Reports File
Posted
a/b

GEORGIA INSTITUTE OF TECHNOLOGY
OFFICE OF RESEARCH ADMINISTRATION

RESEARCH PROJECT INITIATION

Date: May 23, 1974

Project Title: One-Dimensional Investigations of the Sensitivity of the LMFBR Demonstration Plant Breeding Ratio to Cross Section Changes.

Project No: E-26-610

Principal Investigator: Dr. J. M. Kallfelz

Sponsor: Union Carbide Corp. Nuclear Div., Oak Ridge, Tenn.

Agreement Period: From 3-25-74 Until 6-15-74

Type Agreement: Subcontract No. 3986 (under AEC Prime No. W-7405-eng-26)

Amount:

$10,244	UCC funds (E-26-610)
538	GIT Contrib. (E-26-315)
$10,762	Total

Reports Required: Final Technical Report.

Sponsor Contact Person (s):

Technical Matters
Dr. Fred C. Maienschein
Neutron Physics Division
Oak Ridge National Laboratory
P. O. Box X
Oak Ridge, Tenn. 37830

Contractual Matters
Mr. W. S. Rule, Jr.
Contract Administrator
Purchasing Division
Union Carbide Corporation
P. O. Box M
Oak Ridge, Tenn. 37830

Assigned to: School of Nuclear Engineering

COPIES TO:

Principal Investigator	Library
School Director	Rich Electronic Computer Center
Dean of the College	Photographic Laboratory
Director, Research Administration	Project File
Director, Financial Affairs (2)	
Security-Reports-Property Office ✓	
Patent Coordinator	Other

RA-3 (6-71)

GEORGIA INSTITUTE OF TECHNOLOGY
OFFICE OF CONTRACT ADMINISTRATION

SPONSORED PROJECT TERMINATION

Date: June 20, 1978

Project Title: One-Dimensional Investigations of the Sensitivity of the LMFBR Demonstration Plant Breeding Ratio to Cross Section Changes

Project No: E-26-610

Project Director: Dr. J. M. Kallfelz

Sponsor: Union Carbide Corp. Nuclear Div., Oak Ridge, TN

Effective Termination Date: 6/30/78

Clearance of Accounting Charges: 6/30/78

Grant/Contract Closeout Actions Remaining:

X ~~XXXX~~ Invoice ~~XXXXXXXXXXXXXXXX~~ for Supplemental Agreement No. 7--be sure invoice states the period charges were actually incurred.

_ Final Fiscal Report

_ Final Report of Inventions

_ Govt. Property Inventory & Related Certificate

_ Classified Material Certificate

_ Other _____

NOTE: Continued by E-26-633.

Assigned to: Nuclear Engineering (School/Laboratory)

COPIES TO:

Project Director
Division Chief (EES)
School/Laboratory Director
Dean/Director–EES
Accounting Office
Procurement Office
Security Coordinator (OCA) ✓
Reports Coordinator (OCA)
Library, Technical Reports Section
Office of Computing Services
Director, Physical Plant
EES Information Office
Project File (OCA)
Project Code (GTRI)
Other _____

CA–4 (3/76)

GITNE - 78/1

INVESTIGATIONS OF HETEROGENEOUS LMFBR CORES WITH ALTERNATIVE FUEL CYCLES

by J. M. Kallfelz, A. Livrieri and D. M. Rowland

Progress Report for ORNL Subcontract 3986

March 1978

Summary

I. Relation of This Work to National and International Non-Proliferation Studies

Growing concern about the possible illegal use of civilian power reactor fuel for weapons material is reflected in current national and international reassessments of plutonium recycle and LMFBRs based on the plutonium cycle. Such a reassessment is included in the International Fuel Cycle Evaluation (INFCE), which was initiated in the fall of 1977 and is scheduled to be completed in the fall of 1979. One of the tasks of this program is to evaluate various alternative fuel cycles and systems which are potentially more resistant to nuclear proliferation than a system of solely plutonium-fueled LMFBRs.

The Nonproliferation Alternative Systems Assessment Program (NASAP) is a national program which provides technical support to INFCE and provides guidance for the future of nuclear energy development in the U. S. One of the significant sources of input to NASAP is the Thorium Assessment Program (TAP), under which the studies described in this progress report were funded.

II. Areas Investigated

Possible alternative fuel cycles involve the thorium/U-233 breeding cycle. In particular, systems involving "denatured" fresh fuel, which contains a mixture of U-233 and U-238, have been proposed as an alternate which makes recycled breeder fuel more proliferation resistant. A proposed scheme involving this cycle envisions secured energy centers subject to rigorous safeguards, which would be the site for recycle facilities and "transmuter" reactors. These transmuter, or "inside", reactors burn

plutonium and breed U-233, while dispersed from the energy center are the "outside" reactors which operate on denatured fuel. At Oak Ridge National Laboratory, the characteristics of various "symbiotic" systems, involving different combinations of "inside" and "outside" reactor types, are being studied. The work covered in this progress report is part of investigations performed jointly at ORNL's Neutron Physics Division and the Georgia Institute of Technology, concerning the use of LMFBRs as the transmuter reactor or as both an inside and outside reactor type.

"Heterogeneous" LMFBR designs, which have distinct fertile regions interspersed with fissile regions in the reactor core, have been proposed as a means of improving the breeding potential of certain types of LMFBRs. This improvement is particulary important for reactor systems based on alternative fuel cycles for which the doubling times are generally larger than for comparable reactors operating on the (U/Pu) cycle. Furthermore, we recognized that, compared to the standard "homogeneous" LMFBR, the heterogeneous design offers increased design flexibility allowing increased relative production of a particular fissile material, a distinct advantage for alternative fuel cycles. The goal of the studies at the Georgia Institute of Technology is to develop heterogeneous LMFBR designs appropriate for transmuter and denatured reactors, and to investigate their performance characteristics. Basic design assumptions for these reactors are compatible with those made for homogeneous LMFBR designs being studied at the Neutron Physics Division of ORNL, so that the performance indices of the two reactor types can be compared on a consistent basis.

There are various conceivable combinations of fertile and fissile regions possible for heterogeneous LMFBRs in a symbiotic system involving

alternative fuel cycles, and we have considered four basic types:

1. A denatured heterogeneous reactor with $(U\text{-}233/U\text{-}238)O_2$ or $(U\text{-}233/U\text{-}238/Th\text{-}232)O_2$ fuel elements and ThO_2 elements in the internal and external fertile regions.

2. A transmuter reactor with $(Pu/U)O_2$ fuel elements and ThO_2 elements in the internal and external fertile regions.

3. A transmuter reactor like 2. except that $(Pu/Th)O_2$ fuel elements are used.

4. A reference reactor operating only on the Pu/U cycle, with $(Pu/U)O_2$ fuel elements and UO_2 in the internal and external fertile zones.

In developing the various designs for the heterogeneous reactors, a parameter of particular importance is the linear power distribution, which can not violate limits for the material being considered. Thus after picking a basic configuration, we investigated the influence of the fissile region widths on this distribution for the equilibrium cycle. From these investigations we picked the "best" models of those considered.

A significant performance index is the "Compound Fissile Doubling Time" (CFDT), defined in a manner similar to that of the compound system doubling time for a single fuel cycle system. The CFDT is employed because in a symbiotic system some of the bred fissile material produced in a given reactor may not be used for recycle in that reactor. We studied the influence of the fissile region widths on the CFDT, and compared the values of CFDT for the various fuel cycles.

Results for the equilibrium cycle are quite significant for an investigation of reactor performance, but true equilibrium cycle calculations can be rather time-consuming and costly. We therefore investigated the

use of the "quasi-equilibrium" cycle approximation, often employed in Europe to save time and expense, which uses an extended first-cycle calculation to determine approximate results for the equilibrium cycle. In particular, we investigated quasi-equilibrium cycle results for linear power distributions and fissile production.

We have studied some of the basic characteristics of heterogeneous cores and how they differ from those of homogeneous designs, such as neutron energy spectrum changes between the core fissile and fertile regions for the former. Furthermore, we studied various miscellaneous topics related to our models and methods, such as control rod influence and the breeding chain definition, as described in this report.

For all models studied, we analyzed the significant performance parameters and reported the detailed results to the Neutron Physics Division at ORNL, providing input to the studies of symbiotic systems being performed at the laboratory.

III. Summary of Principal Results

1. For initial studies, the quasi-equilibrium cycle approximation is adequate for determining most significant performance parameters of the equilibrium cycle.

2. The base model used for most of these studies had four concentric regions of fissile material, separated by single rows of fertile elements. The three inner fissile regions were two rows, while the outer fissile region contained three rows. To obtain a design for which the maximum linear power was close to the limit for the various materials, fissile elements were replaced with fertile elements, reducing the effective fissile region widths in r - z geometry. The amount of allowable reduction

depended on the driver material. For the cases considered, the best results were obtained for a reduction in all fissile region widths of about 25% and 15%, for the denatured reactors and plutonium fueled reactors, respectively.

3. The models with the best power distribution for the beginning of the first cycle had distributions that were too skewed by the end of the equilibrium cycle. The equilibrium cycle results were used to determine the best models, since the power distribution for the first cycle could be adjusted by various means, e.g. control rod or fuel positioning.

4. For fissile element width reductions up to about 15%, the influence on the CFDT was small. A reduction of 25% led to an increase in the CFDT of about 15% for the denatured case. Thus, for the cases studied, the denatured model which was "best" with respect to the number of fissile elements does not have the best CFDT.

5. For our models, the following rough values of the CFDT were determined for the various heterogeneous LMFBR types:

a.	Denatured	24 years
b.	Transmuter with $(Pu/U)O_2$ fuel and ThO_2 fertile elements	17 years
c.	Transmuter with $(Pu/Th)O_2$ fuel and ThO_2 fertile elements	33 years
d.	Reference reactor with $(Pu/U)O_2$ fuel and UO_2 fertile elements	13 years

6. One of the significant advantages of a heterogeneous core design is the increased design flexibility to influence the components of the bred fissile material, compared to a homogeneous design. For many cases the heterogeneous reactor has a lower CFDT. Even if for some cases,

depending on the cycle, fuel pin size and associated fuel volume fraction, the CFDT for the heterogeneous and homogeneous cases may be about the same, the production of the desired fissile element may be appreciably greater for the former case. For instance, for the case of a transmuter reactor with $(Pu/U)O_2$ fuel and ThO_2 fertile regions, the U-233 production for the heterogeneous reactor is about three times that for the homogeneous case.

7. The design flexibility of the heterogeneous core has a related advantage with regard to materials. An obviously desirable characteristic of a transmuter is a high U-233 production rate. A homogeneous transmuter with $(Pu/U)O_2$ drivers might have an inadequate U-233 production rate. However, based on the discussion in the previous paragraph, this production rate might be adequate for a heterogeneous reactor with $(Pu/U)O_2$ fuel and ThO_2 fertile regions. Thus, the heterogeneous transmuter design might alleviate the necessity to use $(Pu/U/Th)O_2$ or $(Pu/Th)O_2$ fuels, whose properties are presently not nearly as well understood as those of the standard $(Pu/U)O_2$ fuels.

IV. Future Work

The goal of future work on this project will be to obtain a more detailed knowledge of the performance characteristics of heterogeneous LMFBRs operating on alternative fuel cycles, and to make appropriate design changes to improve the models being used for studies of symbiotic systems. We will consider such topics as transport effects, different heterogeneous configurations, and the influence of fuel pin size.

For the future studies particular attention will be given to utilizing and incorporating related information which has become available recently

or should be available in the near future. We will assess the impact of new nuclear data, based on recent and on-going evaluations, for reactions significant to the thorium/U-233 cycle. Further, we will consider the results of the Proliferation-Resistant LMFBR Core Design Study (PRLCDS) as they become available, to determine how the design information from this study can be utilized in our investigations.

CONTENTS

1. Introduction

Growing concern about the possible illegal use of reactor fuel for weapons material is reflected in current national and international reassessment of plutonium recycle and LMFBRs based on the plutonium cycle. There is increasing interest in possible alternative fuel cycles, involving the Th-232/U-233 breeding cycle. In particular the "denatured" (U-233/U-238/Th-232) fuel cycle has been proposed as an alternate which would make recycled breeder fuel more proliferation resistant. A proposed scheme involving this cycle envisions secured energy centers subject to rigorous safeguards. Such centers would be the sites for recycle facilities and "transmuter" reactors, which burn plutonium and produce U-233. Appendix III of this report gives a further discussion of these alternative fuel cycles.

This progress report covers the March 1978 status of investigations performed under ORNL subcontract 3986 at the Georgia Institute of Technology. This work involved studies of "heterogeneous" core designs for LMFBRs operating on various alternative fuel cycles, for both denatured and transmuter reactors. Heterogeneous LMFBR designs, which have distinct fertile regions interspersed with fissile regions in the core, have been proposed as a means of improving the breeding potential of LMFBRs. This improvement is particularly important for alternative fuel cycles, as discussed in Appendix III.

Several of the project participants at Georgia Tech have participated in previous studies of heterogeneous core designs in Europe, including investigations of a possible advanced core for Superphenix type LMFBRs.

Thus in the joint studies with ORNL of alternative fuel cycles for LMFBRs, the work at Georgia Tech concentrated on heterogeneous designs which were compatible with homogeneous LMFBR designs being investigated at ORNL. These joint studies were closely coordinated to insure that the studies at the two sites made compatible design assumptions, so that the heterogeneous and homogeneous design performance indices could be compared on a consistent basis. This consistency was further enhanced by the fact that the calculations at Georgia Tech were performed on the ORNL computer using campus remote terminal facilities. Thus the same codes and basic data were employed in the studies at both sites.

2. Methods and Models Used

2.1. Cross Sections and Codes

The multigroup cross section sets used were generated at ORNL with the code system MINX/SPHINX/AMPX [24-26] and ENDF/B-IV input data, with the exception of the generalized perturbation theory calculations described in section 5.2. For the later calculations, the twenty-six group "Bondarenko" cross section set [27,28] was used. For the "NIRA" models described in section 2.2.1., the ENDF/B-IV cross section set utilized had five groups, while for all other calculations except those for generalized perturbation theory a nine group ENDF/B-IV set was employed.

The results reported here for reactor performance parameters were calculated with the diffusion theory code CITATION [29] using a two-dimensional cylindrical model. The generalized perturbation theory calculations were performed with the one-dimensional diffusion theory codes TAIM [30] and CIAP-1D [31].

2.2. Reactor Models

2.2.1. Models Based on NIRA Investigations

For the initial scoping investigations performed under this subcontract, the reactor models used were based on those used for previous studies by the project director and co-workers at NIRA [9-11,32]. Many of the basic parameters for this model, e.g. the fuel pellet diameter of 5.5 mm, the core height of 100 cm, and the volume fractions for the fuel and radial blanket elements, are as in the French study [12]. The effective annulus thicknesses of 11.2 cm used for the various rows corresponds roughly to the size of the fuel elements for the Phenix reactor.

NIRA models 1 and 2 differed only in the composition of the core fertile regions, which corresponds to that of the axial and radial blankets, respectively. For our calculations we did not include control regions, and the stainless steel concentration was approximately one half of its true value to compensate for an error in the steel cross sections for the five group cross section set. This error was discovered after our initial calculations gave poor comparison with results from NIRA, as discussed in Section 6.1.

For this model, a 300 day full-power cycle (capacity factor of 0.82 and annual refuelling) was assumed. The thermal power was 3000 MWth, a value often assumed by the French for a 1200 MWe reactor. It was assumed that capture gamma energy is approximately 6% of the total, so the assumed power from fission was 2835 MWth.

The figure on page III-24 gives the general layout of this model, and a detailed description thereof has been reported in references 2 and 4.

2.2.2. Models Based on GE LCCEWG Homogeneous Model

To facilitate comparison of results for our heterogeneous core studies and the homogeneous core investigations performed at ORNL, we used a model based on the fuel and fertile elements of the homogeneous core models. These elements are those defined by GE for use in a study of the "Large Core Code Evaluation Working Group" (LCCEWG)[13].

For the base models, the distribution of fissile and fertile rows in the reactor was assumed to be the same as that for the NIRA model, but the annuli thicknesses and core volume were greater than for the NIRA model because the elements of the GE reactor were 13.9 cm flat-to-flat.

Total thermal power for this model was 3085 MWth, as prescribed by GE [13]. The assumed capacity factor was 0.75, corresponding to 273 full power days per cycle for annual refuelling.

Control elements and channels were not included in most of our runs for this model; the influence of this fact is discussed in Section 6.2.

The details of this model have been previously reported [4], and are described in Appendix IV.

2.3. Burn-Up Models: First Cycle, Quasi-Equilibrium Cycle, and Equilibrium Cycle

For the initial calculations of all models, burn-up was considered for the first cycle. The equilibrium cycle, which has different parameters from those of the first cycle, is of more interest.

To obtain detailed and precise values for the equilibrium cycle requires a fairly long and complicated series of iterative runs, using methods developed by Tom Burns at ORNL. To obtain approximate results for the equilibrium cycle we used a method often employed by the French for scoping investigations, the "quasi-equilibrium" cycle method.

This method assumes that the same percentage of elements is replaced at the end of each cycle for all types of elements. To illustrate the method, consider an annual cycle, with 75% capacity factor and refuelling of half of all elements each cycle. The cycle length is then 273 full-power days, and at the beginning of the cycle the average burn-up time of all elements (50% fresh and 50% with 273 day burn-up) is 136.5 days. At the end of this cycle, the average burn-up time is 409.5 days. Assuming linearity, approximate values for the real cycle can be obtained by starting with a fresh core and burning to 409.5 days, then using

the values at 136.5 days and 409.5 days for the BOC and EOC values of the "quasi-equilibrium" cycle.

This technique was used for many of the reactor models that seemed promising. The corresponding runs have .546 in their designation (e.g., see runs 7G and 7H in Appendix I). The BOC and EOC power distributions plotted for these runs in Appendix II are for the quasi-equilibrium cycle.

In sections 3.2 and 4.3 below, we will see that the "quasi-equilibrium" cycle results for many parameters of interest compare well with those of a "true" equilibrium cycle run performed at ORNL.

Considering the breeding "chain", for all runs reported here we have assumed a "short" chain, unless noted otherwise. This "short" chain assumes that all Th^{232} and U^{238} capture leads to U^{233} and Pu^{239}, respectively. All intermediate isotopes (e.g. Pa^{233}, Np^{239}) are ignored, and only Th^{232}, U^{233}, U^{238}, and Pu isotopes 239-242 are considered.

For several cases we utilized an ORNL set of approximate cross sections which contains many of the neglected isotopes, and performed calculations with the "short" chain and a more complicated breeding chain. The results of these calculations are discussed in section 6.3.

2.4. Methods Used to Optimize Power Distribution

Many of the "base" cases (i.e., for the geometry described in Appendix IV) for the models based on the GE LCCEWG reactor have a fairly flat first cycle power distribution, but a P_{max} appreciably lower than the maximum value. Based on economic grounds and other considerations, for an optimized reactor the number of fuel elements should be the minimum consistent with the linear power limit; thus our base models have too many fuel elements.

A parametric study of the influence of reduced fissile element volume was performed by first reducing the width of all fissile element annuli the same percent, while increasing the width of the neighboring fertile elements to keep the outer radius of the radial blanket constant. For this change, the radial distance from the core center of the center of each fertile and fissile zone was not changed. The change was performed in this way because the volume equivalence between the true hexagonal case and the annular (r-z) case is simple; this change is equivalent to replacing a certain number of fuel elements with fertile elements, keeping the total number of element rows in the reactor constant.

The question of the neutronic equivalence of the (r-z) model and the true hexagonal geometry is, of course, a problem not unique to heterogeneous reactors, although for some heterogeneous reactor designs localized changes in the composition of a hexagonal row may occur more often than for a homogeneous reactor.

Tom Burns has indicated that for a heterogeneous GCFR, values from 2-D (r-z) and 3-D (hex) calculations at ORNL are practically the same for many significant parameters (k_{eff}, max. power density, fissile enrichment, total breeding ratio, U^{233} breeding ratio, etc.). For a detailed design some 3-D hexagonal calculations are needed, but for our parametric studies we feel that r-z models are adequate. Such 2-D models were used in the LHRFDS investigations [14,33]. Furthermore, the actual heterogeneous reactors corresponding to our (r-z) models would have a slightly different layout than that shown in Appendix III, e.g. the corners of the hexagonal internal fertile rows might contain control as fuel elements [33].

For the uniform percent reduction in the widths of all fissile regions, the BOC power distribution for the initial cycle became more "skewed" (Proportionally higher in the outer fissile ring). This led in some cases to BOC P_{max} values which exceeded the limits discussed in section 3.1. Hence, we investigated the influence of a further reduction in the width of just the outer fissile ring. The percent values reported for this change in Table V are in percent of this ring width after the initial change, e.g. for case UUTGCS the width of the outer fissile ring is (0.95) (0.90) of its value for the base case, UUTGXS. For this second change, no change was made in the width of the fertile regions, so the radial blanket outer radius decreases.

The only exception to the above described procedure of changing region widths was for model UUTGXD.546, which used a dimension search to obtain the desired k_{eff} at BOL; see the description of Run 7J in Appendix I.

3. Power Density

In this section, we discuss the maximum linear power for various fissile and fertile pins, the relationship between power density distributions for equilibrium, quasi-equilibrium and equilibrium cycles, and the dependence of the power density distribution on the fissile region widths.

3.1 Maximum Linear Power, "Optimum" Power Density Distribution

The information on this parameter is rather sparse for some of the mixed oxides we have used, but for mixed $(Pu/U)O_2$ a value of 16 kW/ft (530 w/cm) is typical [14]. Reference [15] mentions the "higher thermal conductivity and higher melting temperature of $(U/Th)O_2$ relative to $(U/Pu)O_2$, and for one design reports a maximum linear power of 21.3 kW/ft for $(U^{233}/Th)O_2$ fuel in CRBR.

UO_2 and ThO_2 also have superior thermal characteristics compared to mixed $(Pu/U)O_2$ oxides, and a 20 kW/ft limit is stated in Ref. [15] for UO_2 radial blanket pins, while for one CRBR design a peak linear power of 24.4 kW/ft for ThO_2 radial blanket pins is reported. The higher values for the blanket pins can be partially caused by differences in the pellet-clad gap compared to the fuel pins [17], but it appears that for our "denatured" fuel pins of mixed $(U^{233}/U^{238}/Th)O_2$, a maximum linear power of about 20 kW/ft is not excessive. For $(Pu/Th)O_2$, we have not found any definitive values, (Sehgal et al. [16] report that the thermal conductivity of this material is "unavailable"), but based on the above figures it seems likely that its limit is higher than for $(Pu/U)O_2$.

To determine the maximum nominal linear power resulting from a reactor calculation, the above figures should be reduced to allow for 3σ uncertainties and 15% overpower [14]. This typically amounts to about a 25% reduction [18].

For $(Pu/U)O_2$, assuming a maximum linear power of 530 w/cm, the cross sectional area associated with a fuel element of 167.2 cm^2, and 271 pins/asby, we calculate a maximum power density of 858 w/cm^3, or a nominal value of about 690 w/cm^3 allowing about a 25% reduction for 15% overpower and 3σ calculational error. This doesn't include the small decrease due to the fact that 19 elements are control. Further, CITATION power densities do not include the ≈ 6.5% capture gamma contribution, but the gamma energy (including fission gammas) deposition is obviously not all in the pins.

For $(U^{233}/U^{238}/Th)O_2$, based on the above assumptions the corresponding maximum nominal value is around 850 w/cm^3.

Recent results from the "Proliferation-Resistant LMFBR Core Design Studies" (PRLCDS)[21] indicate that advanced fuel pins may have a higher allowable maximum linear power than that indicated above. For instance, maximum values of 18, 19 and 24 kw/ft have been reported for $(Pu\,U)O_2$, $(Pu/Th)O_2$ and $(U^{233}/U^{238})O_2$, respectively [22]. These values include 15% overpower and 12% uncertainty components.

However, Doug Selby has indicated that the grounds for these values are not quite clear [23]. They are at any rate for an advanced fuel pins which are larger (.31 in. for the first two above cases, and .351 in. for the U^{233}/U^{238} case) than those of our model (.26 in. See page III-18), and have the advanced D-9 alloy for the clad. Because of the

better performance of D-9 (an improved SS 316 with an increased silicon content) the clad thickness can be reduced, giving better heat transfer to the pellet.

Doug indicated (22) that WARD is performing power-to-melt (P_M) calculations for this advanced pin, and came to the following results for $(Pu/U)O_2$:

Pin OD (in)	0.27	0.29	0.31
P_M (kw/ft)	18	18.5	19

Doug believes that WARD is now performing such calculations for other fuel element constituents.

Given the preliminary nature of these PRLCDS results, we have used the more conservative limits discussed at the beginning of this section when evaluating our results. However, if further studies confirm conclusively that higher limits are possible, we should use this information in our future studies.

Results for maximum power densities at various times during the cycle are given in Appendix I, while Appendix II reports the detailed power distribution for selected cases. We will discuss below methods to improve the distribution of the base cases for the GE models, and the elimination of cases which violate power distribution restrictions.

Criteria for the "optimum" power distribution are not well defined. While a fairly flat curve for the power distribution in the various fissile regions (i.e. approximately the same maximum value in each region) is desirable, heterogeneous cores have a tendency to change this distribution appreciably during the cycle. Thus, a distribution which

is quite "skewed" at the beginning of the cycle (BOC) may be fairly flat at the end of the cycle (EOC). (E.g., see Run No. 4D, Appendix II.) Furthermore, the equilibrium cycle distribution will be somewhat different from the initial cycle. The general trend is for the power density in regions which initially have a high power and, therefore, a high flux level, to reduce in magnitude relative to this density in the other regions, as burnup progresses.

The "optimum" distribution is, of course, a complicated function of many neutronic, thermal and hydraulic parameters related to performance and safety. For their participation in the LHRFDS [14], ANL investigators chose the following criteria: "The EOEC peak to average ratios have been determined from equilibrium cycle burnup calculations where the feed enrichments were adjusted such that at the end of the cycle the power peaks in the core enrichment zones were the same." [18] This criteria puts the emphasis on the EOC power distribution, presumably due in part to the more stringent restrictions on fuel pin performance at increased irradiation time. However, this requirement can require a fairly "skewed" distribution at BOC (see again Run 4D, Appendix II.)

The HEDL participants in the LHRFDS study [14] used the following criteria: "The power distribution shall be reasonably flattened during the equilibrium cycle." [19] This criteria implies a time-averaged power distribution for the cycle which is fairly flat. It has the advantage that for the models we investigated, the distribution is generally less "skewed" at BOC than it would be for the previous criteria.

3.2 Relationship between Power Density Distributions for the Initial Cycle, Quasi-Equilibrium Cycle and Equilibrium Cycle

Based on the discussion in Section 3.1, it is apparent that since the initial cycle calculation is much simpler than that for the equilibrium cycle, it would be useful to have information on the change in the power density distribution between the former and latter cycles. Furthermore, for all but one class of reactors (the denatured UUT case), we have only performed "quasi-equilibrium" cycle calculations, as discussed in Section 2.3. Thus, an indication of the difference in the power distributions for the quasi-equilibrium and equilibrium cases is desirable; we will address this question first.

Figure 3.1 gives a comparison of the power distribution for a quasi-equilibrium and an equilibrium cycle for model UUTGD (Runs 7H and 7I of Appendix I). As can be seen, the agreement in the core for the two cases is quite good, there being a maximum difference (at BOC) of less than 9%. The true equilibrium cycle is slightly less "skewed" at BOC than the quasi-equilibrium cycle, as illustrated in the associated curves of Appendix II.

Figure 3.2 illustrates that the BOC "skew", shown in the curves for Runs 7E and 7H of Appendix II and indicated by Pmax (outer fissile ring)/ Pmax (inner fissile ring), is reduced by about 40% between the initial and quasi-equilibrium cycles. The EOC skew, in the opposite direction from that for the BOC, is in fact worse for the quasi-equilibrium cycle. Thus, a model with an appreciable power distribution skew for the first cycle can still have an acceptable equilibrium cycle power distribution.

Figure 3.1. Comparison of the Power Distribution in the Core Regions for a Quasi-Equilibrium (A) and an Equilibrium Cycle (B).

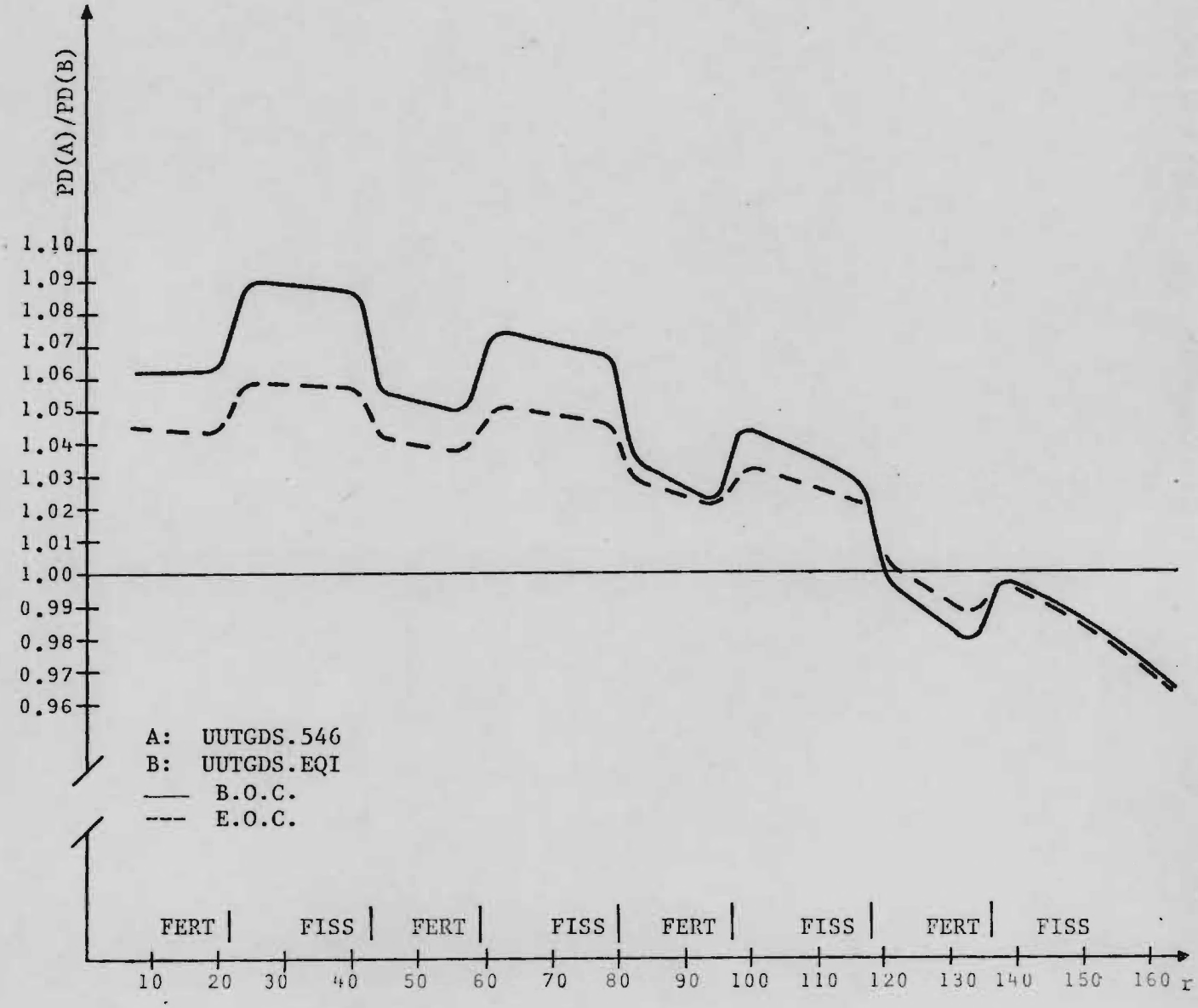

Figure 3.2. Comparison of the Power Distribution of an Initial Cycle (A) and a Quasi-Equilibrium Cycle (B).

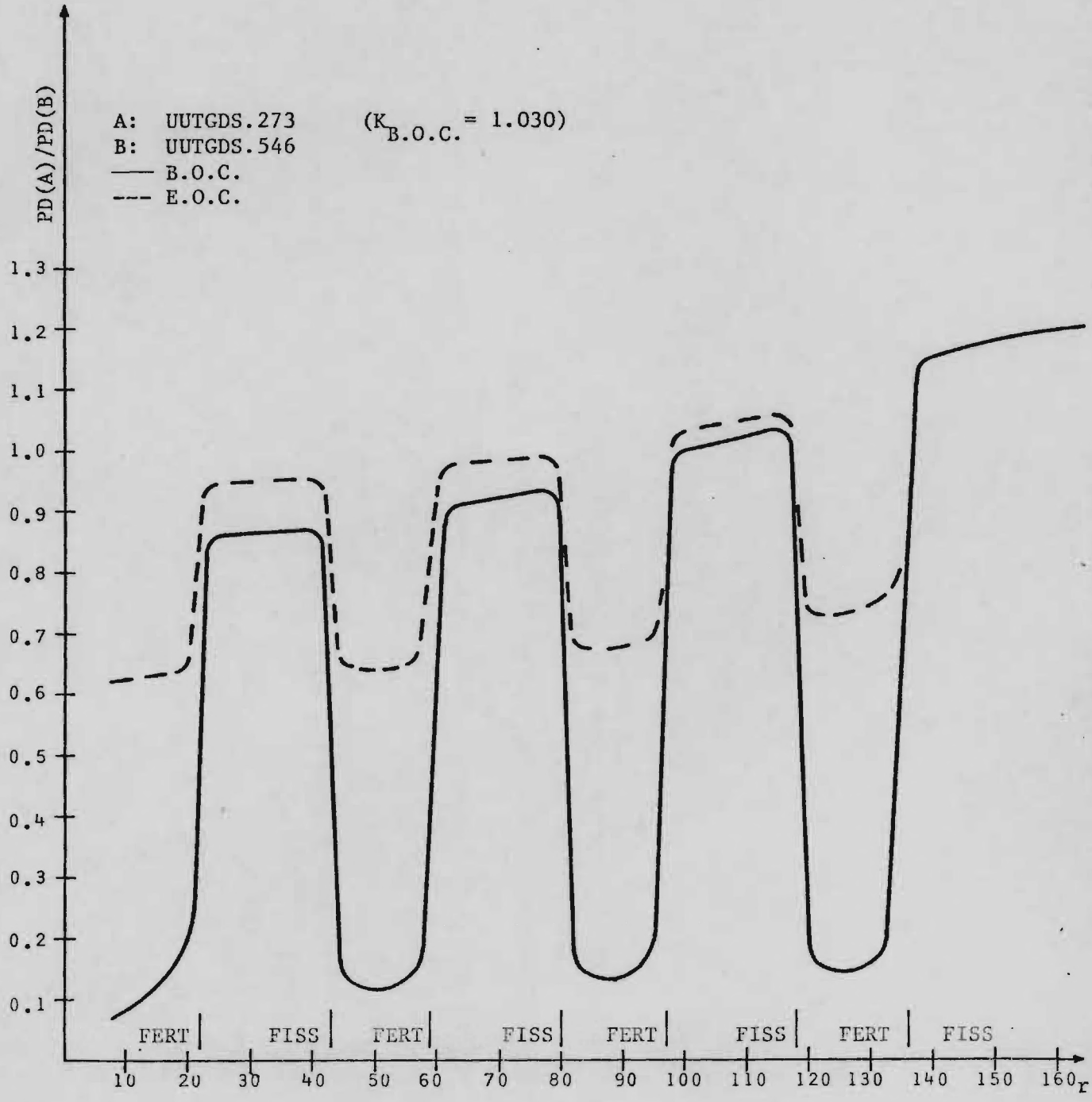

3.3 Influence of Fissile Region Widths on Power Distribution

Many of the base cases reported in Appendix I have a fairly flat initial cycle power distribution, but a Pmax appreciably lower than the maximum value, indicating that the model has too many fissile elements. E.g., see Run 4A of Appendix I, for PUUGX. Pmax during the cycle is 539 w/cc, well below the limit of 690 w/cc mentioned in Section 3.1. Thus, as described in Section 2.4, we studied the influence of reducing the fissile element volume.

The first change we considered was a constant percent decrease in the width (and volume) of all fissile rings. Table 3.1 illustrates that for the BOC values the percent increase in Pmax was appreciably greater than the percent volume decrease; between cases UUTGX and UUTGB these changes were +57% and -25%, respectively. This reflects the fact that the BOC power distribution becomes not only greater in magnitude, but is also more skewed (proportionally higher in the outer fissile ring). This is caused in part by the associated increase in core fertile regions to keep the outer radius of the core constant. Both the size of the outer fissile region and that of the inner fertile region have a strong influence on the amount of "skew."

Figure 3.3 illustrates that the curves for Pmax change versus fissile volume change behave about the same for both the UUT and PUU classes of reactors. Furthermore, it should be noted that the volume change has a much smaller influence on Pmax at EOC than at BOC.

The increased BOC power distribution skew for a uniform percent change in the width of all fissile elements led in some cases to BOC P_{max} values which exceeded the limits discussed in Section 3.1. For

Table 3.1 Maximum Power Density for Base Cases (--X--), and Models with 10% and 25% Reduction in the Fissile Annuli Widths

Type[a]	Pmax (w/cc) (B.O.C.)	Fissile Region No.[b]	Pmax (w/cc) (E.O.C.)	Fissile Region No.
UUTGXS.273	554	4	562	2
UUTGAS.273	655	4	576	2
UUTGBS.273	873	4	639	4
PUUGXS.273	514	4	539	2
PUUGAS.273	609	4	548	2
PUUGBS.273	812	4	597	4
PUTGXS.273	609	4	536	2
PUTGAS.273	737	4		
PUTGBS.273	986	4		
PTTGXS.273	566	4	551	2
PTTGAS.273	684	4	558	2
PTTGBS.273	925	4		

a. Cases ..A.. and ..B.. have a 10% and 25% reduction, respectively, in the thickness of all fissile annuli of Case ..X..

b. Fissile regions are numbered from the core center.

Figure 3.3. Influence of an equal Per Cent Change in the Width (and Volume) of all Fissile Regions.

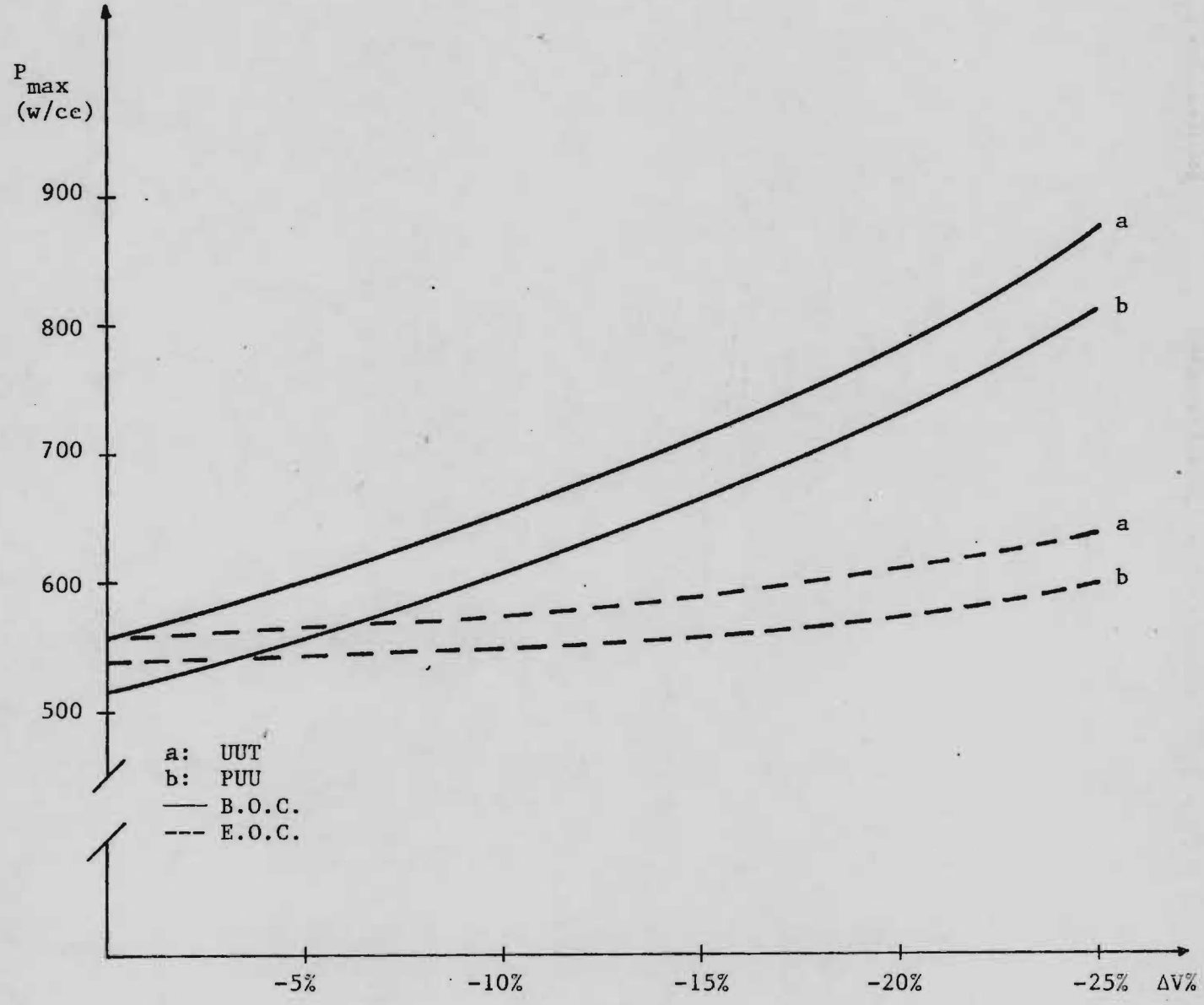

example, note the results for case PUUGBS.273 in Table 3.1 and run No. 4C of Appendix II. Hence, the next logical step was to investigate the influence of reducing the width of just the outer fissile ring.

The influence of such a change for a typical case can be seen in Fig. 3.4. As expected, a reduction in the outer ring size decreases P_{max}, which occurs in this ring. This is accomplished even though the total fuel volume is decreased, because the degree of skew is decreased, with the power density in the inner fissile rings increasing. As for the previous changes, the reduction in the outer fissile ring width had a stronger overall influence on the power distribution at BOC than at EOC; at the later time, the influence of changes made at BOC tend to be compensated during burn-up.

Table V on the last page of this report gives a summary of the various changes in fissile region widths which were considered in this study.

Figure 3.4. Influence on the Power Distribution at a 7% Reduction in the Width of the Outermost Fissile Region.

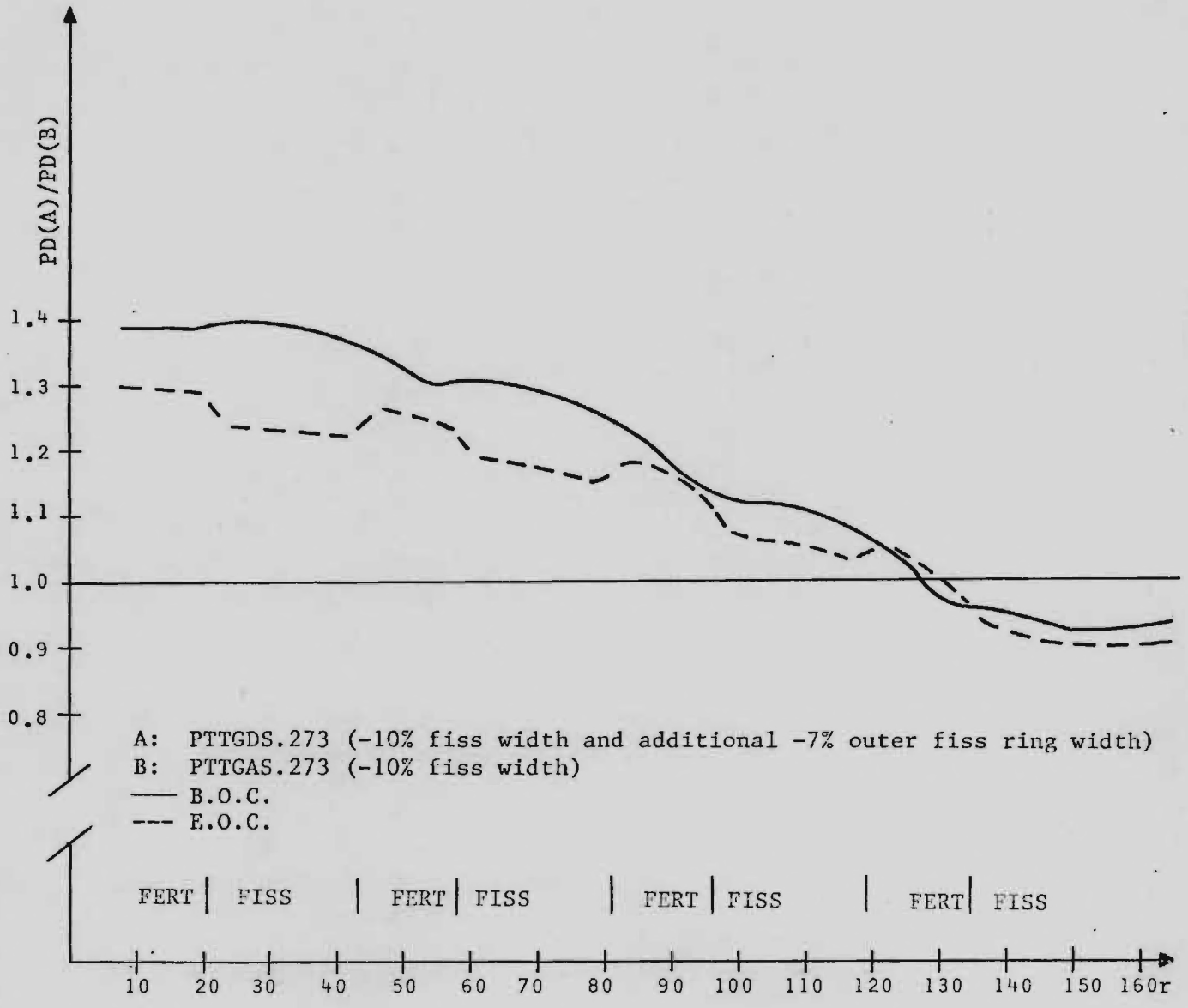

3.4. Cases Which Violate Power Density Distribution Limitations; Selection of "Best" Models

Considering the runs for the initial cycle (all those with a designation ending with .273), the models based on the GE reactor with a constant fissile width reduction of -10% (class A) and -25% (class B), have BOC distributions which are too skewed, with the power density relatively large on the outer fissile annulus. The latter class has P_{max} values in the outer fissile annulus which exceed considerably the P_{max} limitations. We have chosen these limits as 690 w/cc, 700 w/cc and 850 w/cc for $(Pu/U)O_2$, $(Pu/Th)O_2$ and $(U^{233}/U^{238})O_2$ respectively, based on the discussion in section 3.1. For example, the following values are the BOC P_{max} values for the indicated runs:

PUUGBS.273	812	w/cc
PUTGBS.273	986	w/cc
PTTGBS.273	925	w/cc
UUTGBS.273	873	w/cc

Based on the above results, we chose the models which had a further 5% reduction in the outer fissile ring width (generally classes C and D) for the calculation of the quasi-equilibrium cycle; these cases did not have badly skewed BOC power distributions for the initial cycle.

However, comparison of the initial and quasi-equilibrium cycle results showed that for the latter case the power in the outer and inner rings was decreased and increased, respectively, compared to former case (see figure 3.2). Thus, the quasi-equilibrium EOC power

distributions were badly skewed, with the inner fissile ring power too high, for with an added reduction in the outer fissile annulus width, as illustrated by the results shown in Appendix II (runs with a designation ending .546).

Considering the above, with regard to the equilibrium power distributions the models of class A and B are the "best" of the cases considered. Their skewed BOC distributions for the initial cycle can presumably be improved by "shaping" with control rods. The actual amount of constant width reduction for the "best" model depends on the type fuel used. The EOC skew should not be too great, and the limits for the maximum power density of that fuel should not be exceeded. For the UUT cases, the model with a 25% fissile width reduction meets these criterea; see the results for UUTGBS.546, Run 7G, in Appendices I and II. For the $(Pu/U)O_2$ cases the P_{max} limit is exceeded for a 25% fissile width reduction, and the intermediate constant reduction value of 16% as in case PUUGCS.273 apparently gives the "best" results of the cases considered.

Table 4.1. Variation in Breeding Ratio for Two Reactors of the Same Type, Identical Except for the Initial Fissile/Fertile Ratio in the Fissile Regions[a]

TYPE	$\Delta k_i\%$	$\Delta k_f\%$	ΔBR_i	ΔBR_f	$(\Delta BR/\Delta k\%)_i$	$(\Delta BR/\Delta k\%)_f$
UUTGDS	1.5	1.2	-0.037	-0.030	-0.0247	-0.0250
PUUGDS	2.3	1.9	-0.062	-0.066	-0.0270	-0.0347
PUTGCS	3.5	2.8	-0.091	-0.091	-0.0260	-0.0325
PTTGCS	4.5	3.4	-0.097	-0.092	-0.0220	-0.0271

a) i and f correspond to BOC and EOC values, reprectively.

Table 4.2. Variations in the Fissile Production (PF) During a 273 Day Cycle for Two Reactors of the Same Type, Identical Except for the Fissile/Fertile Ratio in the Fissile Regions

TYPE	$\Delta k_i\%$	ΔPF	$\Delta PF/\Delta k_i\%$
UUTGDS.273	1.5	-30.9	-20.6
PUUGDS.273	2.3	-50.5	-21.9
PUTGCS.273	3.5	-75.1	-21.5
PTTGCS.273	4.5	-87.2	-19.4

4. Compound Fissile Doubling Time (CFDT)

The designation of a compound fissile doubling time (CFDT) represents a modification in parameter definition necessitated by the alternative cycles. Since some of the bred fissile material produced in a given reactor may not be available for recycle in the reactor, the commonly used terminology of a "reactor doubling time" is somewhat misleading. The designation of a compound fissile doubling time is employed to emphasize this difference. The parameter, however, is defined in a manner similar to that used for the compound system doubling time for a single fuel cycle system (e.g., Pu/U):

$$\text{CFDT} = \frac{0.693 \times (\text{fissile mass, initial core} + 1 \text{ reload})}{(0.98 \text{ cycle fissile discharge} - \text{cycle fissile charge})} \qquad (4.1)$$

The compound fissile doubling time is thus a measure of the rate of excess fissile production. The value of 0.98 used in Eq. (2) represents a recovery factor (i.e., assumes 2% losses). We have further assumed that one reload is 1/2 an initial core.

4.1 Correction of CFDT for Consistent k_{eff} for Various Cases

As can be seen in Table 4.4, for the initial calculations the minimum k_{eff} during the cycle varied for the different cases. Since k_{eff} depends on the fissile/fertile ratio, a variance of this ratio to obtain a consistent minimum k_{eff} during the cycle will influence the associated breeding ratios and CFDT; thus, the calculated CFDT values for these cases, which vary considerably within a particular reactor class (e.g. PTT), cannot be compared without a correction for this influence. In the following we describe an approximate method for this correction, which for survey calculations negates the necessity to perform several iterative calculations

to obtain the desired minimum k_{eff}.

Let us first consider the influence of a change in the initial k_{eff}, Δk_i, (obtained by varying the fissile/fertile ratio in fissile regions) on the breeding ratio. Table 4.1 shows that the associated change in the initial breeding ratio, ΔBR_i, has approximately the same dependence on Δk_i for all the reactor classes. The value of $(\Delta BR/\Delta k)_i$ of -2.7% for the PUU models is consistent with values obtained at NIRA [1], which determined a value of -2.5% for this parameter for a similar model.

Considering the PUUG--.273 cases, one can see the k_i is 1.030 for all except the first 273 day "cycle" of PUUGDS.546, for which k_i is 1.007. In the following discussion the values for the later cycle will bear the superscript 546, while the superscript 273 will indicate results from PUUGDS.273. The subscripts i and f have the significance given in Table 4.1.

$$\Delta k_i\% = \frac{k_i^{273} - k_i^{546}}{k_i^{546}} \times 100 = 2.3$$

$$\Delta PF = PF^{273} - PF^{546} = -50.5 \text{ kg}$$

Where PF = Fissile production = 0.98 x cycle fissile discharge - cycle fissile charge

The resulting ratio $\frac{\Delta PF}{\Delta k_i\%} = -21.9$

Repeating the same type calculation for cases in the other reactor classes, the values in Table 4.2 result. $\Delta PF/\Delta k_i\%$ is approximately -20 for all reactor types, and this value will be used in the following calculations.

Since the absolute value of k_{eff} is only significant to several percent for the cross sections and methods used, we will correct all cases to a minimum k_{eff} during the cycle of 1.005-1.006, since many of the cases have a minimum k_{eff} close to this range. Thus for the PUT and PTT cases which have $k_i > k_f$ we desire $k_f = 1.006$ and can estimate the desired k_i as illustrated below:

Case	k_i	k_f	$\Delta k_{(f-i)}$
PUUGDS.273	1.030	1.025	-0.005
PUUGDS.273 (from 546)	1.007	1.006	-0.001
PUUGXS.273	1.030	1.028	-0.002
PUUGXS.273 (corrected)	k_f-x	1.006	x

If a linear relationship exists, we can write

$$0.005/0.001 = -0.002/x$$

Thus $x = -0.004$, $k_i = 1.0064$, and the desired $\Delta k_i\%$ for case PUUGSX.273 is -2.3. It follows that $\Delta PF = -2.3 \times - 20 = 46$ kg.

Repeating the calculation of Δk_i for the other PUU cases, a value of approximately - 2.3 always results for $\Delta k_i\%$.

Next we estimate the change in the initial core fissile mass. This calculation is illustrated by Table 4.3.

Considering the results of Table 4.3, we have assumed that $\frac{M_i' - M_i''}{\Delta k_i\%} = 75$ for all cases. Thus referring to Eq. 4.1, the corrected CFDT value for case PUUGXS.273 is

CFDT (Corrected) =

$$\frac{[0.693 \times 1.5 \times (3781 + 574)] - \frac{M_i' - M_i''}{\Delta k_i\%} \times \Delta k_i\%}{\left\{[0.98 \times (4245 + 478)] - (3781 + 574)\right\} + \frac{\Delta PF}{\Delta k_i\%} \times \Delta k_i\%} = 13.6 \text{ yrs}$$

Table 4.3. Variation in the Initial Core Fissile Mass for Two Reactors of the Same Type, Identical Except for the Fissile/Fertile Ratio in the Fissile Regions

TYPE	Initial Core Fissile Mass	$(M_i' - M_i'')/\Delta k_i$ %
PUUGDS.273	M_i' = 3713 + 564 = 4277	74.78
PUUGDS.273(from 546)	M_i''= 3564 + 541 = 4105	
PUTGCS.273	M_i' = 4094 + 622 = 4716	78.76
PUTGCS.273 (from 546)	M_i''= 3855 + 585 = 4440	
PTTGCS.273	M_i' = 4485 + 681 = 5166	75.56
PTTGCS.273 (from 546)	M_i''= 4190 + 636 = 4826	
UUTGDS		75.33

To check the accuracy of this correction, we repeated cases PUUGXS.273 and PUUGCS.273 with k_i such that k_f was approximately 1.005, as shown in Table 4.4. The resulting CFDT from these runs are termed the "actual" values. The following table shows that the agreement between the approximate "corrected" values and the actual values is good.

	CFDT (years)		
	Without Correction	Corrected Value	Actual Value
PUUGXS.273	16.5	13.6	13.4
PUUGCS.273	14.3	12.2	12.1

In a similar manner, we corrected the CFDT for various cases.

As can be seen in Table 4.4, the differences in the corrected values for the various cases in a particular reactor class are generally quite small, in contrast to the wide value spread before the correction was applied.

In closing it should be pointed out that, while correcting to the same minimum k_{eff} during the cycle allows consistent comparison of cases within a reactor class (e.g. UUT), the bias in k_{eff} due to cross section errors is presumably different for different classes, due to their differing fissile and fertile constituents. However, not knowing the cross section errors and associated k_{eff} bias, this comparison is the best we can accomplish between reactor classes.

Table 4.4 Compound Fissile Doubling Time (CFDT) for Various Models

TYPE	$K_{B.O.C.}$	$K_{E.O.C.}$	$\Delta K_{(E-B)}$	Breeding Ratio (E.O.C.)	CFDT (Yr)	CFDT (Yr) Corrected[a]
UUTGXS.273	1.030	1.013	-0.017	1.284	22.8	20.2
AS.273	1.030	1.009	-0.021	1.294	23.0	21.3
CS.273	1.030	1.014	-0.016	1.280	23.4	20.5
DS.273	1.030	1.012	-0.018	1.286	23.6	21.1
DS.273	1.015	1.000	-0.015	1.316	19.5	
ES.273	1.030	1.015	-0.015	1.280	23.7	20.6
BS.546	1.032	1.008	-0.024	1.273	28.8	
DS.546	1.019	1.007	-0.012	1.282	24.5	
DS.EQI	1.012	0.999	-0.013	1.302	23.9	
PUUGXS.273	1.030	1.028	-0.002	1.387	16.5	13.6
AS.273	1.030	1.024	-0.006	1.417	15.3	12.7
CS.273	1.030	1.020	-0.010	1.438	14.5	12.2
DS.273	1.030	1.025	-0.005	1.425	14.6	12.0
DS.273	1.007	1.006	-0.001	1.491	12.0	
ES.273	1.030	1.027	-0.003	1.419	14.5	12.1
DS.546	1.005	1.010	+0.005	1.430	13.3	
XS.273	1.006	1.009	+0.003	1.432	13.4	
CS.273	1.008	1.002	-0.006	1.482	12.1	
PTTGXS.273	1.030	1.040	+0.010	1.235	54.0	34.9
AS.273	1.030	1.033	+0.003	1.269	42.5	29.6
CS.273	1.030	1.039	+0.009	1.257	43.6	30.0
CS.273	0.986	1.005	+0.019	1.349	23.9	
DS.273	1.030	1.041	+0.011	1.252	43.5	29.9
CS.546	0.995	1.014	+0.019	1.277	31.0	
* PUTGXS.273	1.030	1.034	+0.004	1.363	22.0	17.3
CS.273	1.030	1.033	+0.003	1.373	20.9	16.6
CS.273	0.995	1.005	+0.010	1.464	14.9	
CS.546	0.999	1.013	+0.014	1.387	17.3	

[a]Values corrected approximately, as described in text, so that the minimum k_{eff} during the cycle is ≈ 1.005.

*See note, page 4-8.

4.2. CFDT for Various Fissile Element Widths

As discussed in section 4.1, we applied a correction to the CFDT values for various runs to determine the approximate value for a minimum k_{eff} during the cycle of 1.005. The results are given in Table 4.4, which also contains values for many runs for which we did not apply a correction because the minimum k_{eff} during the run was not far from 1.005.

As has been previously noted, the differences in the CFDT values for different models in a particular reactor class are quite small, when they are compared on the consistent basis that the minimum k_{eff} during the cycle is about 1.005. Within the order of accuracy of the correction described above, we can not determine any dependence of CFDT on the fissile width changes for most of the cases reported in Table 4.4., i.e. those involving the -10% and -16% width changes. This seems reasonable, considering that we kept the overall core radius constant or almost constant for most of our changes, increased the fertile volume as the volume of the fissile regions decreased, and increased the fissile enrichment; thus the average core enrichment did not change greatly.

As larger reductions are made in the fissile width, one might expect changes in the CFDT, because among other things the associated increase in fertile width can lead to appreciable flux depression in the fertile regions. This may explain the difference in the results for UUTGBS.546 and UUTGDS.546; the former case, which is for a 25% fissile width reduction, has an appreciably higher CFDT value.

4.3. Comparison of CFDT for Initial Cycle, Quasi-Equilibrium Cycle, and Equilibrium Cycle

The results given in Appendix I are indicative of the differences in fissile mass change for the initial cycle and the quasi-equilibrium cycle. Comparison of the results for these two cycles for all the NIRA model runs, and for the GE models runs with .546 in their designation, indicates the relative shift from one fissile material to another during burnup, and the corresponding changes in the cycle production and burnup rates for the various isotopes. For example, note run 5F (a PUT model). The equilibrium cycle produces less U-233 than the initial cycle, but this effect is partially compensated by the fact that the former cycle also burns up less Pu-239 and Pu-241. This is to be expected, as the equilibrium case has more U-233 and less Pu-239 present during the cycle than does the initial cycle.

This comparison answers the question of interest, namely, can the initial cycle results be used to accurately predict the equilibrium cycle fissile mass balances for the various isotopes? The answer is no, as expected. Thus a comparison of the CFDT for the initial and quasi-equilibrium cycles is somewhat academic. It should further be noted that the minimum k_{eff} values for the two cycles is generally different for the results reported, introducing the question of how this fact should be treated, in light of the discussion in section 4.1.

Clearly the influence of the generally higher k_{eff} values for the initial cycle depends on how this excess k_{eff} is controlled. If control rods perform this function, then the effect on the breeding ratio can be small. If one makes the questionable assumption that the enrichment of

the elements removed at the end of the initial cycle is reduced to reduce k_{eff}, then the influence is like that discussed in section 4.1. for comparison of various models. For this assumption the initial cycle CFDT values are 10%-20% lower than the quasi-equilibrium cycle values, as can be seen in Table 4.4. (e.g., compare the UUTDS.546 CFDT value with the corrected CFDT value of UUTGDS.273).

To compare the results for a quasi-equilibrium and true equilibrium cycle, a run of the latter type was performed for model UUTGDS. by Tom Burns at ORNL, and is reported as run 7I in Appendices I and II. Tables 4.5 and 4.6 compare the results of this run with a quasi-equilibrium run for the same model.

As can be seen, the region-wise BOC and EOC inventories of all fissile isotopes are the same to within several percent for the two cases, with the exception of the radial blanket. For the latter region, six year residence time with annual refuelling of 1/6 of the elements was assumed; thus, its fissile charge should be higher than that of the quasi-equilibrium cycle.

As can be seen in Table 4.6, the region-wise results for the cycle production or burn-up of the various isotopes in the quasi-equilibrium cycle is within 2% of the results for the true equilibrium cycle, even for the radial blanket. Thus we conclude that for our scoping calculations, the quasi-equilibrium cycle runs are adequate to determine the fissile balances and CFDT of the equilibrium cycle.

Table 4.5

Comparison of Fissile Inventories for Equilibrium and "Quasi Equilibrium" Calculations (UUTGDS.EQI/UUTGDS.546)

Inventories

Isotope \ Zone	BOC 1 Fert In	BOC 2 Core Fiss	BOC 3 Fert Out	BOC 4 Ax Blkt	BOC 5 Rad Blkt	EOC 1 Fert In	EOC 2 Core Fiss	EOC 3 Fert Out	EOC 4 Ax Blkt	EOC 5 Rad Blkt
Pu 239		157.8 / 159.4					445.4 / 443.7			
U 233	194.3 / 192.4	3539.7 / 3620.4	34.1 / 31.1	41.0 / 39.8	468.9 / 110.1	536.5 / 538.2	2857.0 / 2923.5	100.0 / 97.6	120.0 / 118.6	646.1 / 290.6
U 235		39.6 / 39.3					33.3 / 33.0			

Change in Cycle Inventory

Isotope \ Zone	1 Fert In	2 Core Fiss	3 Fert Out	4 Ax Blkt	5 Rad Blkt
Δ Pu 239		+287.6 / +284.3			
Δ U 233	+342.2 / +345.8	-682.7 / -696.9	+65.9 / +66.5	+79.0 / +78.8	+177.2 / +180.5
Δ U 235		-6.3 / -6.3			

Table 4.6

Percent Error of "Quasi Equilibrium" Change in Cycle Inventory

$$\left[\frac{\Delta \text{EQI} - \Delta 546}{\Delta \text{EQI}} \times 100\%\right]$$

Zone / Isotope	1 Fert In	2 Core Fiss	3 Fert Out	4 Ax Blkt	5 Rad Blkt
Δ Pu 239		1.15			
Δ U 233	1.05	2.08	1.50	0.25	1.86
Δ U 235		0.0			

4.4. Comparison of CFDT Results for Various Alternative Fuel Cycles

As noted already in section 4.1, correcting to the same minimum k_{eff} during the cycle allows consistent comparison of cases within a reactor class (e.g. UUT), but the bias in k_{eff} due to cross section errors is presumably different for various classes, due to their differing fissile and fertile constituents. However, not knowing the cross section errors, a comparison of various reactors for a minimum k_{eff} during the cycle of 1.0 is the best we can accomplish.

The results for the quasi-equilibrium cycle runs reported in Table 4.4 all have minimum cycle k_{eff} values within about 0.5% of 1.0, and the results for the CFDT should be within several years of the values for a minimum k_{eff} of 1.0. Using the values in the table, we estimate the following rough values of the CFDT for our models and a minimum cycle k_{eff} of 1.0:

Reactor Class	CFDT (yrs)
UUT	24
PUU	13
PTT	33
PUT	17

Note: After preparation of this report, a small error was found in the concentration of U-238 in the fuel region for the PUT cases. Case 5F of Appendix I, model PUTGCS.546, was repeated with the correct U-238 concentration, and the results are given as Run 5G of Appendix I. As can be seen, after the correction the fissile production and fissile mass are both reduced by a small amount. The CFDT for the corrected case is 18.1 years, a 4.6% increase. The increase in the CFDT for all the PUT cases should be about this amount.

5. Characteristics of Heterogeneous Cores

5.1. Problems of Comparison of Heterogeneous and Homogeneous Cores

For various reasons, there is presently some debate about which homogeneous core model should be compared with a heterogeneous core design. Some aspects of this problem are evident from a survey of heterogeneous core references cited in Appendix III, as well as from the results of the LHRFDS study [14]. Various reasons for the problems involved in this comparison are discussed in Appendix III, starting on page III-7.

As discussed further on page III-8 and III-9, in this study we have employed the following procedure for comparing a homogeneous and heterogeneous design. First we have adopted a homogeneous design [13] that is typical for an LMFBR. The fertile and fissile elements of this of this design were then rearranged in heterogeneous designs to determine if the breeding potential is improved for some configuration.

5.2 Generalized Perturbation Theory Calculations for Breeding Parameters

Besides the increased fertile material fraction in the core that can be accomplished with a heterogeneous design, the space dependence of $\phi(E,\vec{r})$ can offer an advantage. We discuss in detail the reasons for this advantage in Appendix III, pages III-8 and III-9, where results are given of generalized perturbation theory calculations for a $(Pu/U)O_2$ fuelled heterogeneous reactor. These calculations give results for the generalized importance function, $\psi_g^*(\vec{r})$, which is the importance of neutrons at $\vec{r}$ in energy group g to a given integral parameter. The results on page III-24 indicate that $\phi(E,r)$ varies in the core in just such a way

as is advantageous to the breeding ratio. There is a "hard" spectrum in the fissile regions and a "soft" spectrum in the fertile regions.

U-233 has a different for for $\eta(E)$ than that of Pu-239, and it is not clear if the spectrum form change offers an appreciable advantage in a U-233 fuelled reactor. Thus we have essentially repeated the generalized perturbation theory calculations of Appendix III for a denatured LMFBR, model UUTGDS.

For these calculations we employed the 1D diffusion theory codes TAIM [30] and CIAP [31], and the Bondarenko cross section set [27,28]. Results are reported in Figure 5-1 and Table 5-1, for ψ^* defined for the breeding ratio of a 1D cylindrical reactor model.

The results are quite similar to those for the $(Pu/U)O_2$ system reported in Appendix III, i.e. $\phi(E)$ has relatively more high energy neutrons where they are more important to the breeding ratio, and more low energy neutrons where they have a greater importance. This is indicated in the curves of ϕ_{15}/ϕ_5 and $\overset{*}{\psi}_{15} - \overset{*}{\psi}_5$ in Figure 5-1, where groups 5 and 15 are for high and low energies, respectively. Table 5-1 gives the absolute values of ϕ_5 and ϕ_{15}, which must also be considered.

This matter is still being investigated at Georgia Tech, since we have some inconsistent results. For the core internal breeding ratio (BI), the behavior of $\overset{*}{\psi}_{15} - \overset{*}{\psi}_5$ is the opposite of that in Fig. 5-1. The reason for this is not understood, since for the $(Pu/U)O_2$ reactor the general behavior of ψ^* for BI and the breeding ratio was the same; thus we are further checking and analyzing these runs.

Figure 5-1. Comparison of Radial Dependence of ϕ_g and the Generalized Adjoint Function (ψ_g^*) for the Breeding Ratio of Model UUTGDS. at BOL. 1D Cylinder Model with ABN Cross Sections (Boundaries of Group 5 and 15 are 0.8 - 1.4 MeV and 0.465 - 1.0 keV, respectively)

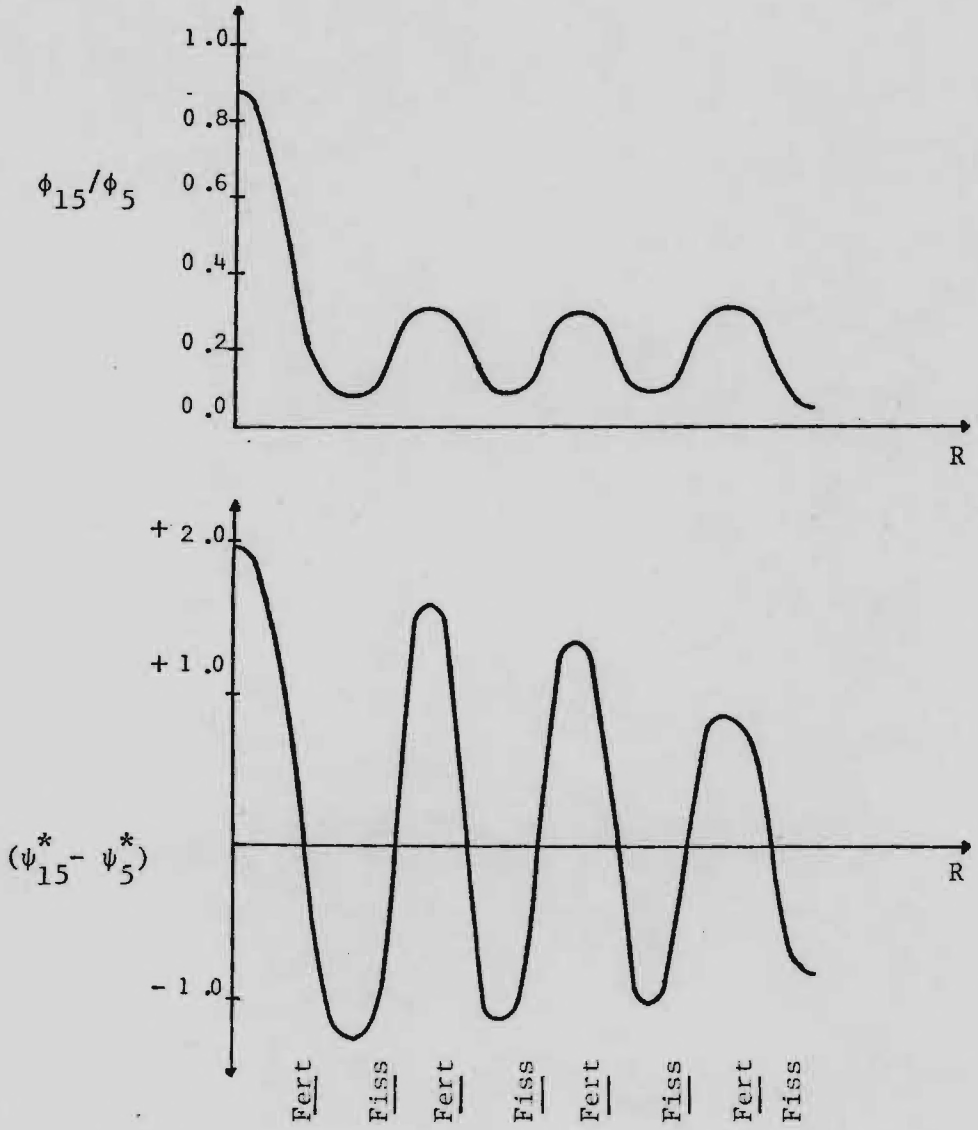

Table 5-1. Comparison of Radial Dependence of ϕ_g and the Generalized Adjoint Function (ψ^*_g) for the Breeding Ratio of Model UUTGDS. at BOL. 1D Cylinder Model with ABN Cross Sections (Boundaries of Group 5 and 15 are 0.8 - 1.4 MeV and 0.465 - 1.0 keV, respectively)

Radius (cm) (region center)	Region	ϕ_{15}	ϕ_5	ϕ_{15}/ϕ_5	ψ^*_{15}	ψ^*_5	$\psi^*_{15} - \psi^*_5$
0.0	1. Fert	11.27	12.87	0.876	+1.479	-0.486	+1.965
31.8	2. Fiss	5.32	81.44	0.065	-3.400	-2.150	-1.250
50.7	3. Fert	11.42	36.53	0.313	+0.232	-1.351	+1.583
69.6	4. Fiss	6.22	95.59	0.065	-3.243	-2.003	-1.240
88.5	5. Fert	13.20	42.22	0.313	+0.459	-0.905	+1.364
107.5	6. Fiss	7.22	110.08	0.066	-2.159	-1.068	-1.091
126.9	7. Fert	15.83	47.73	0.332	+1.080	+0.211	+0.869
150.9	8. Fiss	6.48	143.96	0.045	+0.137	+0.927	-0.790

5.3 Comparison of Some Results for Heterogeneous and Homogeneous Cases

To investigate the influence of the heterogeneous design on the ratio of U-233 production to Pu-239 production for a denatured reactor, we performed a calculation of a 20% denatured reactor equivalent to one of Tom Burn's designs, in which we included 19 control rods with the same procedure used by Tom. Some results are reported as Case 6 in Table III of our 21 June memo [5].

The total reactor U-233/Pu-239 production ratio is 2.27 for the heterogeneous design, compared to 2.05 for the homogeneous reactor. The average per atom ratio Th capture/U-238 capture for the core fissile and fertile regions is 1.27 for this heterogeneous case, compared to a value of 1.13 for the inner core of Tom's homogeneous case. The results apparently indicate the hoped-for benefit of an incresed U-233/Pu-239 production ratio for the heterogeneous cores, due to the spectral change between fertile and fissile regions for these reactors.

Further comparison of results for heterogeneous and homogeneous designs are given in Appendix III, e.g. see the figures on page III-26.

6. Summary of Other Topics Investigated

6.1 Influence of Stainless Steel Cross Sections on Results

The cases starting with numbers 1, 2 and 3 in Appendix I are all based on the NIRA model from Ref.[11], rather than the GE LCCEWG model [13]. These cases were preliminary runs made at the beginning of the project, to compare with results of NIRA [11] for checking our methods and the preliminary ORNL five-group cross section set.

As reported in [2], [3] and [4], the first calculations of these models indicated considerable discrepancy between the results with the NIRA and ORNL σ sets, For models approximately the same as those from the NIRA report [11], our calculations with the ORNL σ set gave BOL k_{eff} and breeding ratio values which were lower than the NIRA results by about 2% and 10%, respectively [2].

Since at NIRA we got good agreement with independent calculations performed by the French at Cadarache, we suspected a possible error in the preliminary ORNL σ set. To allow a direct regionwise comparison of reaction rates in various materials, we performed a CITATION run for a case identical to that of a NIRA model for which the complete output was available at Georgia Tech. As reported in [3] and [4], we found that the absorption in stainless steel with the ORNL cross section set was approximately 100% greater than for the NIRA results.

Concurrently an error was found in the preliminary ORNL sigma set, and this error was not present in the subsequent data sets, which we used for our calculations of the reactor types starting with the numbers 4-7 in Appendix I. For types 1-3, the results in Appendix I are for the stainless steel concentration reduced by the factor 0.536, the ratio of overall stainless steel capture from NIRA and ORNL preliminary cross

section sets for the model discussed in [4]. With this correction the agreement between our results and those of NIRA was satisfactory.

6.2 Influence of Including Control Rods and Channels in Calculation

Our investigations did not include a determination of the reactivity control requirements, which would obviously be necessary to accurately determine the influence of the control assemblies on the results for the performance parameters of our designs. However, we did perform several calculations to give an indication of the impact of control rods, which were not included in our models.

The determination of the amount of reactivity control necessary involves fairly straightforward, but detailed calculations, as discussed in [18]. The French designs have an appreciable decrease in the number of control rods needed for a heterogeneous core compared to a homogeneous core. Even though the rods are generally worth less for the former case due to lower flux levels, this is more than compensated for by the Δk/cycle reduction by about half for the heterogeneous core with its higher conversion ratio [12,34]. However, the HEDL level I results of the LHRFDS [19] had for the heterogeneous design about 50% more control rods than for the homogeneous case, while the GE level II results for the same study [33] had about the same number of control rods for both cases. For our calculations we assumed the same number of control rods, 19, which was prescribed for the homogeneous case [13].

The rods were assumed to be withdrawn into the axial blanket. Since the adjustment of control rods during burnup results in expensive and detailed calculations it is common practice for scoping calculations to assume that the control rods are out of the core during burnup [11,18]. Furthermore, we performed a one-half reactor calculation, and used the

same method used by Tom Burns for including control, i.e., the 19 control rods were smeared uniformly over all core fissile and fertile regions, while the axial blanket had 19/2 control channels and 19/2 control rods smeared uniformly. This method probably overestimates the influence of the control in the axial balnket, since localized fuel rods have some spatial self-shielding.

As discussed in [5], for a denatured reactor case the influence of adding the control as described above to a model which neglected control was fairly small. For this change, the breeding ratio dropped from 1.19 to 1.17, for an enrichment search to the same k_{eff} for both cases. As the models are refined the influence of control should be investigated further.

6.3 Simple and Detailed Breeding Chains

For the calculations reported in Appendix I, we have assumed that all Th-232 capture leads to U-233 production. This is a slight approximation, due to the 27 day half-life of the intermediate isotope, Pa-233, as well as several other details of the breeding chain which have been neglected.

To investigate the influence of this approximation, we performed several calculations of cycles with the "detailed" breeding chain, taken from one of Tom Burns' runs and shown in Fig. 6-1, as well as with two approximations. These calculations were performed with a preliminary cross section set which contained data for the necessary isotopes; therefore, the results can not be compared directly with those of Appendix I, but are of interest to determine relative changes.

The first case we considered was that of a denatured model, UUTGDS., with the detailed breeding chain. Comparison of the results, given in Table 6-1, with those of Table 6-2 for the same case using the "short"

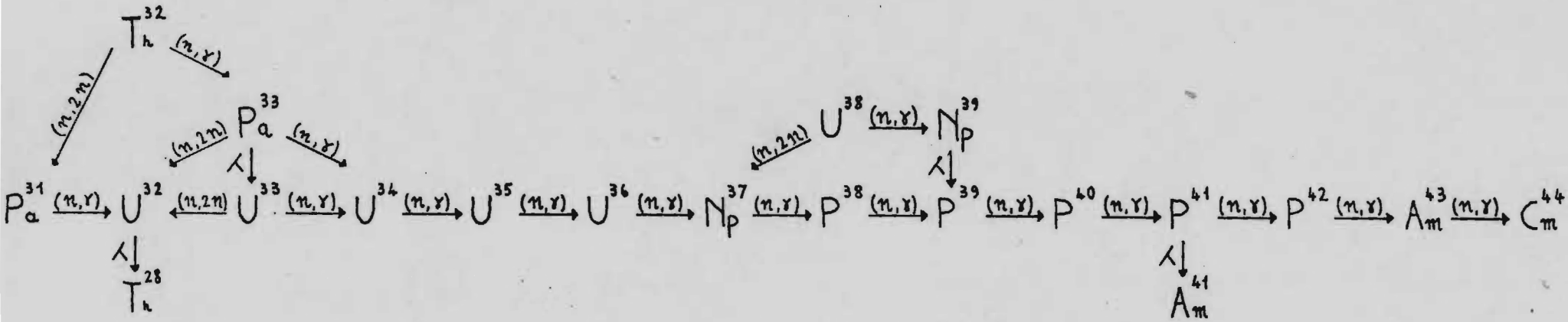

FIG. 6-1. Detailed Breeding Chain

TABLE 6-1

Results for UUTGDS.546 for Detailed Breeding Chain, BOC k_{eff} = 1.03

Cycle Days	0	136.5	273	409.5
K_{eff}	1.030	1.010	1.001	0.996
P_{max} (W/cc)	703	630	653	691
Fissile Mass (FM) [Kg]				
U-233	4051	3928	3921	3929
U-235	43	40	37	36
Pu-239		150	296	430
Pa-233		109	114	115
Np-239		4	4	4
(a) FM(409.5)-FM(136.5) [Kg]			(b)	(a)
(b) FM(273) - FM(0) [Kg]				
U-233			-130	+ 1
U-235			- 6	- 4
Pu-239			+296	+280
Pa-233			+114	+ 6
Np-239			+ 4	0
TOTAL			+278	+283
U-233			-130	+ 1
Pa-233			+114	+ 6
TOTAL			- 16	+ 7

TABLE 6-2

Results for UUTGDS.546 for Simple Breeding Chain, BOC k_{eff} = 1.03

Cycle Days	0	136.5	273	409.5
K_{eff}	1.030	1.018	1.011	1.006
P_{max} (W/cc)	703	628	664	702
Fissile Mass (FM) [Kg]				
U-233	4051	4034	4028	4030
U-235	43	39	36	33
Pu-239		154	298	430
(a) FM(409.5)-FM(136.5) [Kg]			(b)	(a)
(b) FM(273) - FM(0) [Kg]				
U-233			- 23	- 4
U-235			- 7	- 6
Pu-239			+298	+276
TOTAL			+268	+266

chain (which includes only Th-232 and U-233 in the thorium chain, and U-238 and isotopes 239-242 of plutonium in the U/Pu chain) seems to indicate that for the former case the U-233 production is higher! However, this is not a fair comparison, for while both these cases had the same initial k_{eff}, the EOC k_{eff} value is lower for the former case. As discussed in section 4., cases should be compared for the same minimum k_{eff} during the cycle.

Table 6-3 gives results for the detailed breeding chain, with the BOC k_{eff} increased by enrichment so that the EOC k_{eff} is approximately the same as for the case with the short chain. These results indicate that, as expected, there is slightly less U-233 production for the former case. For the quasi-equilibrium cycle, the difference between the EOC and BOC total Pa-233 and U-233 mass is -7 kg for the former case and -4 kg for the latter case. Pu-239 production is practically unchanged, while the U-235 burnup is less for the detailed chain, so that for the two cases the total fissile production is practically unchanged (264 kg and 266 kg for the detailed and simple breeding chain, respectively). These differences are slightly larger for the initial cycle (0 to 273 days), which has almost an identical k_{eff} for the two cases at EOC.

To check on the influence of elements in the detailed breeding chain other than the Pa-233 "loop" (the components of the triangle in Fig. 6-1, with U-232, Pa-233 and U-234 in its corners), a calculation was performed with this loop added to the simple chain. The results for this case, given in Table 6-4, are almost identical with those of the detailed chain in Table 6-1, indicating that the inclusion of the

TABLE 6-3

Results for UUTGDS.546 for Detailed Breeding Chain, BOC k_{eff} = 1.04

Cycle Days	0	136.5	273	409.5
K_{eff}	1.040	1.019	1.010	1.003
P_{max} (W/cc)	701	631	652	688
Fissile Mass (FM) [kg]				
U-233	4128	4000	3986	3987
U-235	43	39	37	36
Pu-239		147	290	421
Pa-233		107	113	113
Np-239		4	4	4
(a) FM(409.5)-FM(136.5) [Kg]			(b)	(a)
(b) FM(273) - FM(0) [Kg]				
U-233			-142	- 13
U-235			- 6	- 3
Pu-239			+290	+274
Pa-233			+113	+ 6
Np-239			+ 4	0
TOTAL			+259	+264
U-233			-142	- 13
Pa-233			+113	+ 6
TOTAL			- 29	- 7

TABLE 6-4

Results for UUTGDS.546 for Simple Breeding Chain + Loop for Pa-233, BOC k_{eff} = 1.03

Cycle Days	0	136.5	273	409.5
K_{eff}	1.030	1.010	1.001	0.996
P_{max} (W/cc)	703	629	654	691
Fissile Mass (FM) [Kg]				
U-233	4051	3928	3921	3929
U-235	43	39	36	33
Pu-239		154	300	434
Pa-233		109	114	115
(a) FM(409.5)-FM(136.5) [Kg]			(b)	(a)
(b) FM(273) - FM(0) [Kg]				
U-233			-130	+ 1
U-235			- 7	- 6
Pu-239			+300	+280
Pa-233			+114	+ 6
TOTAL			+277	+281
U-233			-130	+ 1
Pa-233			+114	+ 6
TOTAL			- 16	+ 7

elements not in the loop is not significant for the overall fissile production.

At the end of cycle for the case with the detailed breeding chain, the relative decay and capture rates of Pa-233 were 0.712 and 0.004, respectively. Thus Pa-233 capture should have only a small influence on the U-233 production results.

6.4 GE Model From LHRFDS Study

For the Proliferation-Resistant LMFBR Core Design Studies (PRLCDS) [21], the GE heterogeneous level II design [33] of the Large Heterogenous Reference Fuel Design Study (LHRFDS) [14] was chosen as the reference $(U/Pu)O_2$ design. The PRLCDS guidelines state that this reference design shall be updated only if necessary. Given the present interest in this model, we have initiated calculations using it as our base design.

The GE report [33] gives a description of their design, and we have used the r-z model described therein for our calculations. From the data given in this reference [33], we were unable to derive consistent values for the atom densities in the various regions. Since the fuel pins used in this model are those of the CRBR, we used the CRBR region densities given in Ref. [35] for our preliminary calculations, changing only the fuel enrichment to obtain criticality. Our calculations should not reproduce the GE results precisely, since GE used slightly larger fuel elements than for CRBR (271 vs. 217 pins/element) and fertile pins smaller than those of CRBR. However, our preliminary calculations are adequate to investigate the general characteristics of the GE model.

Results for our calculations of this model are given in Table 6-5, and Figs. 6-2 and 6-3. The GE report [33] does not define the time in the cycle for which the performance indices are quoted, but assuming their breeding ratio value of 1.336 is for the middle of the equilibrium cycle, our value of 1.348 for the middle of the quasi-equilibrium cycle is in good agreement. Figure 6-3 presents the radial layout of the various core regions for this model, and allows a comparison of the radial linear power profile for our results and those of GE. Due to the approximations in our model discussed above, we would not expect precise agreement, but the general behavior of the curves is approximately the same for the two cases, with the GE power distribution being somewhat flatter than for our case.

The breeding ratio for the GE model is about 0.10 smaller than the results for our PUUG cases in section 4 of Appendix I. The fissile loading for the GE LHRFDS model is also somewhat higher than the latter cases. Thus, the 16.7 year doubling time of the GE model [33] is somewhat higher than the values given in Table 4.4 for our models. The principal reason for this difference is probably the fact that for the LHRFDS use of CRBR fuel pins was required. The base model we used [13] had somewhat larger fuel pins and a larger fuel volume fraction than for the CRBR. Various studies have indicated that the minimum doubling time for a heterogeneous core is obtained with a fuel pin somewhat larger than that of the CRBR.

Studies of this model are continuing for various alternative fuel cycles.

Table 6-5 . Results for GE PUU Heterogeneous Model from LHRFDS [33] .

CYCLE DAYS	0	136.5	273	409.5
K_{eff}	1.007	1.010	1.013	1.015
Breeding Ratio	1.408	1.389	1.348	1.294
Pmax (W/cc)	672	692	693	684
Fissile Mass (FM) [kg]				
Pu-239	4472	4756	5007	5230
Pu-241	677	614	562	518
U-235	327	305	286	269
(a) FM(409.5)-FM(136.5) [kg]			(b)	(a)
(b) FM(273)-FM(0) [kg]				
Pu-239			+535	+474
Pu-241			-115	- 96
U-235			- 41	- 36
Total			+379	+342

Figure 6-2 . Power Distribution for GE Heterogeneous PUU Model from LHRFDS [33].

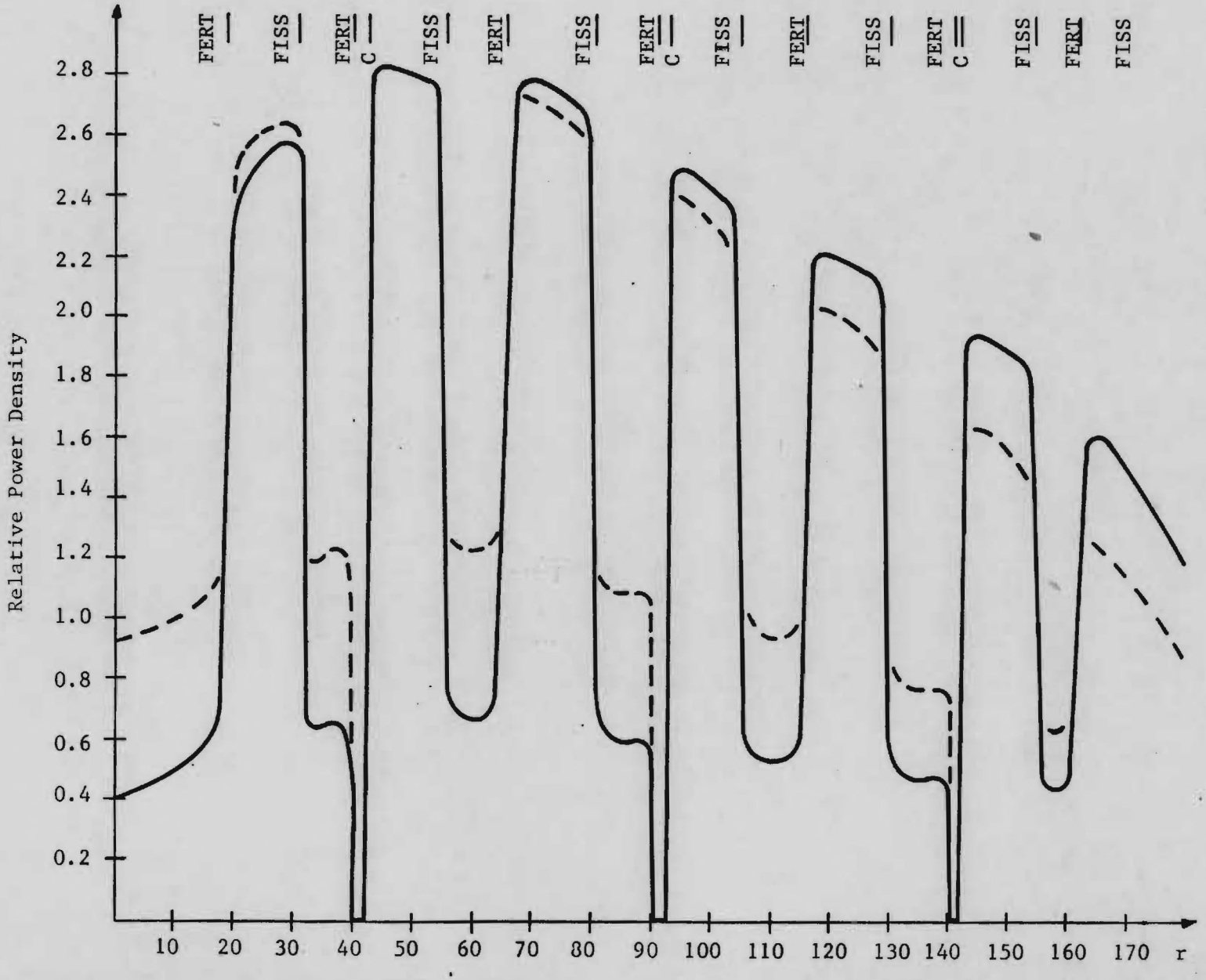

Fig. 6-3. Radial Linear Power Profile (Core Midplane) for GE Heterogeneous PUU Model from LHRFDS [33].

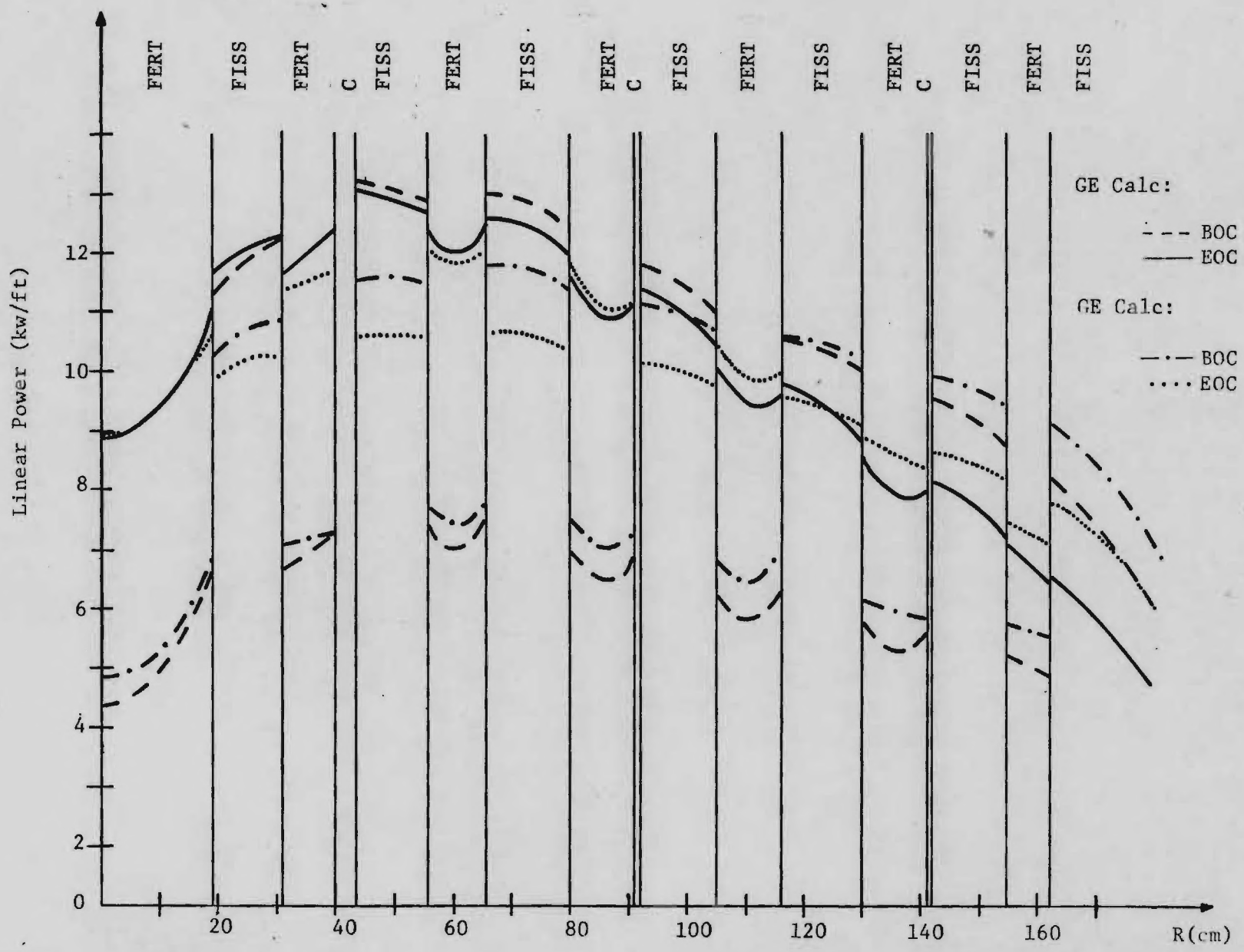

References

1. J. Kallfelz, letter to F. Mynatt and D. Bartine "Tasks under ORNL Subcontract 3986," 11 February 1977.

2. J. Kallfelz, "ORNL Project Report," attachment to agenda for meeting with T. Burns at Georgia Tech, 8 March 1977.

3. J. Kallfelz, letter to D. Bartine and T. Burns "Comments Related to ORNL Subcontract Work," 22 April 1977.

4. J. Kallfelz, "ORNL Progress Report," attachment to agenda for meeting with D. Bartine at Georgia Tech, 5-6 May 78.

5. J. Kallfelz, letter to D. Bartine and T. Burns,"Investigators Under Subcontract 3986," 21 June 1977.

6. D. Rowland, letter to T. Burns, "Investigations Under Subcontract 3986" 22 July 1977.

7. G. B. Bruna, G. P. Cecchini, G. Gastaldo, J. M. Kallfelz, G. Palmiotti, M. Salvatores, D. Rowland, D. Bartine, T. Burns, "Studies of the Heterogeneous LMFBR Core Concept for Several Fuel Cycles and Its Sensitivity to Design and Cross-Section Changes," Trans. Am. Nucl. Soc., 26, 558 (June 1977).

8. D. E. Bartine, T. J. Burns, J. R. White, J. M. Kallfelz and D. M. Rowland, "Alternative Fuel Cycles for Breeder Reactors," Proceedings of the International Conference on Alternative Energy Sources, Miami, December 1977.

9. G. Bruna, J. M. Kallfelz and G. Palmiotti, "Advances in the Heterogeneous Core Concept," NIRA External Report T-NA-E-10004-F, Nucleare Italiana Reattori Avanzati, Genoa (1976).

10. G. Bruna, J. M. Kallfelz and G. Palmiotti, "Ricerca di un Modello Alternativo di Core per il Miglioramento del Tempo di Raddoppio di un Reattore Veloce di Potenza da 1200 Mwt. Elettrici," ("Investigation of an Alternative Core Model for Improvement of the Doubling Time for a 1200 MWe LMFBR"), NIRA External Report SEC I-01-7, Nucleare Italiana Reattori Avanzati, Genova (February 1976).

11. G. B. Bruna, G. P. Cecchini, J. M. Kallfelz, G. Palmiotti, and M. Salvatores, "Studies of the Heterogeneous LMFBR Core Concept and Its Sensitivity to Design and Cross Sections Variations," NIRA Report, T-NA-E-344047-F, Nucleare Italiana Reattori Avanzati, Genoa, Italy (1977).

12. J. C. Mougniot, J. Y. Barre, P. Clauzon, D. Giancometti, G. Neviere, J. Ravier and B. Sicard, "Gains de Regeneration des Reacteurs Rapides a Combustible Oxyde et a Refrigerant Sodium," Nuclear Energy Maturity, Proceedings of the Paris Conference. Progress in Nuclear Energy Series 1976. Pergamon Press, Oxford and New York.

13. Letter from Edouard Kujawski, Fast Breeder Reactor Department, General Electric, to Members of the Large Core Code Evaluation Working Group, SUBJECT: Transmittal of Design for Use in Large Core Code Evaluation, (January 29, 1976).

14. "Ground Rules, Large Heterogeneous Reference Fuel Design Study," Combustion Engineering, Inc., Windsor, Conn. (October 22, 1976).

15. T. G. Ayers, M.T. Benedict, F. L. Culler, Jr., J. L. Everett, III, R. V. Laney, C. D. Perkins, C. Starr, C. Walske, "LMFBR Program Review by the Following Members of the LMFBR Review Steering Committee." See Addendum to Vol. II, "Addendum to the Report of the Task Force - Role of the CRBRP. Alternative Plan," Energy Research and Development Administration (April 6, 1977).

16. B. R. Sehgal, J. A. Naser, C. L. Lin and W. Loewenstein, "Thorium-Based Fuels in Fast Breeder Reactors," Nucl Tech 35, 635, October 1977.

17. Private communication, meeting at WARD with P. Dickson, R. Doncals, T. Paxson, R. Markley, R. Vijuk, G. Paik, J. Lake and G. Calame, 2 May 1977.

18. W. P. Barthold and C. P. Tzanos, "Performance Potential of Reference Fuel in 1200 MWE LMFBRs," FRA-TM-104, Argonne National Laboratory, Nov. 15, 1977. (Report of ANL results for LHRFDS [14])

19. J. C. Chandler et al., "Large Heterogeneous Reference Fuel Design Study-Final Report," Hanford Engineering Development Laboratory, May 1977.

20. Y. I. Chang et al., "Alternative Fuel Cycle Options: Performance Characteristics and Impact on Nuclear Power Growth Potential", ANL-77-70, Argonne National Laboratory, September 1977.

21. C. E. Weber (RDD/TA), telex to F. Mynatt, Subject: "Proliferation-Resistant LMFBR Core Design Studies," September 21, 1977.

22. G. F. Flanagan, Memo to T. E. Cole and H. F. Bauman, Subject: "Revised Reactor Design Characteristics for Use by Burns and Roe for Fuel Center Calculations," with enclosures (December 14, 1977).

23. D. Selby, private communication, March 1978.

24. C. R. Weisbin, P. D. Soran, R. E. MacFarlane, D. R. Harris, R. J. LaBauve, J. S. Hendricks, J. E. White and R. B. Kidman, "MINX: a Multigroup Interpretation of Nuclear X-Sections from ENDF/B," LA-6488-MS (ENDF-237) Los Alamos Scientific Laboratory (September 1976).

25. N. C. Paik, et al, "Physics Evaluations and Applications Quarterly Progress Report for Period Ending July 31, 1974," WARD-XS-3042-7, Westinghouse Advanced Reactors Div. (July 1974).

26. N. M. Greene, J. L. Lucius, L. M. Petrie, W. E. Ford, III, J. E. White and R. Q. Wright, "AMPX: A Modular Code System for Generating Coupled Multigroup Neutron-Gamma Libraries from ENDF/B," ORNL-TM-3706, Oak Ridge National Laboratory (March 1976).

27. I. I. Bondarenko (Ed.), "Group Constants for Nuclear Reactor Calculations," Consultants Bureau, New York (1964).

28. J. M. Kallfelz and O. W. Hermann, "Bondarenko Cross-Section Set for Reactor Calculations," ORNL internal memo, ORNL Central Files Number 73-12-13 (December 14, 1973).

29. T. B. Fowler, D. R. Vondy and G. W. Cunningham, "Nuclear Reactor Core Analysis Code: CITATION," ORNL-TM-2496, Rev. 2, Oak Ridge National Laboratory (July 1971).

30. I. Dal Bono, "TAIM: Multigroup One-Dimensional Diffusion Code," CNEN Doc. CEC.(66)-12, Comitato Nazionale per l'Energia Nucleare, Bologna (1966).

31. I. Dal Bono, V. Leproni and M. Salvatores, "The CIAP-1D Code," RT/FI (68)9, Comitato Nazionale Energia Nucleare, Rome (1968).

32. G. B. Bruna, G. P. Cecchini, G. Gastaldo, J. M. Kallfelz, G. Palmiotti, M. Salvatores, D. Rowland, D. Bartine, T. Burns, "Studies of the Heterogeneous LMFBR Core Concept for Several Fuel Cycles and Its Sensitivity to Design and Cross-Section Changes," Trans. Am. Nucl. Soc., 26, 558 (June 1977).

33. D. P. Johnson, "Large Heterogeneous Reference Fuel Design Study," GEFR 00110 (L), General Electric Fast Breeder Reactor Department, Sunnyvale, Calif. (May 1977).

34. B. Sicard, J. C. Mougniot et al., "Preliminary Physics Studies of a Large Fast Core Based on the Heterogeneous Concept," Trans. Am. Nucl. Soc. 26, 553 (1977).

35. J. Lake, "LMFBR Nuclear Analytical Model," WARD Internal Memo LRA-73-251, August 17, 1973.

APPENDIX I.

Summary of significant parameters for heterogeneous reactor models.

Tabulated results for the various runs are ordered as follows:

Runs are numbered "NL", where

N = number, same for a general reactor type.
L = letter, designating variations within the type.

N = 1 PUU reactors [$(Pu/U)O_2$ fissile regions, UO_2 fertile] based on NIRA models [11].

N = 2 PUT reactors [$(Pu/U)O_2$ fissile regions, ThO_2 fertile] based on NIRA models [11].

N = 3 PTT reactors [$(Pu/Th)O_2$ fissile regions, ThO_2 fertile] based on NIRA models [11].

N = 4 PUU reactors based on GE model [13].

N = 5 PUT reactors based on GE model [13].

N = 6 PTT reactors based on GE model [13].

N = 7 UUT denatured reactors [$(U^{233}/U^{238})O_2$ or $(U^{233}/U^{238}/Th)O_2$ fissile regions, ThO_2 fertile regions] based on GE model.

HETEROGENEOUS CORE PERFORMANCE PARAMETERS
ORNL/GA. TECH LMFBR ALTERNATIVE FUEL CYCLE STUDIES

RUN NO. 1A MODEL DESIGNATION PUU1SS.372

CONDENSED DESCRIPTION: Based on NIRA Model 1 [4, 11]. (Axial blanket in core fertile regions). LWR Pu, no control. $(Pu/U)O_2$ fissile, UO_2 fertile. 5-group σ set, stainless steel corrected [4, 5].

Cycle Days	0	150	300	450
k_{eff}	1.042	1.020	1.002	0.986
Breeding Ratio	1.297	1.300	1.305	1.307
Pmax (w/cc)	800	793	789	782
Fissile Mass (FM) [kg]				
Pu-239	2689	2886	3076	3258
Pu-241	405	354	313	281
U-233				
U-235	21	20	19	18
(a) FM(450)-FM(150) [kg]			(b)	(a)
(b) FM(t)-FM(0) [kg.]				
Pu-239			+387	+372
Pu-241			- 92	- 73
U-233				
U-235			- 2	- 2
Total			+293	+297
Capture Rates [sec^{-1}]				
Th-232				
U-238	.379			
Pu-240	.016			

HETEROGENEOUS CORE PERFORMANCE PARAMETERS
ORNL/GA. TECH LMFBR ALTERNATIVE FUEL CYCLE STUDIES

RUN NO. 1B MODEL DESIGNATION PUU2SS.372

CONDENSED DESCRIPTION: Based on NIRA Model 2 [4, 11]. (Radial blanket in core fertile regions). LWR Pu, no control. $(Pu/U)O_2$ fissile, UO_2 fertile. 5-group σ-set, stainless steel corrected [4, 5].

Cycle Days	0	150	300	450
k_{eff}	1.033	1.014	1.000	0.988
Breeding Ratio	1.376	1.378	1.378	1.370
Pmax (w/cc)	736	738	733	736
Fissile Mass (FM) [kg]				
Pu-239	2809	3041	3265	3478
Pu-241	423	372	330	298
U-233				
U-235	22	21	20	19
(a) FM(450)-FM(150) [kg]			(b)	(a)
(b) FM(t)-FM(0) [kg]				
Pu-239			+456	+437
Pu-241			- 93	- 74
U-233				
U-235			- 2	- 2
Total			+361	+361
Capture Rates [sec^{-1}]				
Th-232				
U-238	.395			
Pu-240	.015			

HETEROGENEOUS CORE PERFORMANCE PARAMETERS
ORNL/GA. TECH LMFBR ALTERNATIVE FUEL CYCLE STUDIES

RUN NO. 2A MODEL DESIGNATION PUTT1SS.372

CONDENSED DESCRIPTION: Based on NIRA Model 1 [4, 11]. (Axial blanket in core fertile regions). LWR Pu, no control. $(Pu/U)O_2$ fissile, ThO_2 fertile. 5-group σ-set, stainless steel corrected [4, 5].

Cycle Days	0	150	300	450
k_{eff}	1.032	1.015	1.001	0.989
Breeding Ratio	1.292	1.290	1.286	1.277
Pmax (w/cc)	835	822	817	804
Fissile Mass (FM) [kg]				
Pu-239	2824	2647	2489	2350
Pu-241	425	371	329	394
U-233	0	361	689	988
U-235	25	22	19	16
(a) FM(450)-FM(150) [kg]			(b)	(a)
(b) FM(t)-FM(0) [kg]				
Pu-239			-335	-297
Pu-241			- 96	- 77
U-233			+689	-627
U-235			- 6	- 6
Total			+252	+247
Capture Rates [sec^{-1}]				
Th-232	.246			
U-238	.140			
Pu-240	.016			

HETEROGENEOUS CORE PERFORMANCE PARAMETERS
ORNL/GA. TECH LMFBR ALTERNATIVE FUEL CYCLE STUDIES

RUN NO. 2B MODEL DESIGNATION PUT2SS.372

CONDENSED DESCRIPTION: Based on NIRA Model 2 [4, 11]. (Radial blanket in core fertile regions). LWR Pu, no control. $(Pu/U)O_2$ fissile, ThO_2 fertile. 5-group σ-set, stainless steel corrected [4, 5].[2]

Cycle Days	0	150	300	450
k_{eff}	1.027	1.011	1.000	0.991
Breeding Ratio	1.352	1.350	1.344	1.326
Pmax (w/cc)	754	761	755	751
Fissile Mass (FM) [kg]				
Pu-239	3001	2808	2636	2484
Pu-241	452	397	353	318
U-233	0	404	774	1111
U-235	25	22	19	16
(a) FM(450)-FM(150) [kg]			(b)	(a)
(b) FM(t)-FM(0) [kg]				
Pu-239			-365	-324
Pu-241			- 99	- 79
U-233			+774	+707
U-235			- 6	- 6
Total			+304	+298
Capture Rates [sec^{-1}]				
Th-232	.274			
U-238	.127			
Pu-240	.016			

HETEROGENEOUS CORE PERFORMANCE PARAMETERS
ORNL/GA. TECH LMFBR ALTERNATIVE FUEL CYCLE STUDIES

RUN NO. 3A MODEL DESIGNATION PTT1SS.372

CONDENSED DESCRIPTION: Based on NIRA Model 1. [4, 11]. (Axial blanket in core fertile regions). LWR Pu, no control. $(Pu/Th)O_2$ fissile, UO_2 fertile. 5-group σ-set, stainless steel corrected [4, 5].

Cycle Days	0	150	300	450
k_{eff}	1.023	1.013	1.003	0.993
Breeding Ratio	1.230	1.221	1.209	1.195
Pmax (w/cc)	846	837	827	811
Fissile Mass (FM) [kg]				
Pu-239	3067	2658	2308	2008
Pu-241	462	404	358	321
U-233	0	561	1046	1468
U-235				
(a) FM(450)-FM(150) [kg]			(b)	(a)
(b) FM(t)-FM(0) [kg]				
Pu-239			-759	-650
Pu-241			-104	- 83
U-233			+1046	+907
U-235				
Total			+183	+174
Capture Rates [sec^{-1}]				
Th-232	.388			
U-238	0			
Pu-240	.016			

HETEROGENEOUS CORE PERFORMANCE PARAMETERS
ORNL/GA. TECH LMFBR ALTERNATIVE FUEL CYCLE STUDIES

RUN NO. 3B MODEL DESIGNATION PTT2SS.372

CONDENSED DESCRIPTION: Based on NIRA Model 2 [4, 11]. (Radial blanket in core fertile regions). LWR Pu, no control. $(Pu/Th)O_2$ fissile, UO_2 fertile. 5-group σ-set, stainless steel corrected [4, 5].

Cycle Days	0	150	300	450
k_{eff}	1.018	1.008	1.001	0.994
Breeding Ratio	1.291	1.282	1.267	1.245
Pmax (w/cc)	769	771	762	761
Fissile Mass (FM) [kg]				
Pu-239	3247	2840	2489	2185
Pu-241	489	430	383	345
U-233	0	589	1105	1557
U-235				
(a) FM(450)-FM(150) [kg]				
(b) FM(t)-FM(0) [kg]				
Pu-239			-758	-655
Pu-241			-106	- 85
U-233			+1105	+968
U-235				
Total			+241	+228
Capture Rates [sec^{-1}]				
Th-232	.401			
U-238	0			
Pu-240	.016			

HETEROGENEOUS CORE PERFORMANCE PARAMETERS
ORNL/GA. TECH LMFBR ALTERNATIVE FUEL CYCLE STUDIES

RUN NO. 4A MODEL DESIGNATION PUUGXS.273

CONDENSED DESCRIPTION: Standard GE LMFBR model using Pu drivers and fertile U in the driver, fertile, and blanket regions. Isotope search (Pu vs. U) for K = 1.03, followed by 273 day burnup.

Cycle Days	0	91	182	273
k_{eff}	1.030	1.029	1.0281	1.0282
Breeding Ratio	1.445	1.436	1.417	1.387
Pmax (w/cc)	514	508	525	539
Fissile Mass (FM) [kg]				
Pu-239	3781	3944	4099	4245
Pu-241	574	538	507	478
U-233				
U-235	254	245	237	229
FM(t)-FM(0) [kg]				
Pu-239				+464
Pu-241				- 96
U-233				
U-235				- 25
Total				+343
Capture Rates [sec^{-1}]				
Th-232				
U-238	.496			
Pu-240	.0181			

HETEROGENEOUS CORE PERFORMANCE PARAMETERS
ORNL/GA. TECH LMFBR ALTERNATIVE FUEL CYCLE STUDIES

RUN NO. 4B MODEL DESIGNATION PUUGAS.273

CONDENSED DESCRIPTION: Same as Run 4A, but the widths of all fissile regions are reduced by 10%. Fertile region widths are increased by a corresponding amount to maintain overall reactor dimensions.

Cycle Days	0	91	182	273
k_{eff}	1.030	1.027	1.025	1.024
Breeding Ratio	1.468	1.460	1.444	1.417
Pmax (w/cc)	609	556	526	548
Fissile Mass (FM) [kg]				
Pu-239	3769	3939	4101	4255
Pu-241	572	537	505	476
U-233				
U-235	260	251	242	235
FM(t)-FM(0) [kg]				
Pu-239				+486
Pu-241				- 96
U-233				
U-235				- 25
Total				+365
Capture Rates [sec^{-1}]				
Th-232				
U-238	.501			
Pu-240	.0177			

HETEROGENEOUS CORE PERFORMANCE PARAMETERS
ORNL/GA. TECH LMFBR ALTERNATIVE FUEL CYCLE STUDIES

RUN NO. 4C MODEL DESIGNATION PUUGBS.273

CONDENSED DESCRIPTION: Same as Run 4A, but the widths of all fissile regions are reduced by 25%. Fertile region widths are increased by a corresponding amount to maintain overall reactor dimensions.

Cycle Days	0	91	182	273
k_{eff}	1.030	1.022	1.017	1.013
Breeding Ratio	1.505	1.499	1.492	1.475
Pmax (w/cc)	812	739	666	597
Fissile Mass (FM) [kg]				
Pu-239	3706	3885	4059	4227
Pu-241	562	527	496	467
U-233				
U-235	269	260	251	243
FM(t)-FM(0) [kg]				
Pu-239				+521
Pu-241				- 95
U-233				
U-235				- 26
Total				+400
Capture Rates [sec^{-1}]				
Th-232				
U-238	.508			
Pu-240	.017			

HETEROGENEOUS CORE PERFORMANCE PARAMETERS
ORNL/GA. TECH LMFBR ALTERNATIVE FUEL CYCLE STUDIES

RUN NO. 4D MODEL DESIGNATION PUUGCS.273

CONDENSED DESCRIPTION: Same as Run 4A, but the widths of all fissile regions are reduced by 16%. Fertile region widths are increased by a corresponding amount to maintain overall reactor dimensions.

Cycle Days	0	91	182	273
k_{eff}	1.030	1.025	1.022	1.020
Breeding Ratio	1.482	1.475	1.462	1.438
Pmax (w/cc)	682	620	562	551
Fissile Mass (FM) [kg]				
Pu-239	3750	3923	4090	4250
Pu-241	569	534	502	473
U-233				
U-235	264	254	246	238
FM(t)-FM(0) [kg]				
Pu-239				+500
Pu-241				- 96
U-233				
U-235				- 26
Total				+378
Capture Rates [sec^{-1}]				
Th-232				
U-238	.504			
Pu-240	.017			

HETEROGENEOUS CORE PERFORMANCE PARAMETERS
ORNL/GA. TECH LMFBR ALTERNATIVE FUEL CYCLE STUDIES

RUN NO. 4E MODEL DESIGNATION PUUGDS.273

CONDENSED DESCRIPTION: Same as Run 4A, but the widths of all fissile regions are reduced by 16% with corresponding increases in the fertile region widths. The outermost fissile ring is also reduced by an additional 5%.

Cycle Days	0	91	182	273
k_{eff}	1.030	1.0269	1.0253	1.0250
Breeding Ratio	1.484	1.475	1.456	1.425
Pmax (w/cc)	645	580	604	626
Fissile Mass (FM) [kg]				
Pu-239	3713	3886	4051	4208
Pu-241	564	528	497	468
U-233				
U-235	260	251	242	234
FM(t)-FM(0) [kg]				
Pu-239				+495
Pu-241				- 96
U-233				
U-235				- 26
Total				+373
Capture Rates [sec^{-1}]				
Th-232				
U-238	.504			
Pu-240	.0174			

HETEROGENEOUS CORE PERFORMANCE PARAMETERS
ORNL/GA. TECH LMFBR ALTERNATIVE FUEL CYCLE STUDIES

RUN NO. 4F MODEL DESIGNATION PUUGES.273

CONDENSED DESCRIPTION: Same as Run 4A, but the widths of all fissile regions are reduced by 16% with corresponding increases in the fertile region widths. The outermost fissile ring is also reduced by an additional 7%.

Cycle Days	0	91	182	273
k_{eff}	1.0300	1.0277	1.0268	1.0270
Breeding Ratio	1.485	1.4744	1.4536	1.4192
Pmax (w/cc)	627	613	638	664
Fissile Mass (FM) [kg]				
Pu-239	3695	3868	4033	4188
Pu-241	561	526	494	466
U-233				
U-235	259	250	241	233
FM(t)-FM(0) [kg]				
Pu-239				+493
Pu-241				- 95
U-233				
U-235				- 26
Total				+372
Capture Rates [sec^{-1}]				
Th-232				
U-238	.504			
Pu-240	.0174			

HETEROGENEOUS CORE PERFORMANCE PARAMETERS
ORNL/GA. TECH LMFBR ALTERNATIVE FUEL CYCLE STUDIES

RUN NO. 4G MODEL DESIGNATION PUUGYS.273

CONDENSED DESCRIPTION: Same as Run 4A, but the width of all fissile regions are reduced by 16% with corresponding increases in the fertile region widths. The outermost fissile ring is also reached by an additional 33%.

Cycle Days	0	91	182	273
k_{eff}	1.030	1.034	1.037	1.040
Breeding Ratio	1.489	1.468	1.428	1.379
Pmax (w/cc)	1181	1139	1098	1061
Fissile Mass (FM) [kg]				
Pu-239	3295	3467	3624	3768
Pu-241	500	466	436	409
U-233				
U-235	242	233	225	217
FM(t)-FM(0) [kg]				
Pu-239				+473
Pu-241				- 91
U-233				
U-235				- 25
Total				+357
Capture Rates [sec^{-1}]				
Th-232				
U-238	.506			
Pu-240	.018			

HETEROGENEOUS CORE PERFORMANCE PARAMETERS
ORNL/GA. TECH LMFBR ALTERNATIVE FUEL CYCLE STUDIES

RUN NO. 4H MODEL DESIGNATION PUUGDS.546

CONDENSED DESCRIPTION: Same as Run 4E (PUUGDS.273), except with 546 day burnup.

Cycle Days	0	136.5	273	409.5
k_{eff}	1.007	1.005	1.006	1.010
Breeding Ratio	1.546	1.527	1.491	1.430
Pmax (w/cc)	643	593	630	669
Fissile Mass (FM) [kg]				
Pu-239	3564	3846	4105	4341
Pu-241	541	490	447	411
U-233				
U-235	261	247	234	223
(a) FM(409.5)-FM(136.5) [kg]			(b)	(a)
(b) FM(t)-FM(0) [kg]				
Pu-239			+541	+495
Pu-241			- 94	- 79
U-233				
U-235			- 27	- 24
Total			+420	+392
Capture Rates [sec^{-1}]				
Th-232				
U-238	.513			
Pu-240	.017			

HETEROGENEOUS CORE PERFORMANCE PARAMETERS
ORNL/GA. TECH LMFBR ALTERNATIVE FUEL CYCLE STUDIES

RUN NO. 4I MODEL DESIGNATION PUUG1S.273

CONDENSED DESCRIPTION: Same as Run 4A, except that the width of the outermost fissile ring is reduced by 33%.

Cycle Days	0	91	182	273
k_{eff}	1.030	1.033	1.036	1.038
Breeding Ratio	1.452	1.434	1.399	1.356
Pmax (w/cc)	933	913	894	874
Fissile Mass (FM) [kg]				
Pu-239	3239	3402	3551	3688
Pu-241	492	457	427	401
U-233				
U-235	229	220	212	204
FM(t)-FM(0) [kg]				
Pu-239				+449
Pu-241				- 91
U-233				
U-235				- 25
Total				+333
Capture Rates [sec^{-1}]				
Th-232				
U-238	.50			
Pu-240	.018			

HETEROGENEOUS CORE PERFORMANCE PARAMETERS
ORNL/GA. TECH LMFBR ALTERNATIVE FUEL CYCLE STUDIES

RUN NO. 5A MODEL DESIGNATION PUTGXS.273

CONDENSED DESCRIPTION: Standard GE LMFBR model using Pu drivers, fertile U in the driver regions, and Th in all fertile/blanket regions. Isotope search (Pu vs. U) for K = 1.03, followed by 273 day burnup.

Cycle Days	0	91	182	273
k_{eff}	1.030	1.030	1.032	1.034
Breeding Ratio	1.435	1.422	1.399	1.363
Pmax (w/cc)	609	550	521	536
Fissile Mass (FM) [kg]				
Pu-239	4138	4060	3987	3918
Pu-241	628	591	557	526
U-233		230	447	649
U-235	58	55	51	48
FM(t)-FM(0) [kg]				
Pu-239				-220
Pu-241				-102
U-233				+649
U-235				- 10
Total				+317
Capture Rates [sec^{-1}]				
Th-232	.299			
U-238	.204			
Pu-240	.018			

HETEROGENEOUS CORE PERFORMANCE PARAMETERS
ORNL/GA. TECH LMFBR ALTERNATIVE FUEL CYCLE STUDIES

RUN NO. 5B MODEL DESIGNATION PUTG1S.273

CONDENSED DESCRIPTION: Same as Run 5A, except that the width of the outermost fissile ring is reduced by 33%.

Cycle Days	0	91	182	273
k_{eff}	1.030	1.039	1.047	1.052
Breeding Ratio	1.430	1.405	1.360	1.307
Pmax (w/cc)	1028	995	965	936
Fissile Mass (FM) [kg]				
Pu-239	3593	3502	3419	3341
Pu-241	546	509	476	448
U-233		240	456	651
U-235	46	43	40	37
FM(t)-FM(0) [kg]				
Pu-239				-252
Pu-241				- 98
U-233				+651
U-235				- 9
Total				+292
Capture Rates [sec^{-1}]				
Th-232	.316			
U-238	.189			
Pu-240	.018			

HETEROGENEOUS CORE PERFORMANCE PARAMETERS
ORNL/GA. TECH LMFBR ALTERNATIVE FUEL CYCLE STUDIES

RUN NO. 5C MODEL DESIGNATION PUTGAS.273

CONDENSED DESCRIPTION: Same as Run 5A, but the widths of all fissile regions are reduced by 10%. Fertile region widths are increased by a corresponding amount to maintain overall reactor dimensions.

Cycle Days	0	91	182	273
k_{eff}	1.030	1.028	1.027	
Breeding Ratio	1.451	1.440	1.422	1.401
Pmax (w/cc)	737	664	595	
Fissile Mass (FM) [kg]				
Pu-239	4127	4029	3936	3848
Pu-241	627	589	555	524
U-233		256	498	725
U-235	51	48	45	42
FM(t)-FM(0) [kg]				
Pu-239				-279
Pu-241				-103
U-233				+725
U-235				- 9
Total				+334
Capture Rates [sec^{-1}]				
Th-232	.331			
U-238	.176			
Pu-240	.018			

HETEROGENEOUS CORE PERFORMANCE PARAMETERS
ORNL/GA. TECH LMFBR ALTERNATIVE FUEL CYCLE STUDIES

RUN NO. 5D MODEL DESIGNATION PUTGBS.273

CONDENSED DESCRIPTION: Same as Run 5A, but the widths of all fissile regions are reduced by 25%. Fertile region widths are increased by a corresponding amount to maintain overall reactor dimensions.

Cycle Days	0	91	182	273
k_{eff}	1.030	1.023	1.017	
Breeding Ratio	1.478	1.469	1.461	1.448
Pmax (w/cc)	986	893	800	
Fissile Mass (FM) [kg]				
Pu-239	4060	3931	3810	3697
Pu-241	616	579	544	513
U-233		292	571	836
U-235	40	38	35	33
FM(t)-FM(0) [kg]				
Pu-239				-363
Pu-241				-103
U-233				+836
U-235				- 7
Total				+363
Capture Rates [sec^{-1}]				
Th-232	.377			
U-238	.138			
Pu-240	.017			

HETEROGENEOUS CORE PERFORMANCE PARAMETERS
ORNL/GA. TECH LMFBR ALTERNATIVE FUEL CYCLE STUDIES

RUN NO. 5E MODEL DESIGNATION PUTGCS.273

CONDENSED DESCRIPTION: Same as Run 5A, but the widths of all fissile regions are reduced by 10% with corresponding increases in the fertile region widths. The outermost fissile ring is also reduced by an additional 5%.

Cycle Days	0	91	182	273
k_{eff}	1.030	1.030	1.031	1.033
Breeding Ratio	1.4506	1.4369	1.413	1.373
Pmax (w/cc)	702	622	588	611
Fissile Mass (FM) [kg]				
Pu-239	4094	3991	3895	3805
Pu-241	622	584	550	519
U-233		259	502	728
U-235	49	46	43	41
FM(t)-FM(0) [kg]				
Pu-239				-289
Pu-241				-103
U-233				+728
U-235				- 8
Total				+328
Capture Rates [sec^{-1}]				
Th-232	.336			
U-238	.172			
Pu-240	.018			

HETEROGENEOUS CORE PERFORMANCE PARAMETERS
ORNL/GA. TECH LMFBR ALTERNATIVE FUEL CYCLE STUDIES

RUN NO. 5F MODEL DESIGNATION PUTGCS.546

CONDENSED DESCRIPTION: Same as Run 5E (PUTGCS.273), except with 546 day burnup.

Cycle Days	0	136.5	273	409.5
k_{eff}	0.995	0.999	1.005	1.013
Breeding Ratio	1.542	1.514	1.464	1.387
Pmax (w/cc)	704	580	615	650
Fissile Mass (FM) [kg]				
Pu-239	3855	3720	3599	3490
Pu-241	585	531	485	447
U-233		402	763	1083
U-235	50	45	41	37
(a) FM(409.5)-FM(136.5) [kg]			(b)	(a)
(b) FM(t)-FM(0) [kg]				
Pu-239			-256	-230
Pu-241			-100	- 84
U-233			+763	+681
U-235			- 9	- 8
Total			+398	+359
Capture Rates [sec^{-1}]				
Th-232	0.342			
U-238	0.179			
Pu-240	0.017			

HETEROGENEOUS CORE PERFORMANCE PARAMETERS
ORNL/GA. TECH LMFBR ALTERNATIVE FUEL CYCLE STUDIES

RUN NO. 5G MODEL DESIGNATION PUTGCS.546

CONDENSED DESCRIPTION: Same as Run 5F (PUTGCS.273), except that error in the uranium concentration in the fuel is corrected. (see note, p. 4-8.)

Cycle Days	0	136.5	273	409.5
k_{eff}	0.995	0.998	1.004	1.011
Breeding Ratio	1.516	1.489	1.441	1.366
Pmax (w/cc)	690	581	617	651
Fissile Mass (FM) [kg]				
Pu-239	3788	3633	3493	3368
Pu-241	575	521	475	437
U-233		414	784	1112
U-235	44	40	36	33
(a) FM(409.5)-FM(136.5) [kg]			(b)	(a)
(b) FM(t)-FM(0) [kg]				
Pu-239			-295	-265
Pu-241			-100	- 84
U-233			+784	+698
U-235			- 8	- 7
Total			+381	+342
Capture Rates [sec^{-1}]				
Th-232	0.353			
U-238	0.165			
Pu-240	0.018			

HETEROGENEOUS CORE PERFORMANCE PARAMETERS
ORNL/GA. TECH LMFBR ALTERNATIVE FUEL CYCLE STUDIES

RUN NO. 6A MODEL DESIGNATION PTTGXS.273

CONDENSED DESCRIPTION: Standard GE LMFBR model using Pu drivers and Th in the driver, fertile and blanket regions. Isotope search (Pu vs. Th) for K = 1.03, followed by 273 day burnup.

Cycle Days	0	91	182	273
k_{eff}	1.030	1.033	1.037	1.040
Breeding Ratio	1.306	1.293	1.270	1.235
Pmax (w/cc)	566	528	536	551
Fissile Mass (FM) [kg]				
Pu-239	4572	4010	4067	3843
Pu-241	694	653	615	582
U-233		380	730	1052
U-235				
FM(t)-FM(0) [kg]				
Pu-239				-729
Pu-241				-112
U-233				+1052
U-235				
Total				+ 211
Capture Rates [sec^{-1}]				
Th-232	.495			
U-238				
Pu-240	.020			

HETEROGENEOUS CORE PERFORMANCE PARAMETERS
ORNL/GA. TECH LMFBR ALTERNATIVE FUEL CYCLE STUDIES

RUN NO. 6B MODEL DESIGNATION PTTG1S.273

CONDENSED DESCRIPTION: Same as Run 6A, except that the width of the outermost fissile ring is reduced by 33%.

Cycle Days	0	91	182	273
k_{eff}	1.030	1.041	1.049	1.055
Breeding Ratio	1.310	1.287	1.247	1.200
Pmax (w/cc)	1003	969	940	912
Fissile Mass (FM) [kg]				
Pu-239	3929	3667	3434	3216
Pu-241	597	556	521	490
U-233		378	714	1015
U-235				
FM(t)-FM(0) [kg]				
Pu-239				-713
Pu-241				-107
U-233				+1015
U-235				
Total				+ 195
Capture Rates [sec^{-1}]				
Th-232	.498			
U-238				
Pu-240	.020			

HETEROGENEOUS CORE PERFORMANCE PARAMETERS
ORNL/GA. TECH LMFBR ALTERNATIVE FUEL CYCLE STUDIES

RUN NO. 6C MODEL DESIGNATION PTTGAS.273

CONDENSED DESCRIPTION: Same as Run 6A, but the widths of all fissile regions are reduced by 10%. Fertile region widths are increased by a corresponding amount to maintain overall dimensions.

Cycle Days	0	91	182	273
k_{eff}	1.030	1.030	1.031	1.033
Breeding Ratio	1.331	1.319	1.300	1.269
Pmax (w/cc)	684	612	552	558
Fissile Mass (FM) [kg]				
Pu-239	4538	4278	4037	3813
Pu-241	689	648	610	577
U-233		386	743	1074
U-235				
FM(t)-FM(0) [kg]				
Pu-239				-725
Pu-241				-112
U-233				+1074
U-235				
Total				+ 237
Capture Rates [sec^{-1}]				
Th-232	.501			
U-238				
Pu-240	.019			

HETEROGENEOUS CORE PERFORMANCE PARAMETERS
ORNL/GA. TECH LMFBR ALTERNATIVE FUEL CYCLE STUDIES

RUN NO. 6D MODEL DESIGNATION PTTGBS.273

CONDENSED DESCRIPTION: Same as Run 6A, but the widths of all fissile regions are reduced by 25%. Fertile region widths are increased by a corresponding amount to maintain overall reactor dimensions.

Cycle Days	0	91	182	273
k_{eff}	1.030	1.024	1.021	
Breeding Ratio	1.371	1.361	1.351	1.337
Pmax (w/cc)	925	830	739	
Fissile Mass (FM) [kg]				
Pu-239	4424	4167	3927	3705
Pu-241	672	631	594	560
U-233		394	764	1110
U-235				
FM(t)-FM(0) [kg]				
Pu-239				-719
Pu-241				-112
U-233				+1110
U-235				
Total				+ 279
Capture Rates [sec^{-1}]				
Th-232	.509			
U-238				
Pu-240	.018			

HETEROGENEOUS CORE PERFORMANCE PARAMETERS
ORNL/GA. TECH LMFBR ALTERNATIVE FUEL CYCLE STUDIES

RUN NO. 6E MODEL DESIGNATION PTTGCS.273

CONDENSED DESCRIPTION: Same as Run 6A, but the widths of all fissile regions are reduced by 10% with corresponding increases in the fertile region widths. The outermost fissile ring is also reduced by an additional 5%.

Cycle Days	0	91	182	273
k_{eff}	1.030	1.032	1.0355	1.0389
Breeding Ratio	1.3325	1.3186	1.2940	1.2568
Pmax (w/cc)	650	586	610	628
Fissile Mass (FM) [kg]				
Pu-239	4485	4225	3984	3762
Pu-241	681	640	603	569
U-233		386	741	1066
U-235				
FM(t)-FM(0) [kg]				
Pu-239				-723
Pu-241				-112
U-233				+1066
U-235				
Total				+231
Capture Rates [sec^{-1}]				
Th-232	.502			
U-238				
Pu-240	.0195			

HETEROGENEOUS CORE PERFORMANCE PARAMETERS
ORNL/GA. TECH LMFBR ALTERNATIVE FUEL CYCLE STUDIES

RUN NO. 6F MODEL DESIGNATION PTTGDS.273

CONDENSED DESCRIPTION: Same as Run 6A, but the widths of all fissile regions are reduced by 10% with corresponding increases in the fertile region widths. The outermost fissile ring is also reduced by an additional 7%.

Cycle Days	0	91	182	273
k_{eff}	1.0300	1.0333	1.0372	1.0411
Breeding Ratio	1.333	1.318	1.291	1.252
Pmax (w/cc)	633	620	643	660
Fissile Mass (FM) [kg]				
Pu-239	4461	4201	3961	3739
Pu-241	677	636	599	566
U-233		386	739	1063
U-235				
FM(t)-FM(0) [kg]				
Pu-239				-722
Pu-241				-111
U-233				+1063
U-235				
Total				+ 230
Capture Rates [sec^{-1}]				
Th-232	.502			
U-238				
Pu-240	.0195			

HETEROGENEOUS CORE PERFORMANCE PARAMETERS
ORNL/GA. TECH LMFBR ALTERNATIVE FUEL CYCLE STUDIES

RUN NO. 6G MODEL DESIGNATION PTTGCS.546

CONDENSED DESCRIPTION: Same as Run 6E (PTTGCS.273), except with 546 day burnup.

Cycle Days	0	136.5	273	409.5
k_{eff}	0.986	0.995	1.005	1.014
Breeding Ratio	1.430	1.400	1.349	1.277
Pmax (w/cc)	650	603	634	663
Fissile Mass (FM) [kg]				
Pu-239	4190	3806	3471	3176
Pu-241	636	577	527	485
U-233		611	1141	1600
U-235				
(a) FM(409.5)-FM(136.5) [kg]			(b)	(a)
(b) FM(t)-FM(0) [kg]				
Pu-239			-719	-630
Pu-241			-109	- 92
U-233			+1141	+989
U-235				
Total			+ 313	+267
Capture Rates [sec^{-1}]				
Th-232	0.517			
U-238				
Pu-240	0.003			

HETEROGENEOUS CORE PERFORMANCE PARAMETERS
ORNL/GA. TECH LMFBR ALTERNATIVE FUEL CYCLE STUDIES

RUN NO. 7A MODEL DESIGNATION IIITGXS.273

CONDENSED DESCRIPTION: Standard GE LMFBR model using U drivers and Th in all fertile/blanket regions. U isotope search (U-233 vs. U-235 & U-238) for K = 1.03, followed by 273 day burnup.

Cycle Days	0	91	182	273
k_{eff}	1.030	1.023	1.018	1.013
Breeding Ratio	1.291	1.291	1.290	1.284
Pmax (w/cc)	554	535	548	562
Fissile Mass (FM) [kg]				
Pu-239		143	278	407
Pu-241				
U-233	3939	3885	3838	3796
U-235	55	52	49	46
FM(t)-FM(0) [kg]				
Pu-239				407
Pu-241				
U-233				-143
U-235				- 9
Total				+255
Capture Rates [sec^{-1}]				
Th-232	.308			
U-238	.200			
Pu-240				
Percent Denatured	15.2			

HETEROGENEOUS CORE PEROFRMANCE PARAMETERS
ORNL/GA. TECH LMFBR ALTERNATIVE FUEL CYCLE STUDIES

RUN NO. 7B MODEL DESIGNATION UUTGAS.273

CONDENSED DESCRIPTION: Same as Run 7A, but the widths of all fissile regions are reduced by 10%. Fertile regions widths are increased by a corresponding amount to maintain reactor dimensions.

Cycle Days	0	91	182	273
k_{eff}	1.030	1.022	1.015	1.009
Breeding Ratio	1.292	1.293	1.296	1.294
Pmax (w/cc)	655	598	556	576
Fissile Mass (FM) [kg]				
Pu-239		122	239	350
Pu-241				
U-233	4012	3978	3950	3929
U-235	48	46	43	41
FM(t)-FM(0) [kg]				
Pu-239				350
Pu-241				
U-233				-83
U-235				- 7
Total				+260
Capture Rates [sec^{-1}]				
Th-232	.339			
U-238	.172			
Pu-240				
Percent Denatured	17.4			

HETEROGENEOUS CORE PERFORMANCE PARAMETERS
ORNL/GA. TECH LMFBR ALTERNATIVE FUEL CYCLE STUDIES

RUN NO. 7C MODEL DESIGNATION UUTGBS.273

CONDENSED DESCRIPTION: Same as Run 7A, but the widths of all fissile regions are reduced by 25%. Fertile regions widths are increased by a corresponding amount to maintain overall reactor dimensions.

Cycle Days	0	91	182	273
k_{eff}	1.030	1.018	1.008	1.0007
Breeding Ratio	1.293	1.296	1.307	1.316
Pmax (w/cc)	873	794	715	639
Fissile Mass (FM) [kg]				
Pu-239		94	185	271
Pu-241				
U-233	4084	4078	4079	4086
U-235	38	36	34	32
FM(t)-FM(0) [kg]				
Pu-239				+271
Pu-241				
U-233				+2
U-235				-6
Total				+267
Capture Rates [sec^{-1}]				
Th-232	.382			
U-238	.133			
Pu-240				
Percent Denatured	21.2			

HETEROGENEOUS CORE PERFORMANCE PARAMETERS
ORNL/GA. TECH LMFBR ALTERNATIVE FUEL CYCLE STUDIES

RUN NO. 7D MODEL DESIGNATION UUTGCS.273

CONDENSED DESCRIPTION: Same as Run 7A, but the widths of all fissile regions are reduced by 10% with corresponding increases in the fertile region widths. The outermost fissile ring is also reduced by an additional 5%.

Cycle Days	0	91	182	273
k_{eff}	1.0300	1.0235	1.0184	1.0144
Breeding Ratio	1.2916	1.2910	1.2889	1.2804
Pmax (w/cc)	623	608	630	645
Fissile Mass (FM) [kg]				
Pu-239		119	233	341
Pu-241				
U-233	3974	3942	3916	3894
U-235	47	44.1	41.6	39
FM(t)-FM(0) [kg]				
Pu-239				+341
Pu-241				
U-233				- 80
U-235				- 8
Total				+253
Capture Rates [sec^{-1}]				
Th-232	.343			
U-238	.168			
Pu-240				
Percent Denatured	17.6			

HETEROGENEOUS CORE PERFORMANCE PARAMETERS
ORNL/GA. TECH LMFBR ALTERNATIVE FUEL CYCLE STUDIES

RUN NO. 7E MODEL DESIGNATION UUTGDS.273

CONDENSED DESCRIPTION: Same as Run 7A, but the widths of all fissile regions are reduced by 16% with corresponding increases in the fertile region widths. The outermost fissile ring is also reduced by an additional 5%.

Cycle Days	0	91	182	273
k_{eff}	1.0300	1.0225	1.0167	1.0123
Breeding Ratio	1.292	1.292	1.292	1.286
Pmax (w/cc)	693	626	644	665
Fissile Mass (FM) [kg]				
Pu-239		108	211	308
Pu-241				
U-233	4022	4002	3987	3977
U-235	43	40	38	36
FM(t)-FM(0) [kg]				
Pu-239				308
Pu-241				
U-233				-45
U-235				- 7
Total				+256
Capture Rates [sec^{-1}]				
Th-232	.361			
U-238	.152			
Pu-240				
Percent Denatured	19.1			

HETEROGENEOUS CORE PERFORMANCE PARAMETERS
ORNL/GA. TECH LMFBR ALTERNATIVE FUEL CYCLE STUDIES

RUN NO. 7F MODEL DESIGNATION UUTGES.273

CONDENSED DESCRIPTION: Same as Run 7A, but the widths of all fissile regions are reduced by 16% with corresponding increases in the fertile region widths. The outermost fissile ring is also reduced by an additional 7%.

Cycle Days	0	91	182	273
k_{eff}	1.030	1.023	1.0184	1.0147
Breeding Ratio	1.2917	1.2910	1.2889	1.280
Pmax (w/cc)	674	656	681	707
Fissile Mass (FM) [kg]				
Pu-239		107	209	305
Pu-241				
U-233	4008	3989	3975	3964
U-235	42	40	38	36
FM(t)-FM(0) [kg]				
Pu-239				+305
Pu-241				
U-233				- 44
U-235				- 6
Total				+255
Capture Rates [sec^{-1}]				
Th-232	.363			
U-238	.150			
Pu-240				
Percent Denatured	19.4			

HETEROGENEOUS CORE PERFORMANCE PARAMETERS
ORNL/GA. TECH LMFBR ALTERNATIVE FUEL CYCLE STUDIES

RUN NO. 7G MODEL DESIGNATION UUTGBS.546

CONDENSED DESCRIPTION: Same as Run 7C (UUTGBS.273), except with 546 day burnup.

Cycle Days	0	136.5	273	409.5
k_{eff}	1.0498	1.0320	1.0180	1.0083
Breeding Ratio	1.245	1.251	1.267	1.273
Pmax (w/cc)	870	760	652	630
Fissile Mass (FM) [kg]				
Pu-239		133	258	375
Pu-241				
U-233	4242	4222	4218	4225
U-235	38	35	32	30
(a) FM(409.5)-FM(136.5) [kg]			(b)	(a)
(b) FM(t)-FM(0) [kg]				
Pu-239			+258	+242
Pu-241				
U-233			-24	+3
U-235			-6	-5
Total			+228	+240
Capture Rates [sec^{-1}]				
Th-232	.378			
U-238	.129			
Pu-240				
Percent Denatured	21.8			

HETEROGENEOUS CORE PERFORMANCE PARAMETERS
ORNL/GA. TECH LMFBR ALTERNATIVE FUEL CYCLE STUDIES

RUN NO. 7H MODEL DESIGNATION UUTGDS.546

CONDENSED DESCRIPTION: Same as Run 7E (UUTGDS.273), except with 546 day burnup.

Cycle Days	0	136.5	273	409.5
k_{eff}	1.030	1.0192	1.0118	1.0071
Breeding Ratio	1.292	1.292	1.290	1.282
Pmax (w/cc)	693	630	664	701
Fissile Mass (FM) [kg]				
Pu-239		159	307	444
Pu-241				
U-233	4022	3994	3977	3968
U-235	43	39	36	33
(a) FM(409.5)-FM(136.5) [kg]			(b)	(a)
(b) FM(t)-FM(0) [kg]				
Pu-239			+307	+285
Pu-241				
U-233			- 45	- 26
U-235			- 7	- 6
Total			+255	+253
Capture Rates [sec^{-1}]				
Th-232	.361			
U-238	.152			
Pu-240				
Percent Denatured	19.1			

HETEROGENEOUS CORE PERFORMANCE PARAMETERS
ORNL/GA. TECH LMFBR ALTERNATIVE FUEL CYCLE STUDIES

RUN NO. 7I MODEL DESIGNATION UUTGDS.EQI

CONDENSED DESCRIPTION: Same as Run 7E (UUTGDS.273), except that a refueling scheme was incorporated to allow the core to reach equilibrium conditions. One-half of the core fissile, core fertile, and axial blanket regions were refueled annually while one-sixth of the radial blanket was refueled annually.

Cycle Days	0	91	182	273
k_{eff}	1.0118	1.0065	1.0027	0.9999
Breeding Ratio*	1.317	1.314	1.310	1.302
Pmax (w/cc)	600	615	635	662
Fissile Mass (FM) [kg]				
Pu-239	158	259	355	445
Pu-241				
U-233	.4278	4268	4262	4260
U-235	40	37	35	33
FM(t)-FM(0) [kg]				
Pu-239				+287
Pu-241				
U-233				- 18
U-235				- 7
Total				+262
Capture Rates [sec^{-1}]				
Th-232	.360			
U-238	.151			
Pu-240				
Percent Denatured	19.1			

*For this run, U-235 is defined as fertile for BR calculation.

HETEROGENEOUS CORE PERFORMANCE PARAMETERS
ORNL/GA. TECH LMFBR ALTERNATIVE FUEL CYCLE STUDIES

RUN NO. 7J MODEL DESIGNATION UUTGXD.546

CONDENSED DESCRIPTION: Same as Run 7A, except that a dimension search (-23%/+23% changes in all Core Fiss/Fert Region widths) is used for K = 1.03 and the burnup time is 546 days. The resulting reactor has a smaller radius than the standard GE model.

Cycle Days	0	136.5	273	409.5
k_{eff}	1.030	1.017	1.009	1.003
Breeding Ratio	1.286	1.287	1.287	1.280
Pmax (w/cc)	782	685	680	694
Fissile Mass (FM) [kg]				
Pu-239		158	303	436
Pu-241				
U-233	3678	3649	3633	3628
U-235	39	35	32	29
(a) FM(409.5)-FM(136.5) [kg]			(b)	(a)
(b) FM(t)-FM(0) [kg]				
Pu-239			+303	+278
Pu-241				
U-233			- 45	- 21
U-235			- 7	- 6
Total			+251	+251
Capture Rates [sec^{-1}]				
Th-232	.361			
U-238	.151			
Pu-240				
Percent Denatured	19.2			

HETEROGENEOUS CORE PERFORMANCE PARAMETERS
ORNL/GA. TECH LMFBR ALTERNATIVE FUEL CYCLE STUDIES

RUN NO. 7K MODEL DESIGNATION UUTGAS.27A

CONDENSED DESCRIPTION: Same as Model 7B (UUTGAS.273), except that the search option was altered to keep a constant 19.1% enrichment, i.e. U-233, 235, 238 exchanged with Th.

Cycle Days	0	91	182	273
k_{eff}	1.030	1.022	1.015	1.010
Breeding Ratio	1.280	1.281	1.283	1.282
Pmax (w/cc)	650	595	557	578
Fissile Mass (FM) [kg]				
Pu-239		108	212	311
Pu-241				
U-233	4077	4053	4035	4022
U-235	43	41	39	36
FM(t)-FM(0) [kg]				
Pu-239				+311
Pu-241				
U-233				- 55
U-235				- 7
Total				+249
Capture Rates [sec^{-1}]				
Th-232	.357			
U-238	.153			
Pu-240				
Percent Denatured	19.1			

APPENDIX II.

Plots of power distribution for selected cases reported in Appendix I, ordered as follows:

N = number, same for a general reactor type.

L = letter, designating variations within the type.

N = 4 PUU reactors based on GE model [13].

N = 5 PUT reactors based on GE model [13].

N = 6 PTT reactors based on GE model [13].

N = 7 UUT denatured reactors [$(U^{233}/U^{238})O_2$ or $(U^{233}/U^{238}/Th)O_2$ fissile regions, ThO_2 fertile regions] based on GE model.

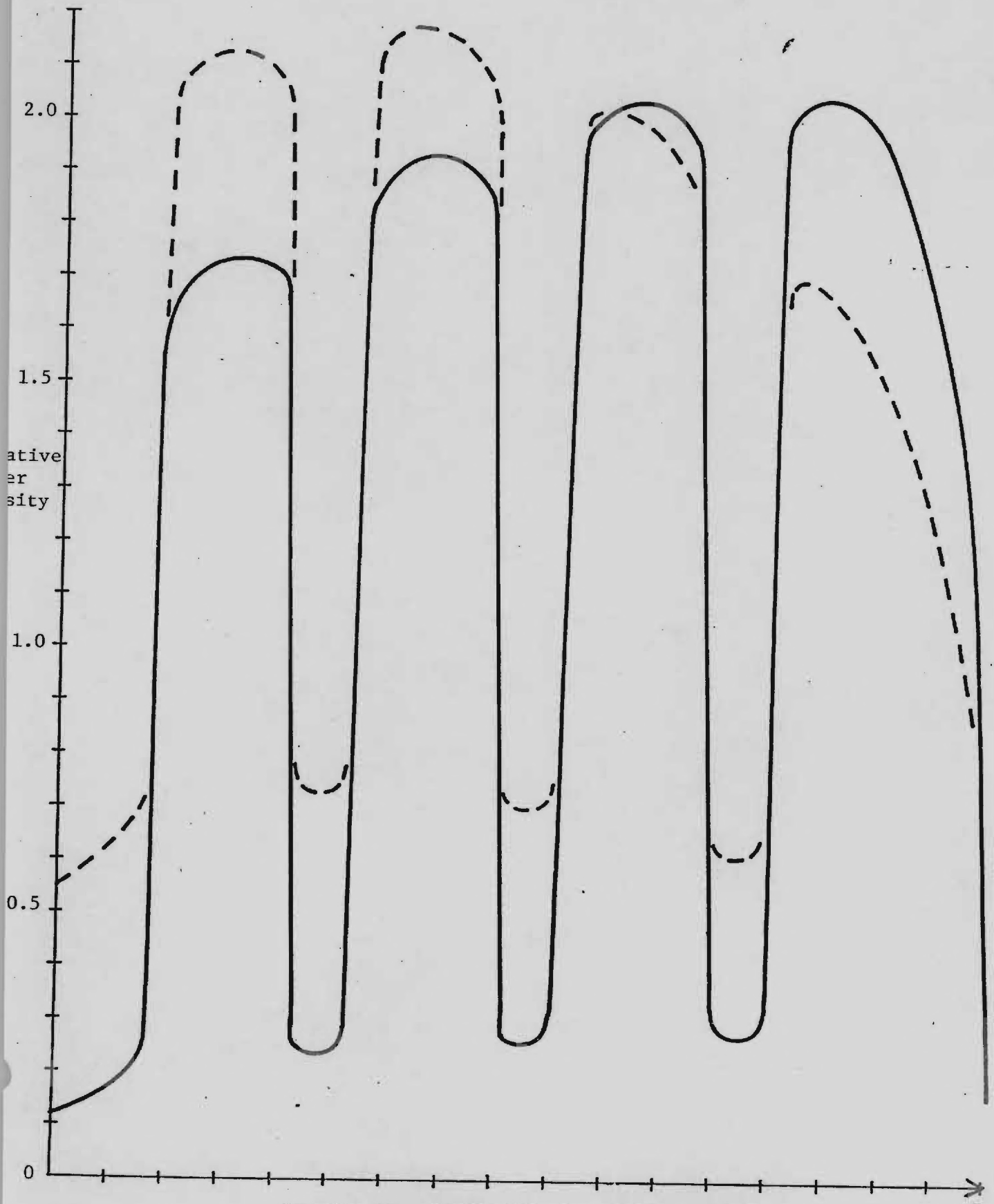

Run No. 4A. PUUGXS.273 (—— BOC, --- EOC).

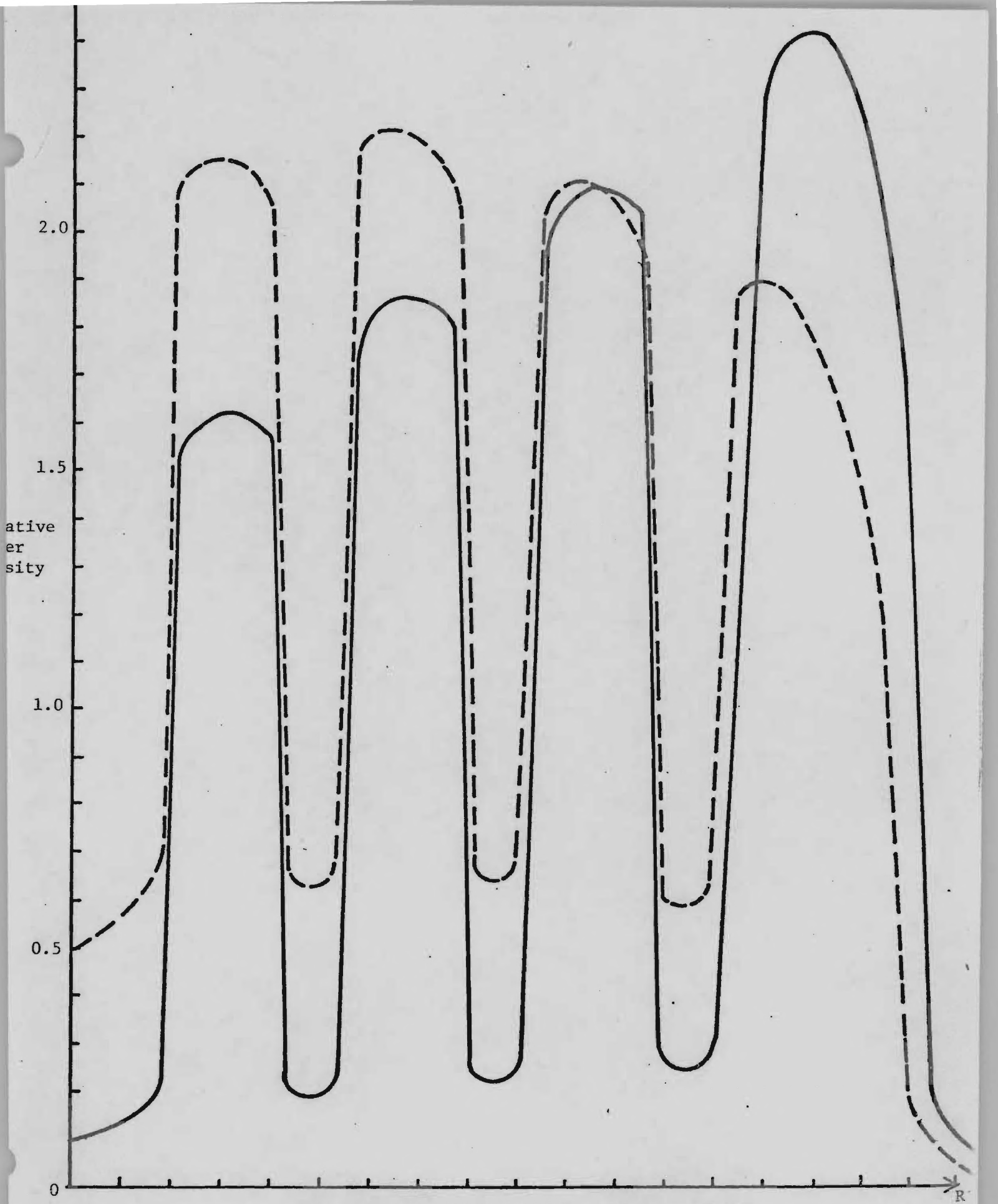

Run No. 4B. PUUGAS.273 (—— BOC, --- EOC).

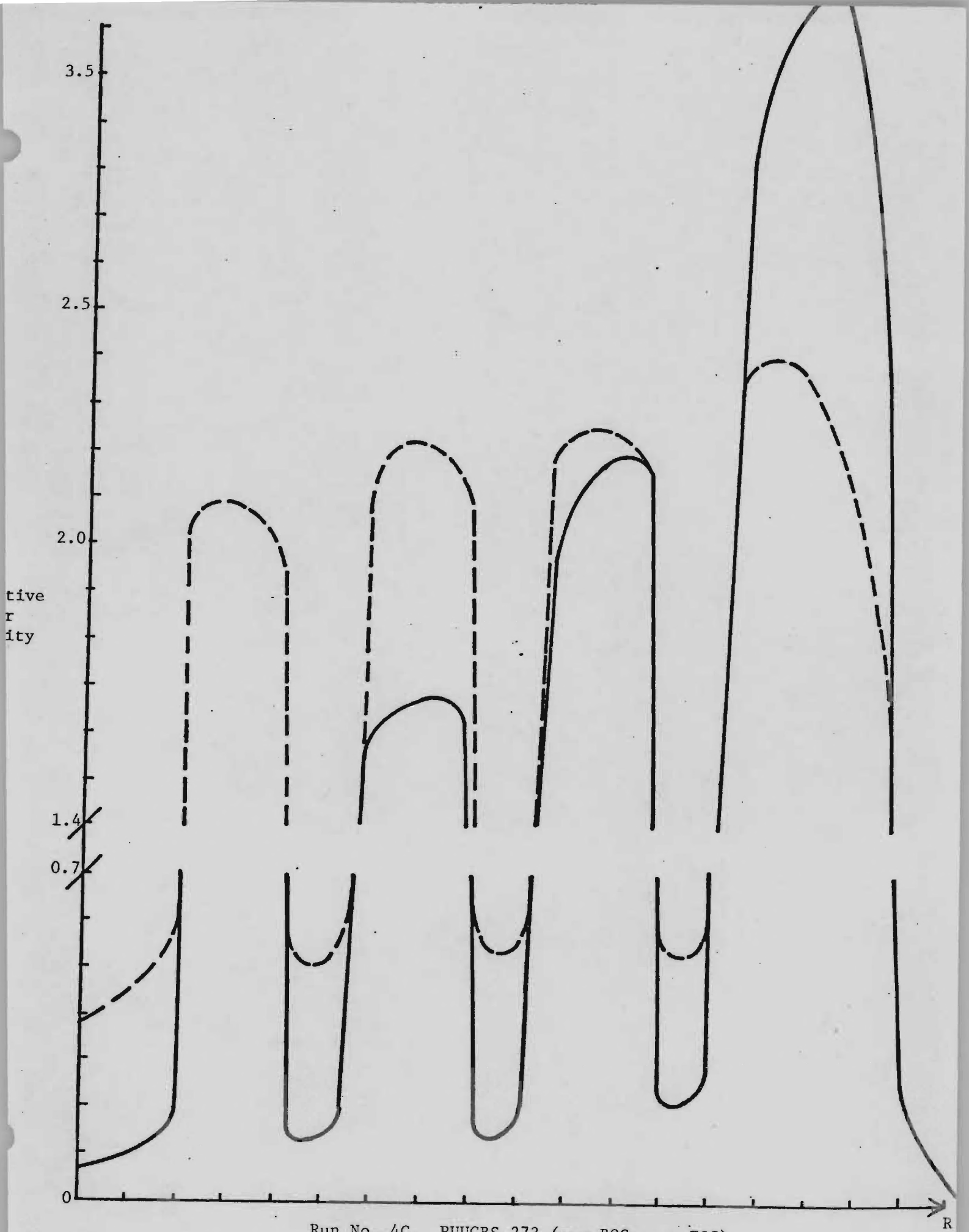

Run No. 4C. PUUGBS.273 (—— BOC, --- EOC).

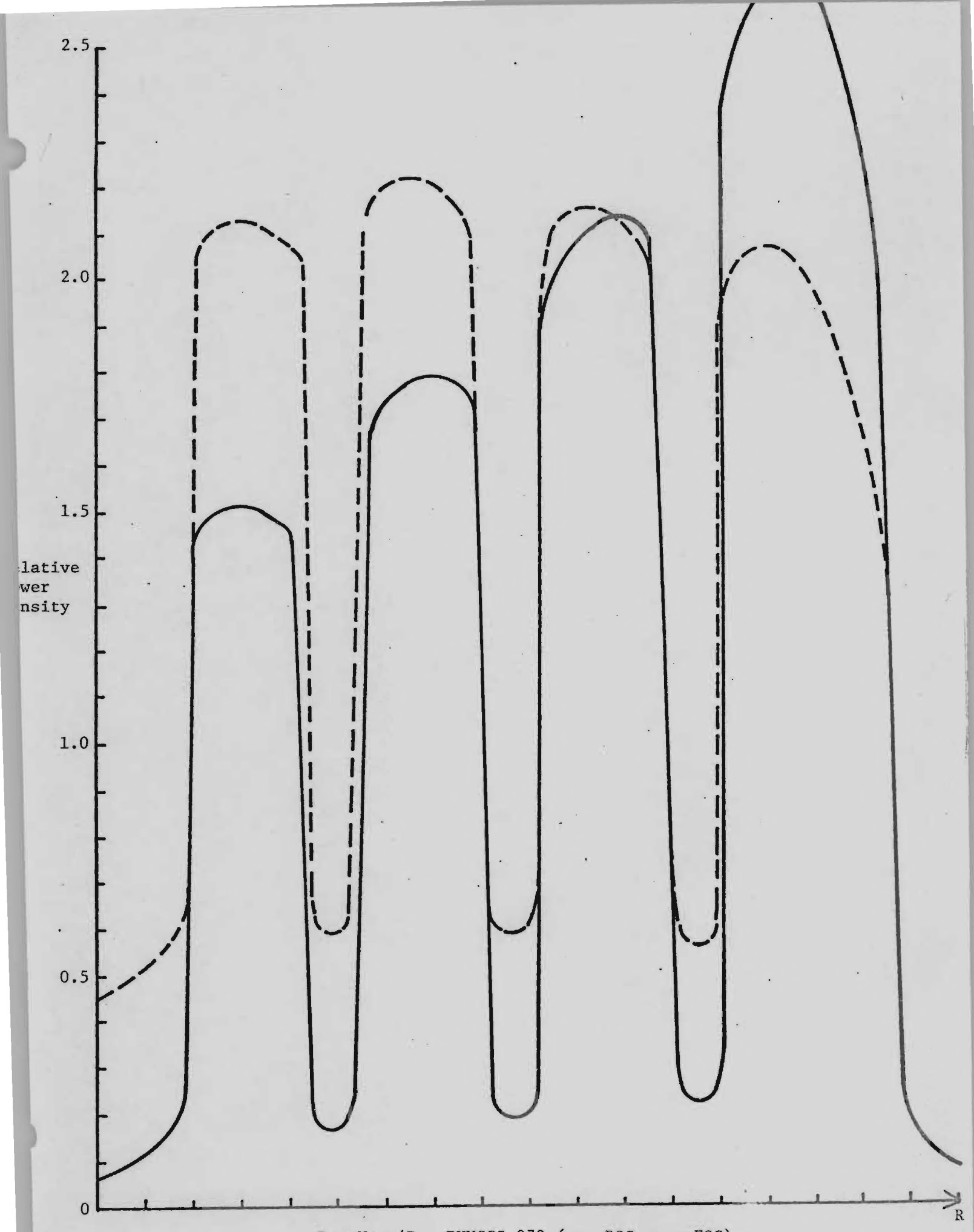

Run No. 4D. PUUGCS.273 (—— BOC, --- EOC).

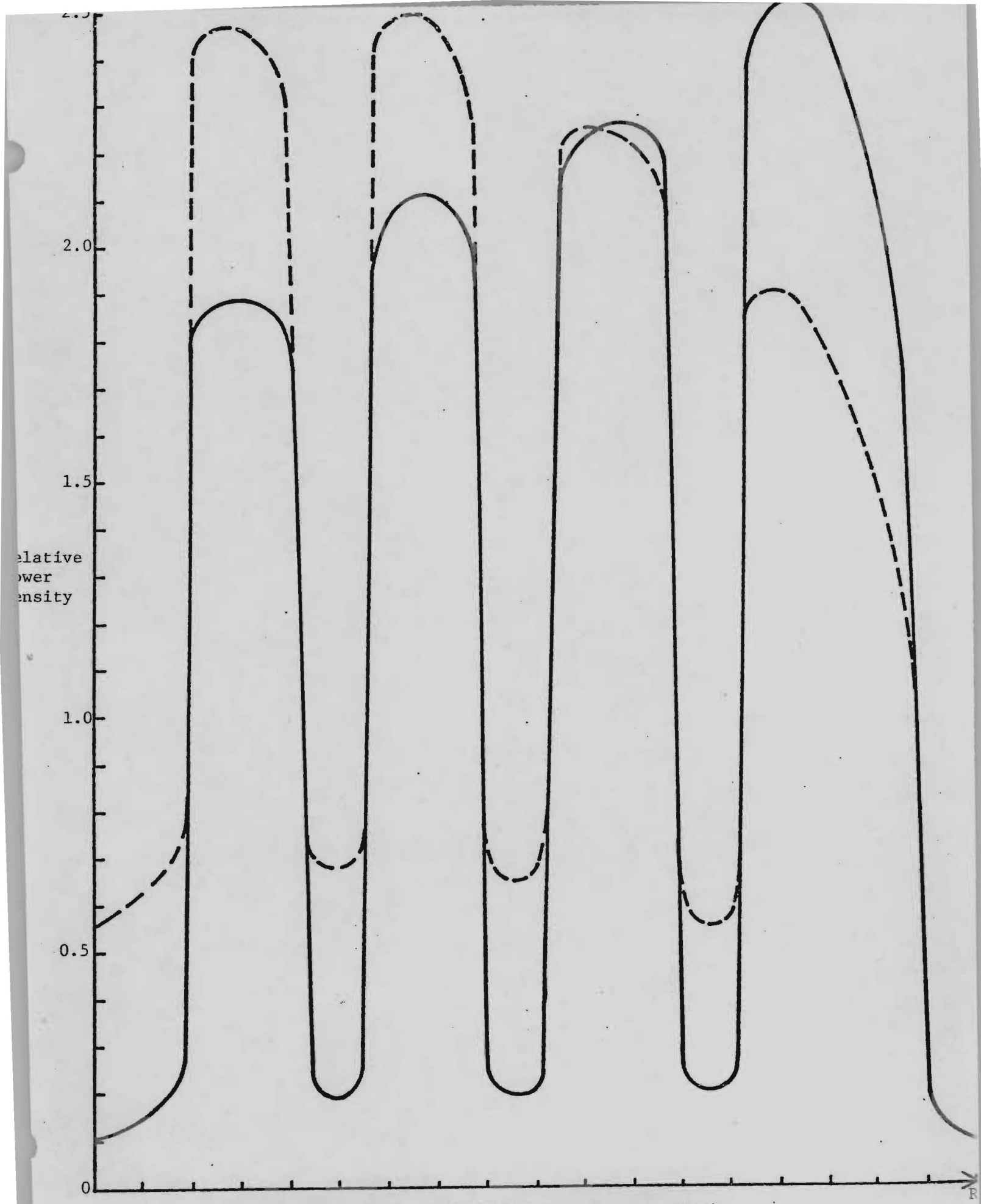

Run No. 4E. PUUGDS.273 (—— BOC, --- EOC).

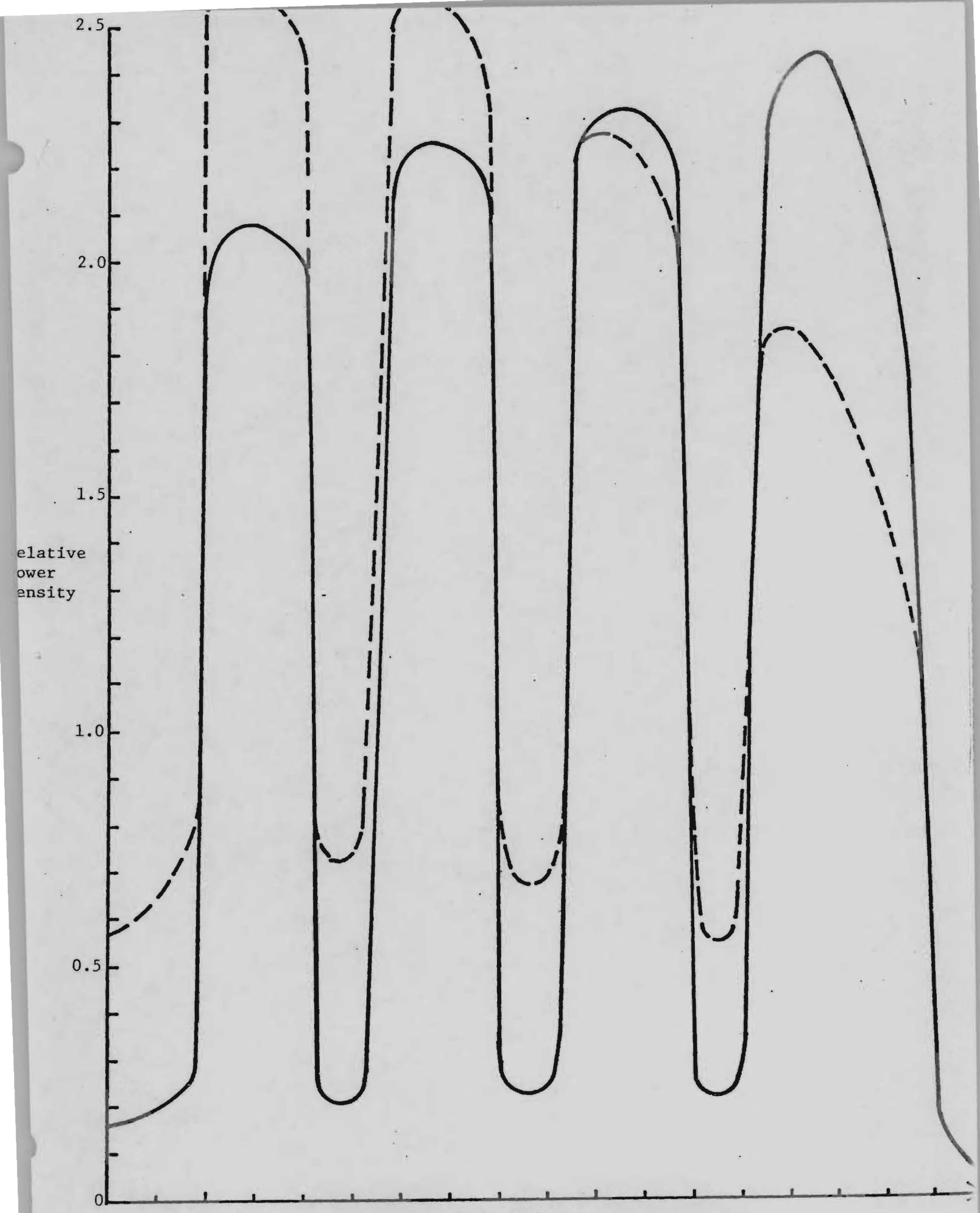

Run No. 4F. PUUGES.273 (—— BOC, --- EOC).

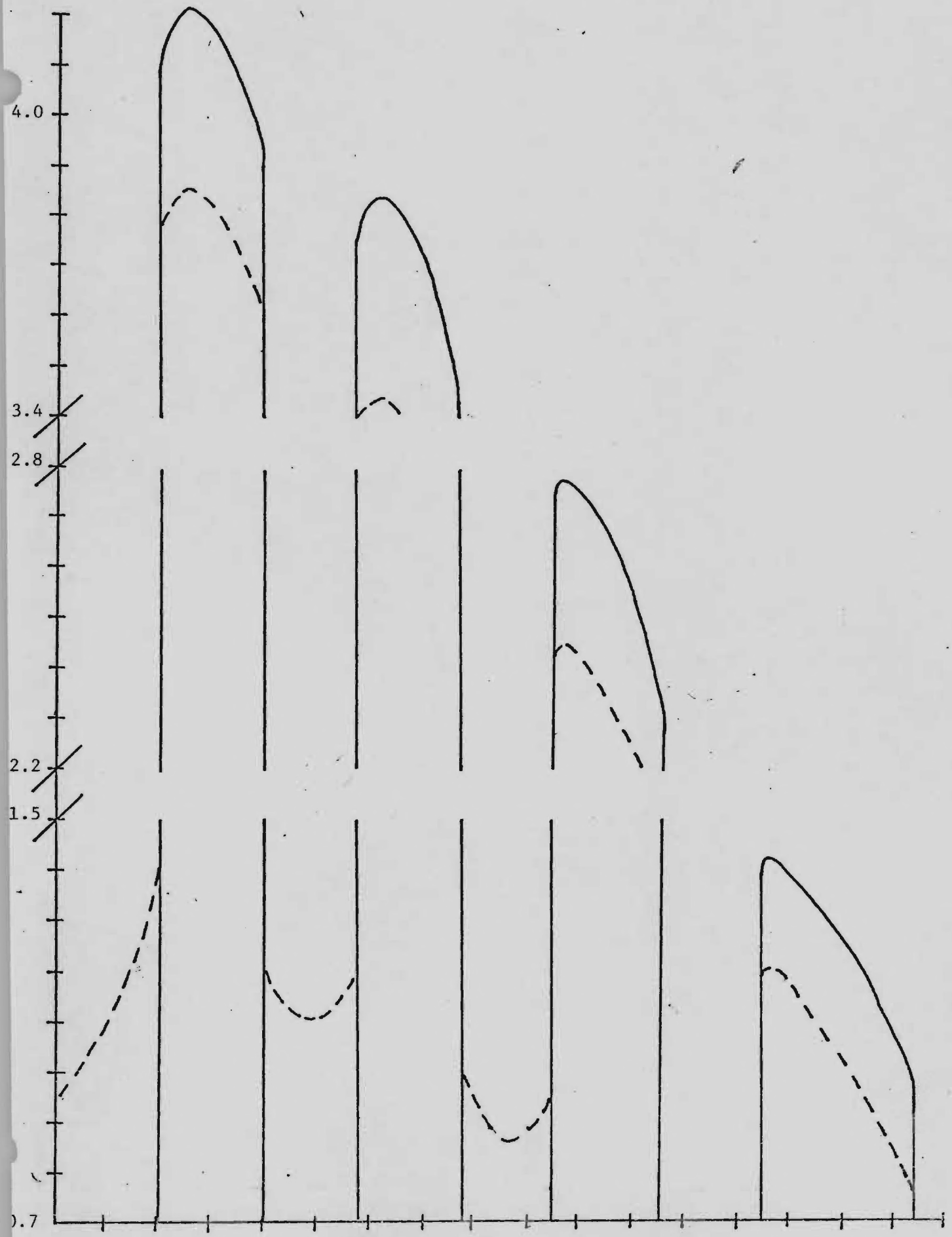

Run No. 4G. PUUGYS.273 (—— BOC, --- EOC).

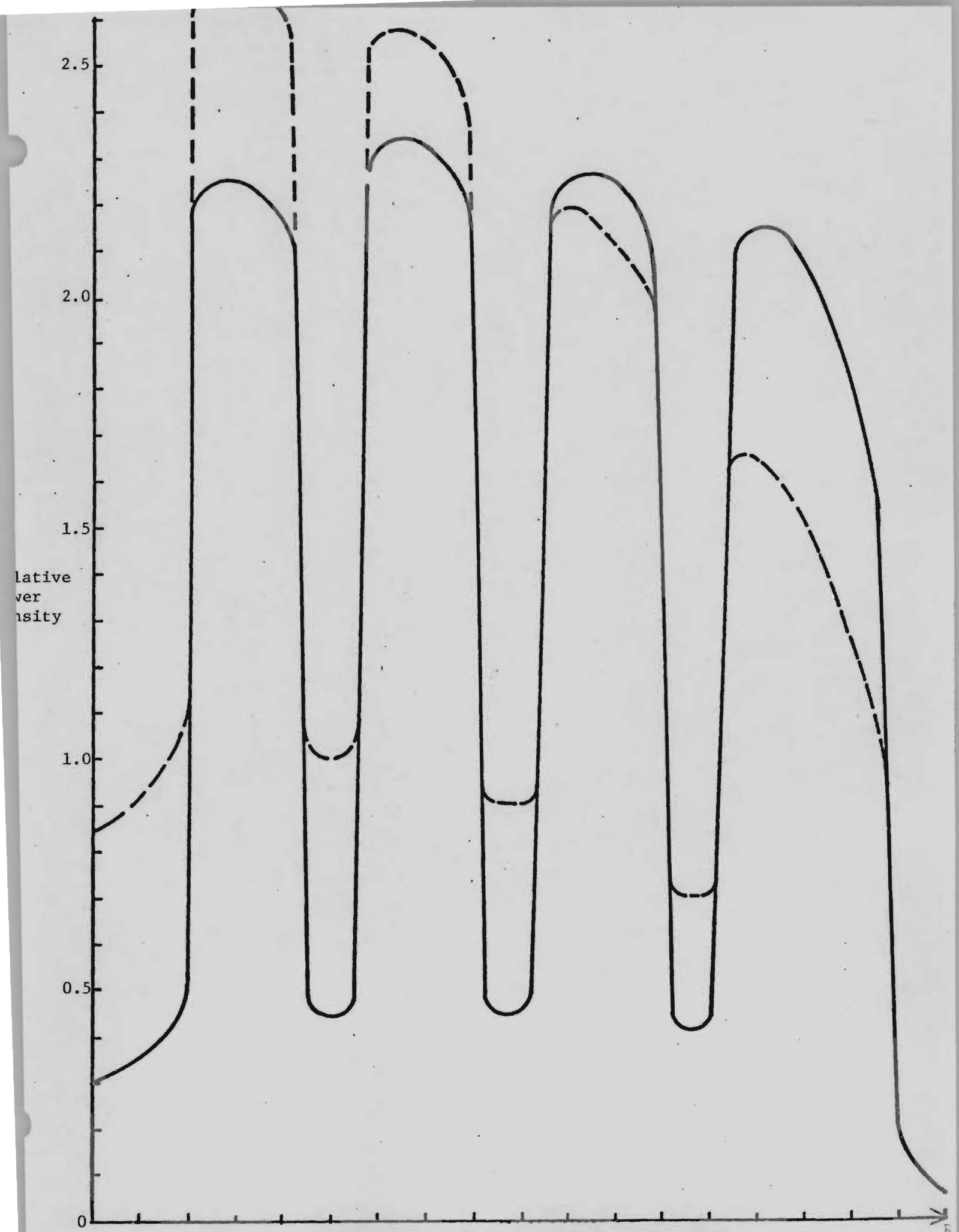

Run No. 4H. PUUGDS.546 (—— BOC, --- EOC).

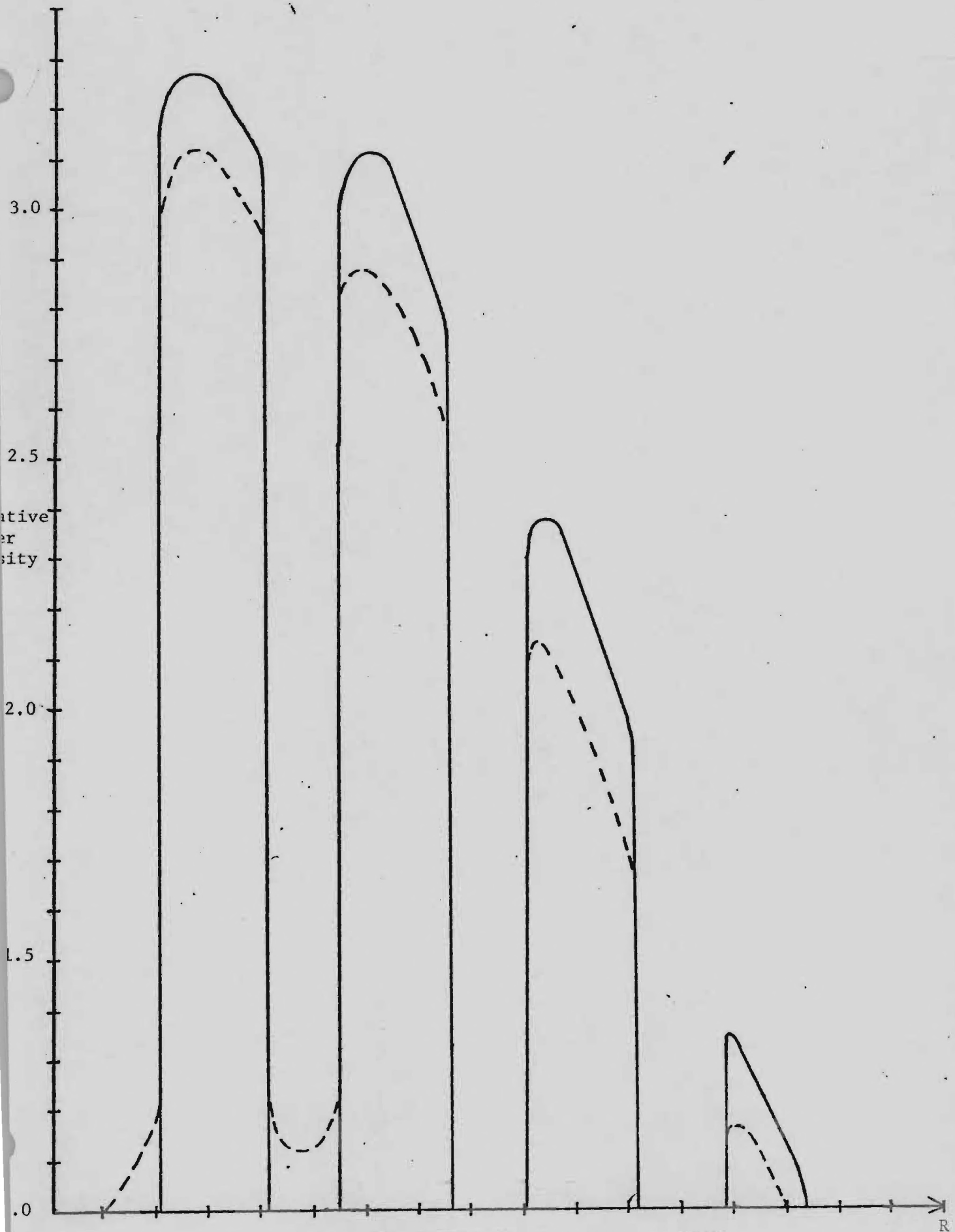

Run No. 4I. PUUG1S.273 (—— BOC, --- EOC).

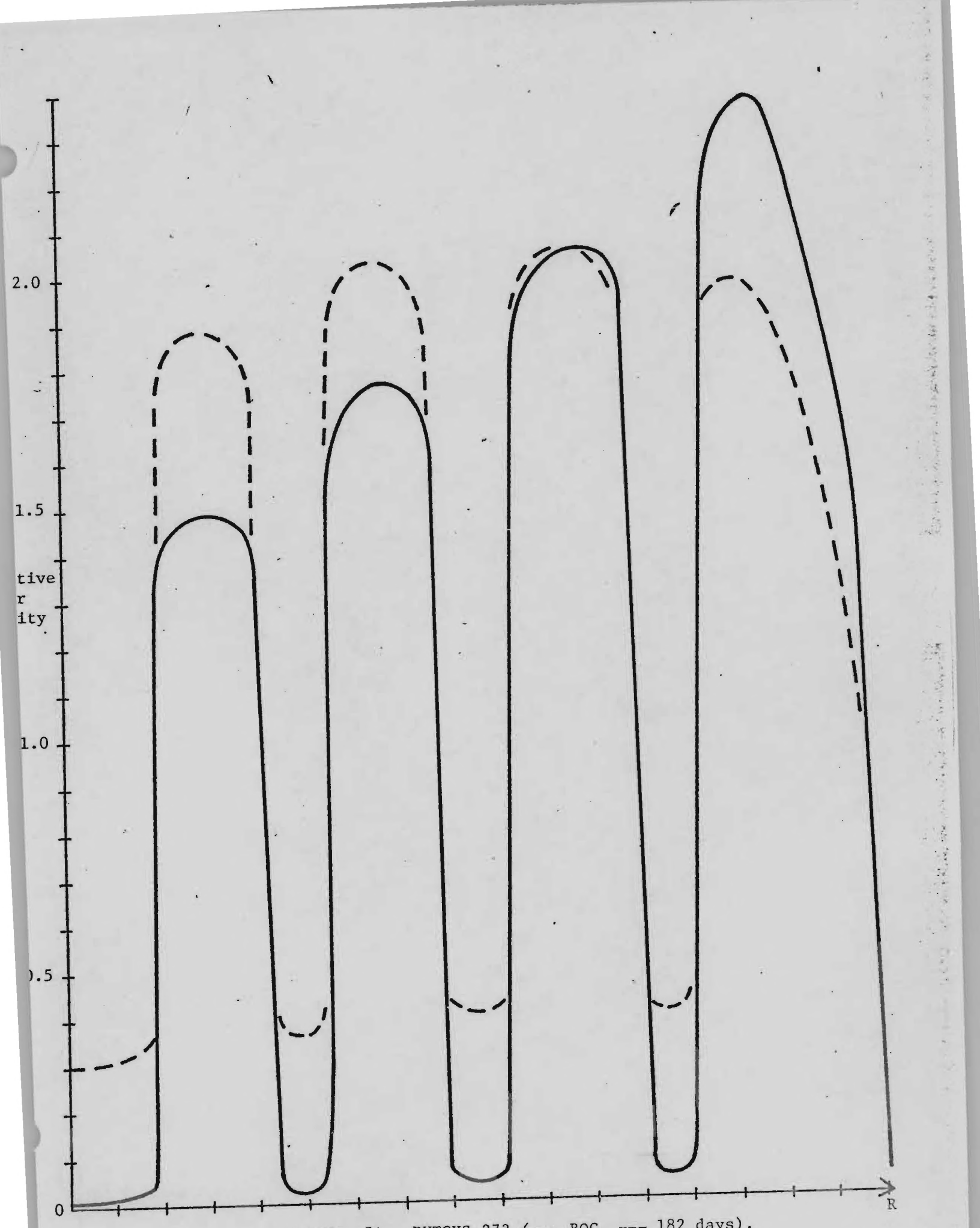

Run No. 5A. PUTGXS.273 (—— BOC, --- 182 days).

Run No. 5B. PUTG1S.273 (—— BOC, --- EOC).

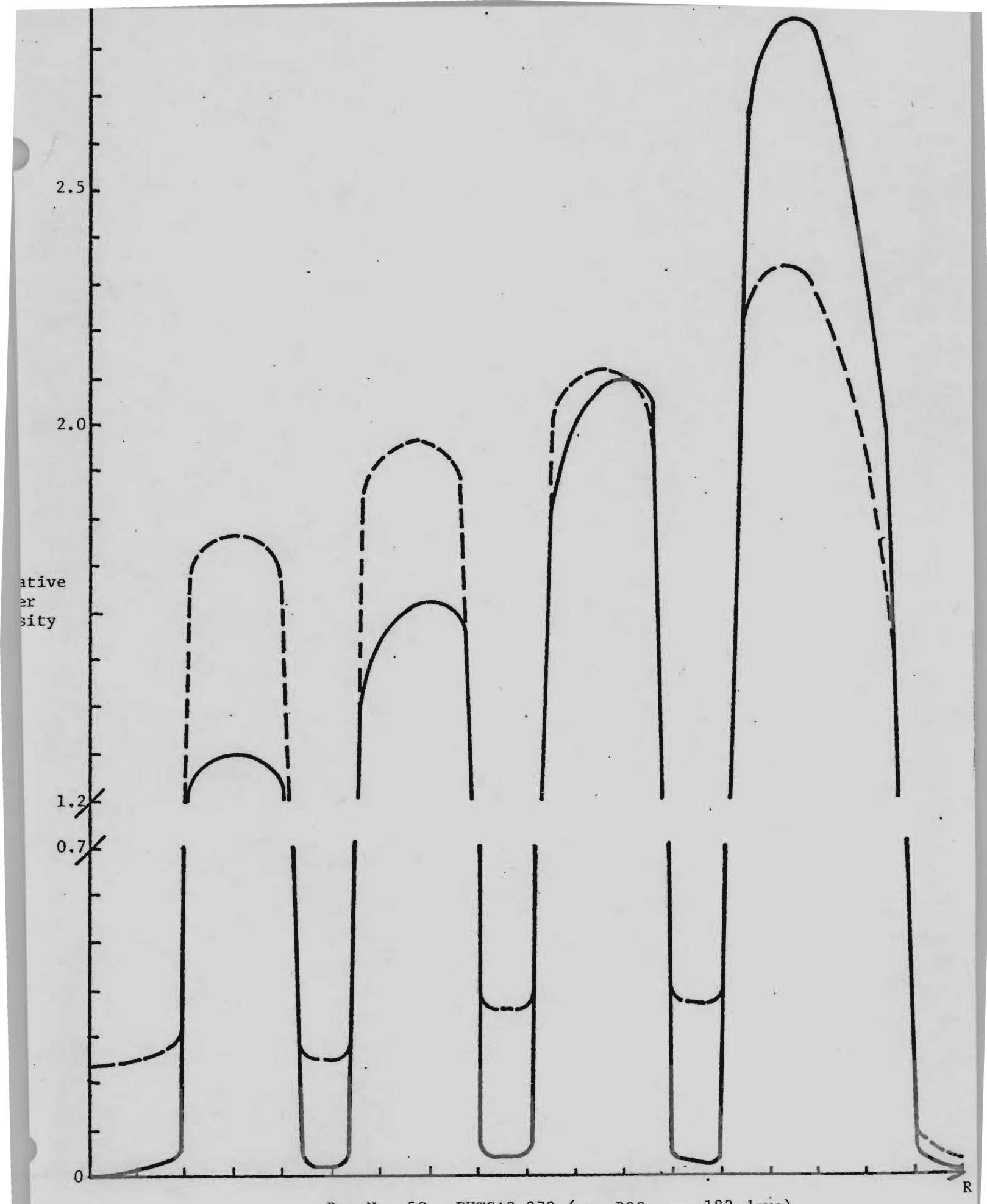

Run No. 5C. PUTGAS.273 (—— BOC, --- 182 days).

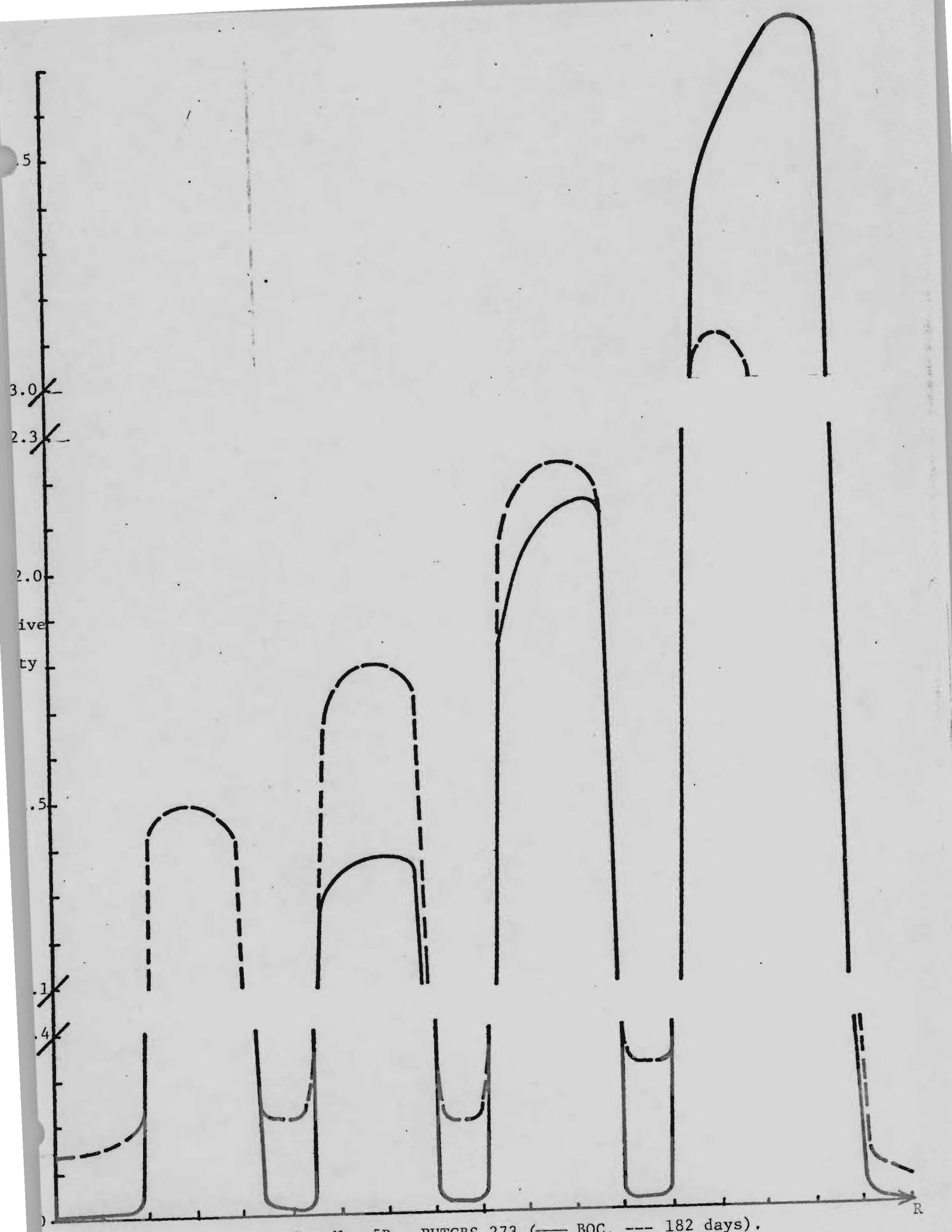

Run No. 5D. PUTGBS.273 (—— BOC, --- 182 days).

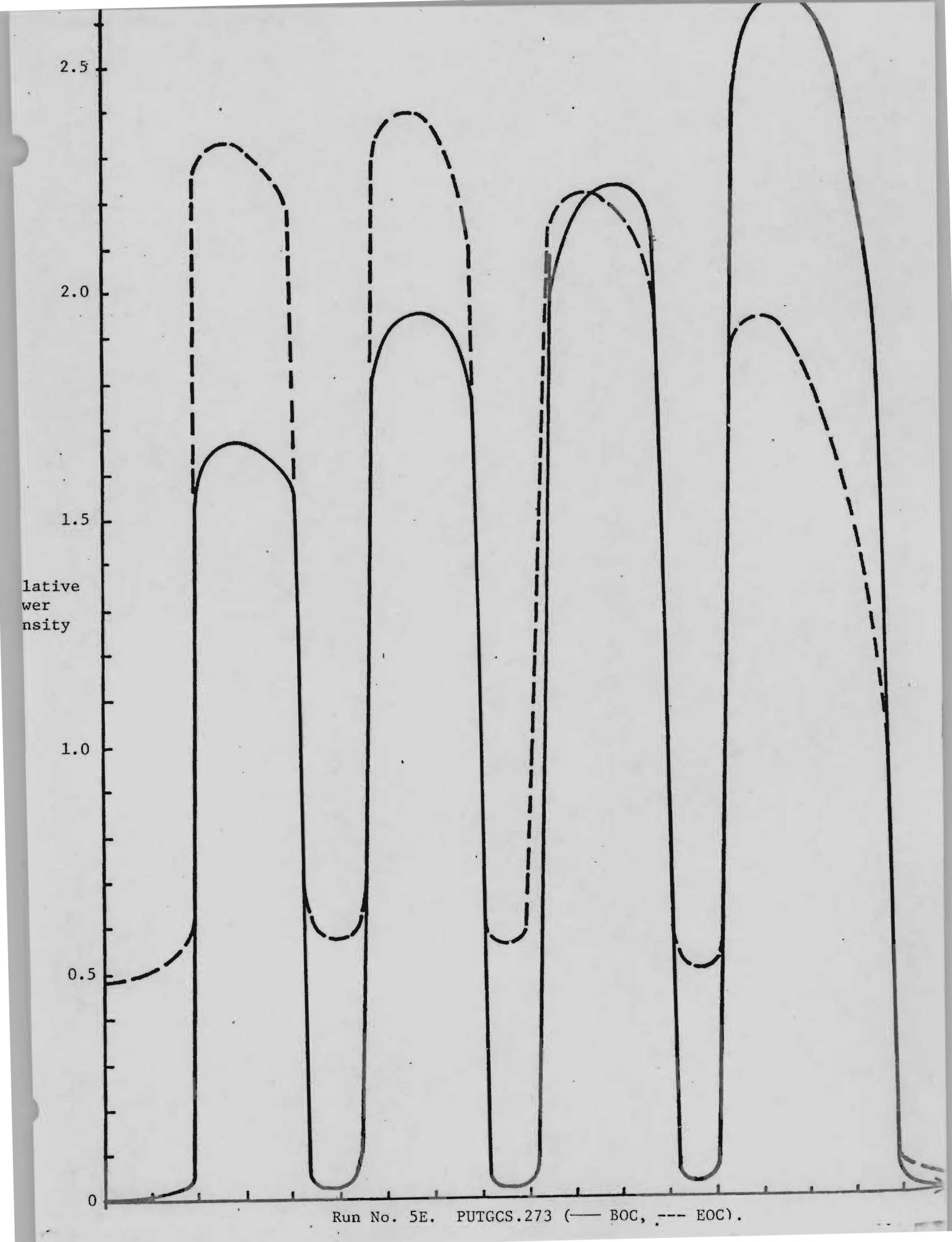

Run No. 5E. PUTGCS.273 (—— BOC, --- EOC).

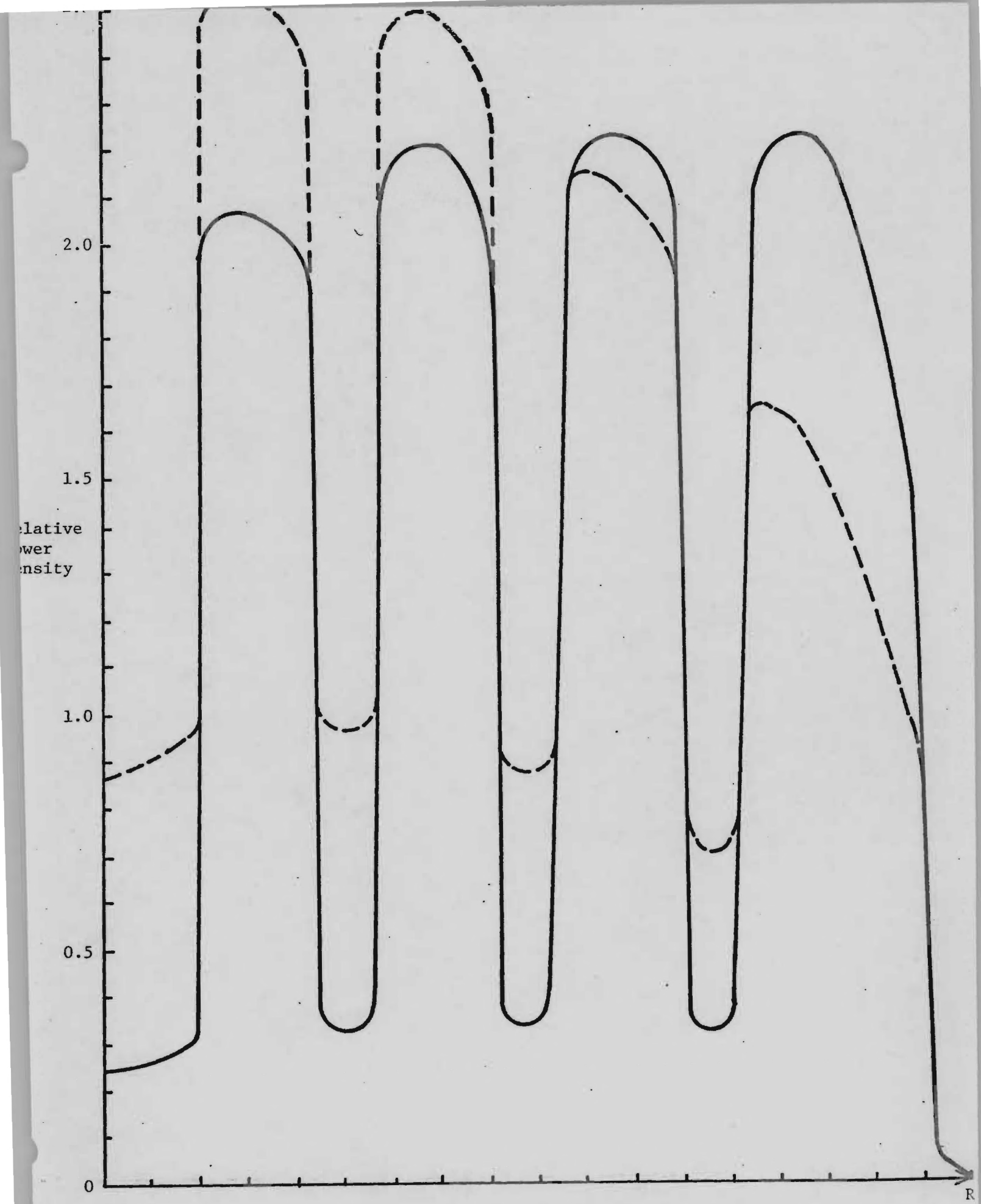

Run No. 5F. PUTGCS.546 (—— BOC, --- EOC).

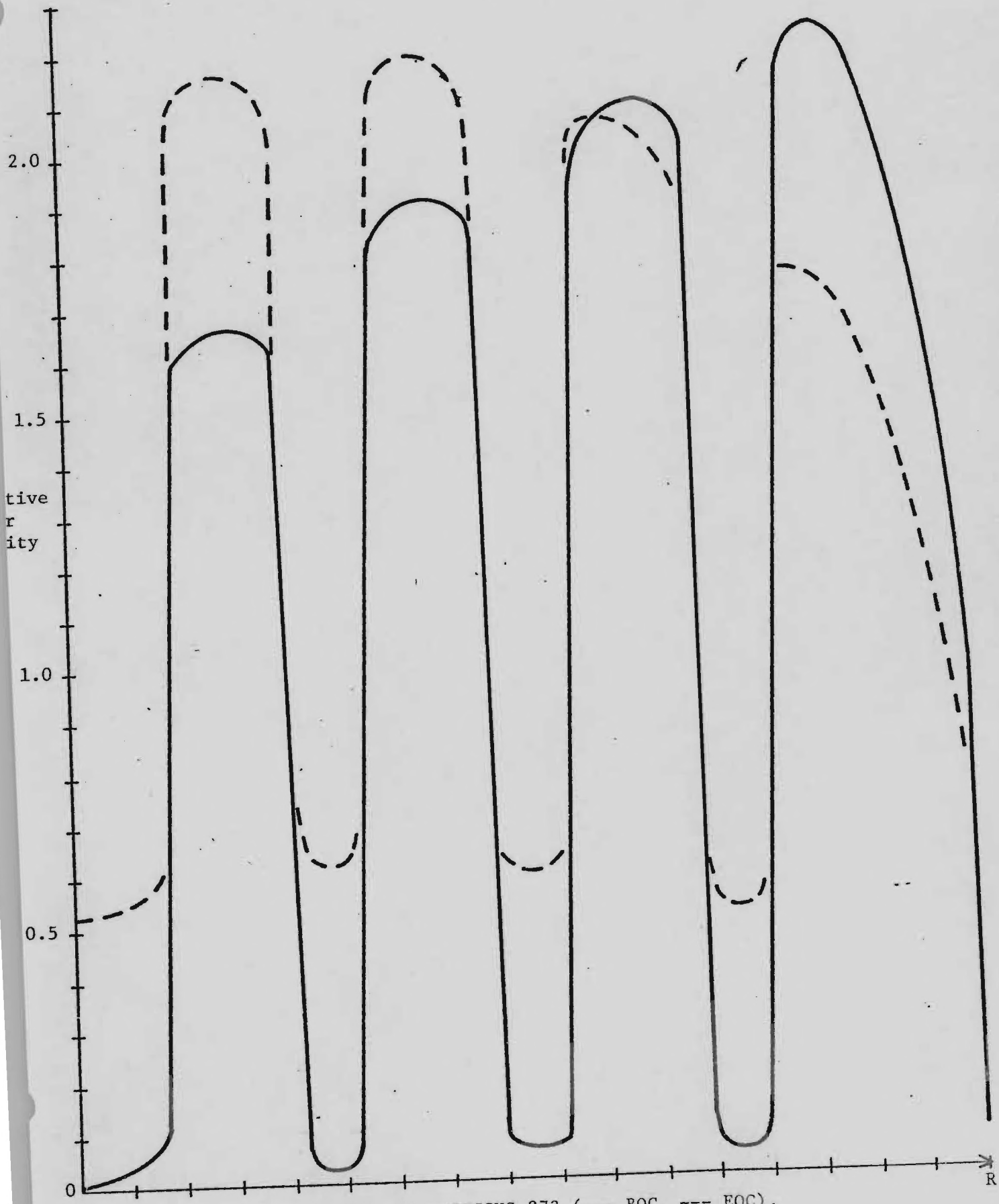

Run No. 6A. PTTGXS.273 (—— BOC, --- EOC).

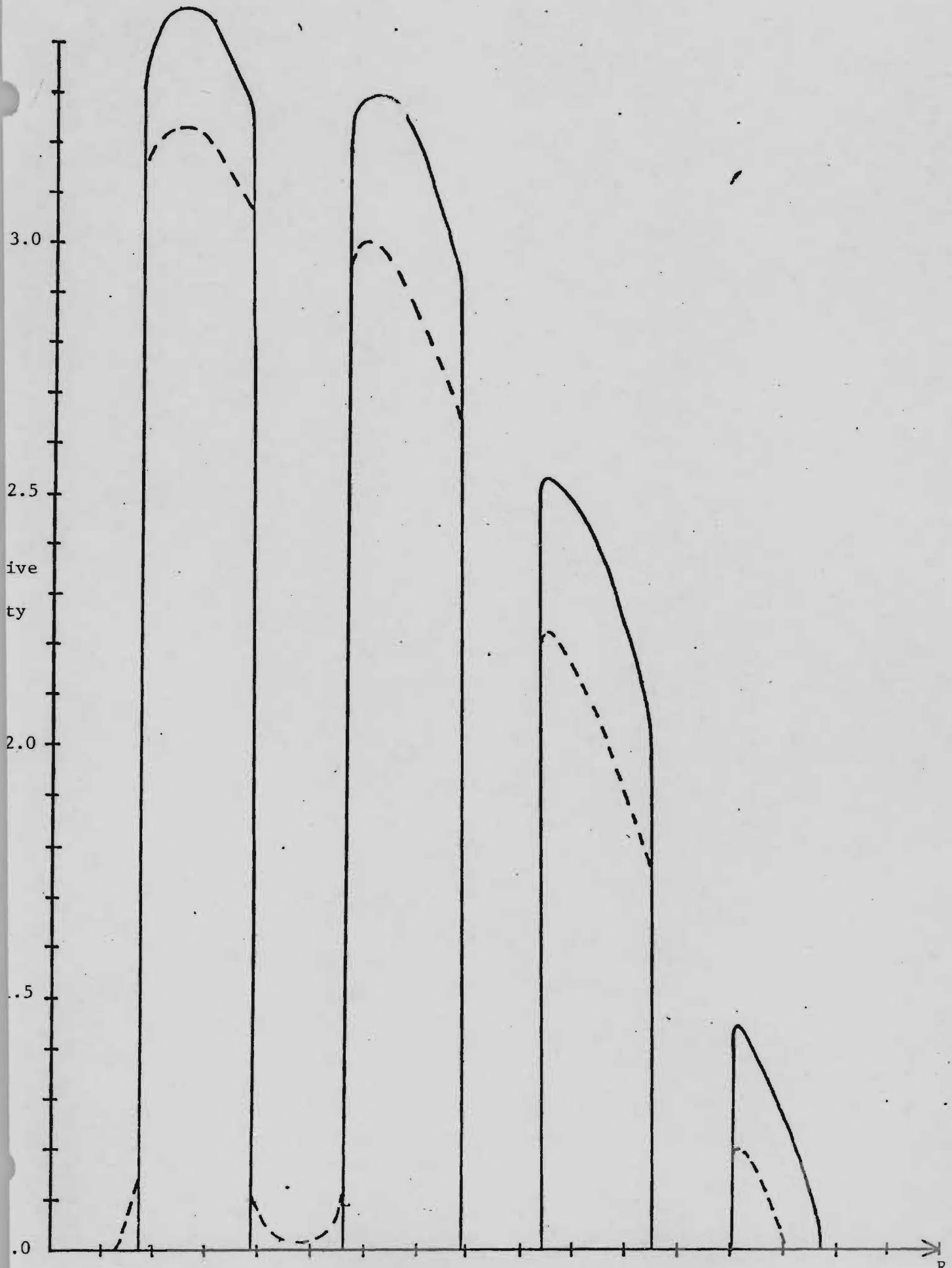

Run No. 6B. PTTG1S.273 (—— BOC, --- EOC).

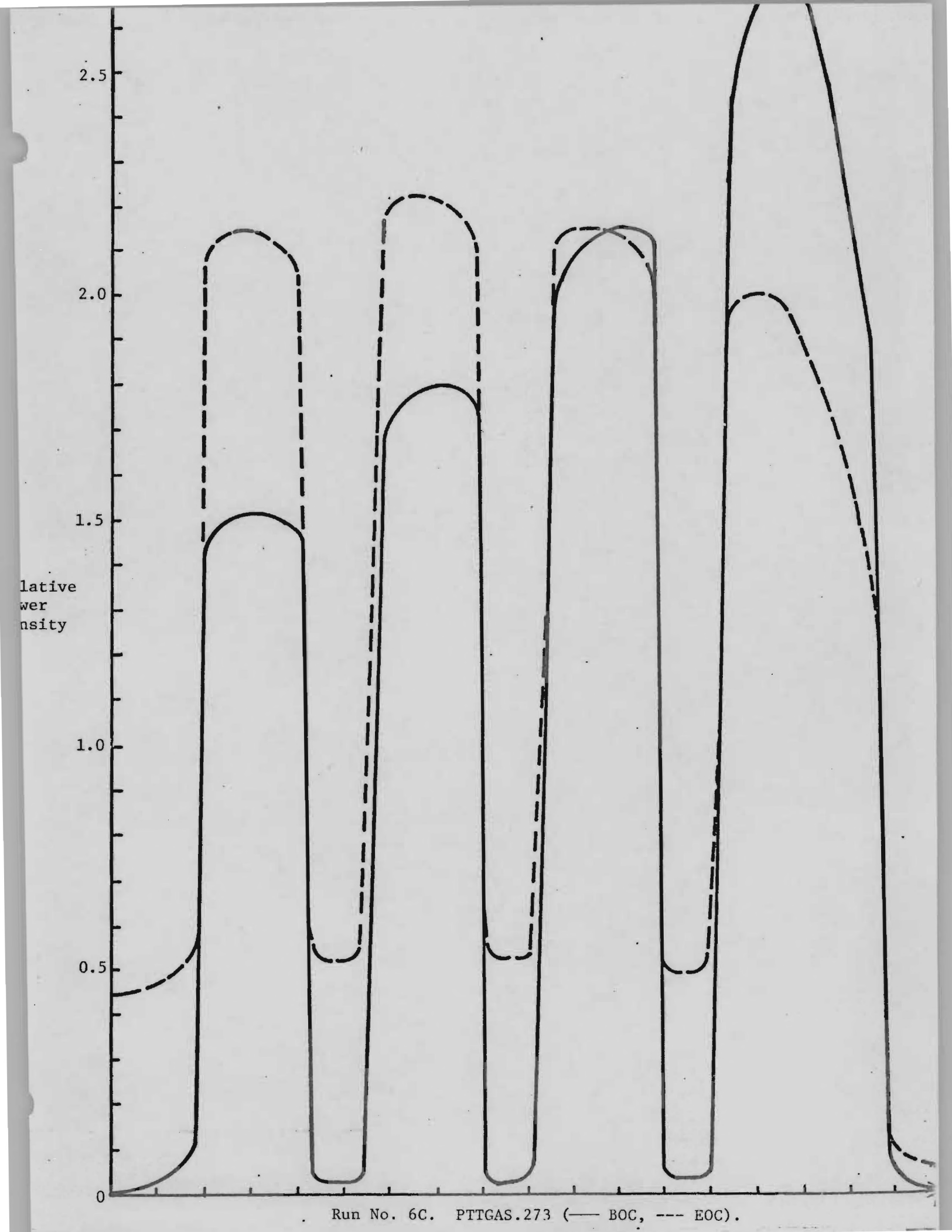

Run No. 6C. PTTGAS.273 (—— BOC, --- EOC).

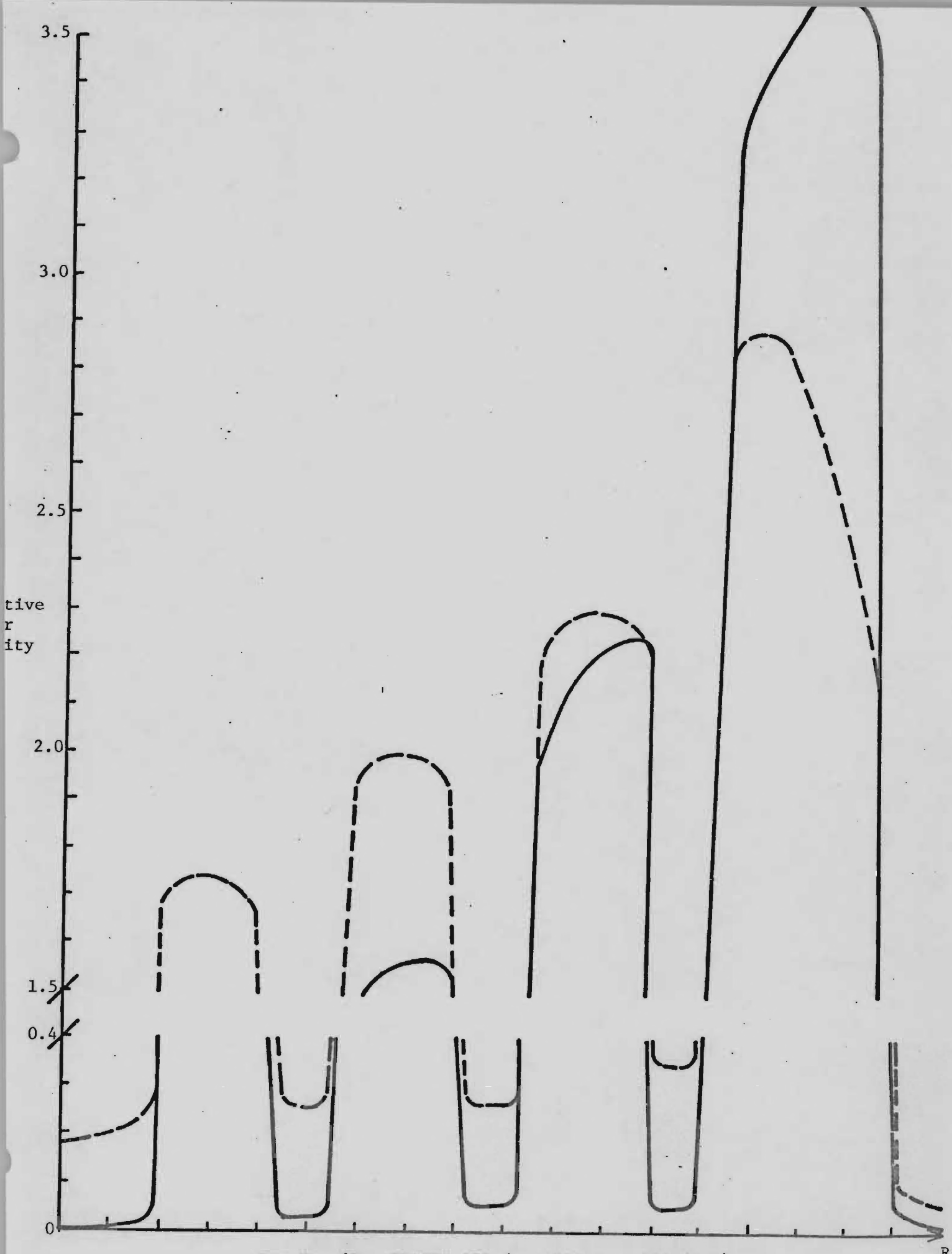

Run No. 6D. PTTGBS.273 (—— BOC, --- 182 days).

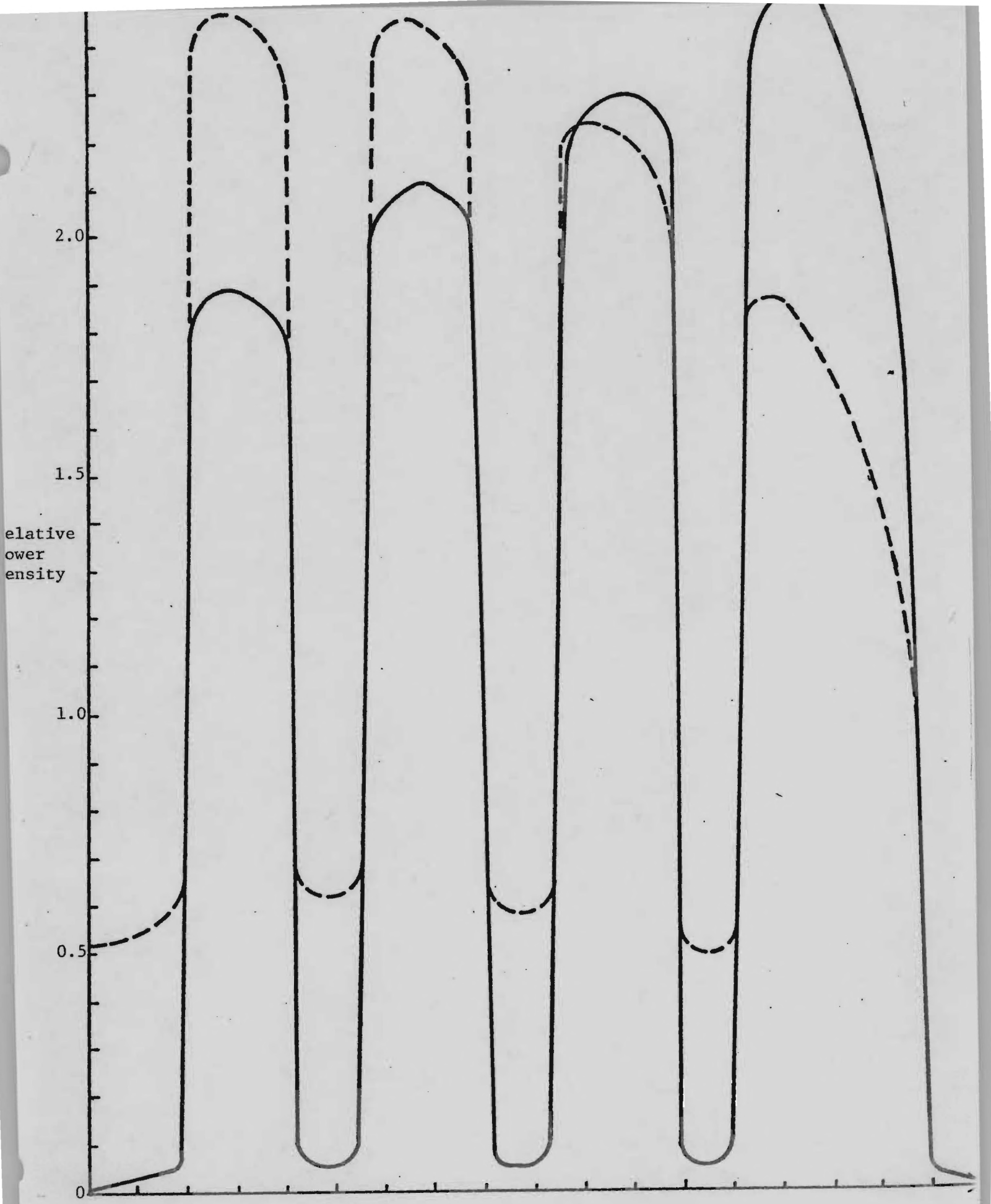

Run No. 6E. PTTGCS.273 (—— BOC, --- EOC).

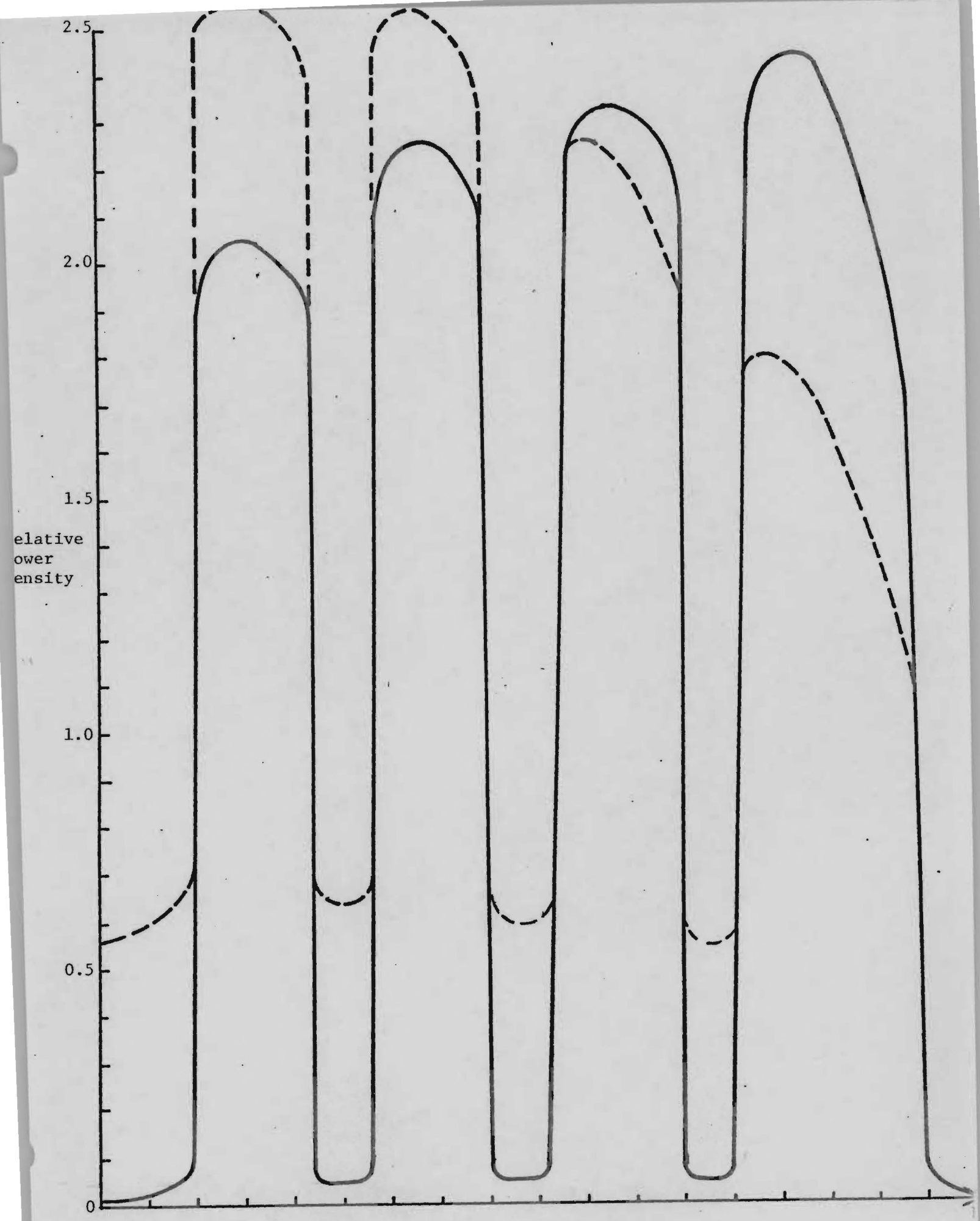

Run No. 6F. PTTGDS.273 (—— BOC, --- EOC).

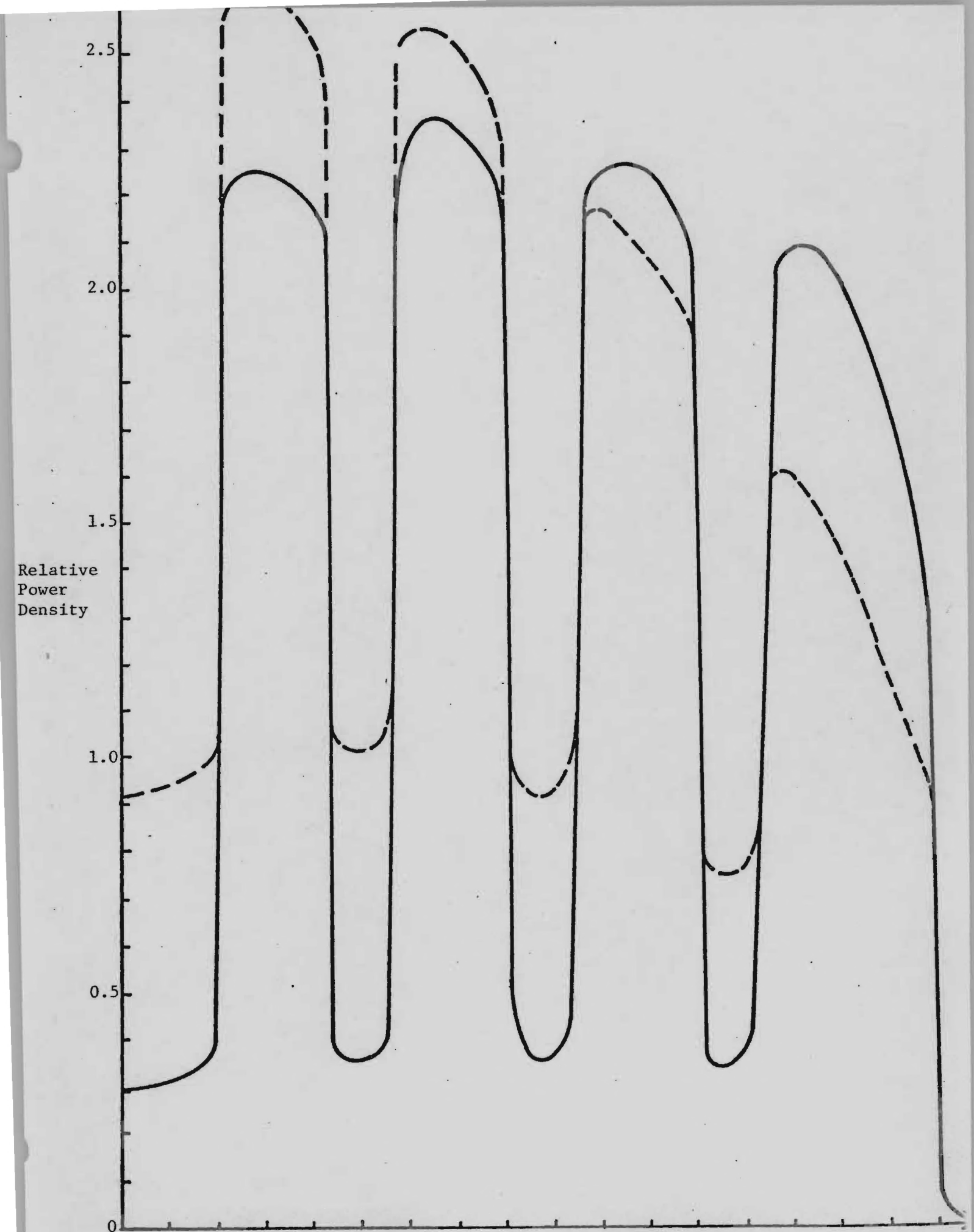

Run No. 6G. PTTGCS.546 (—— BOC, --- EOC).

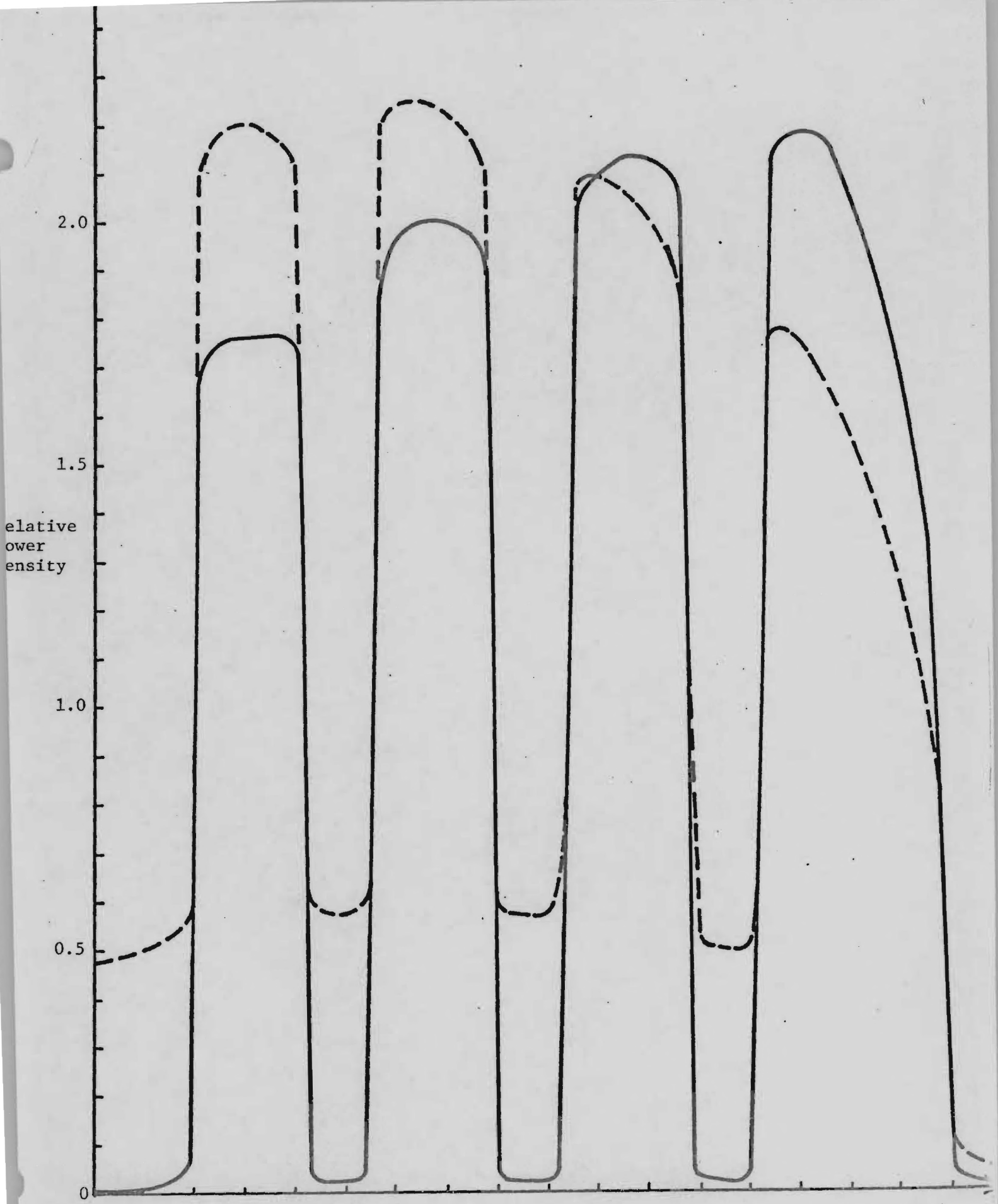

Run No. 7A. UUTGXS.273 (—— BOC, --- EOC).

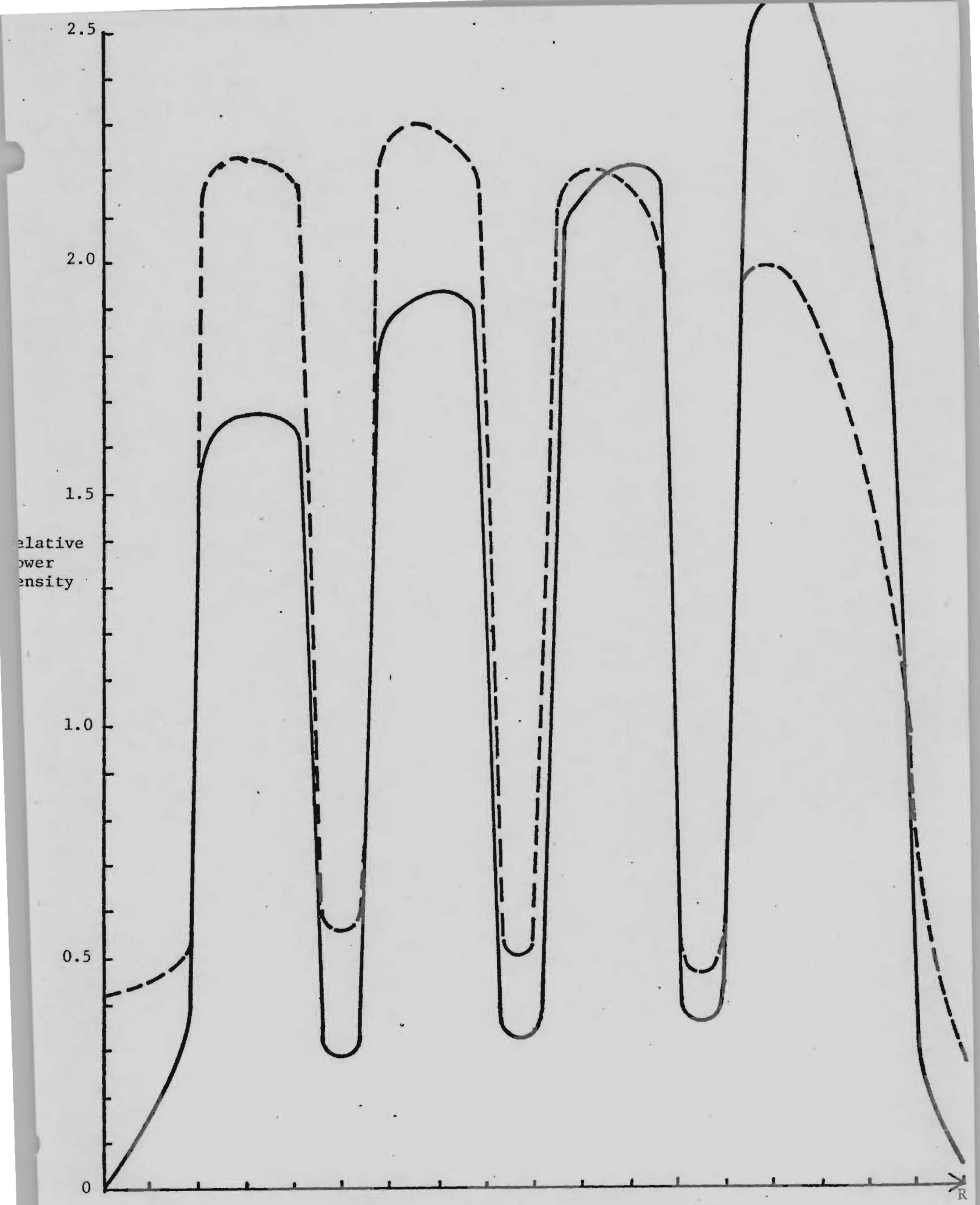

Run No. 7B. UUTGAS.273 (—— BOC, --- EOC).

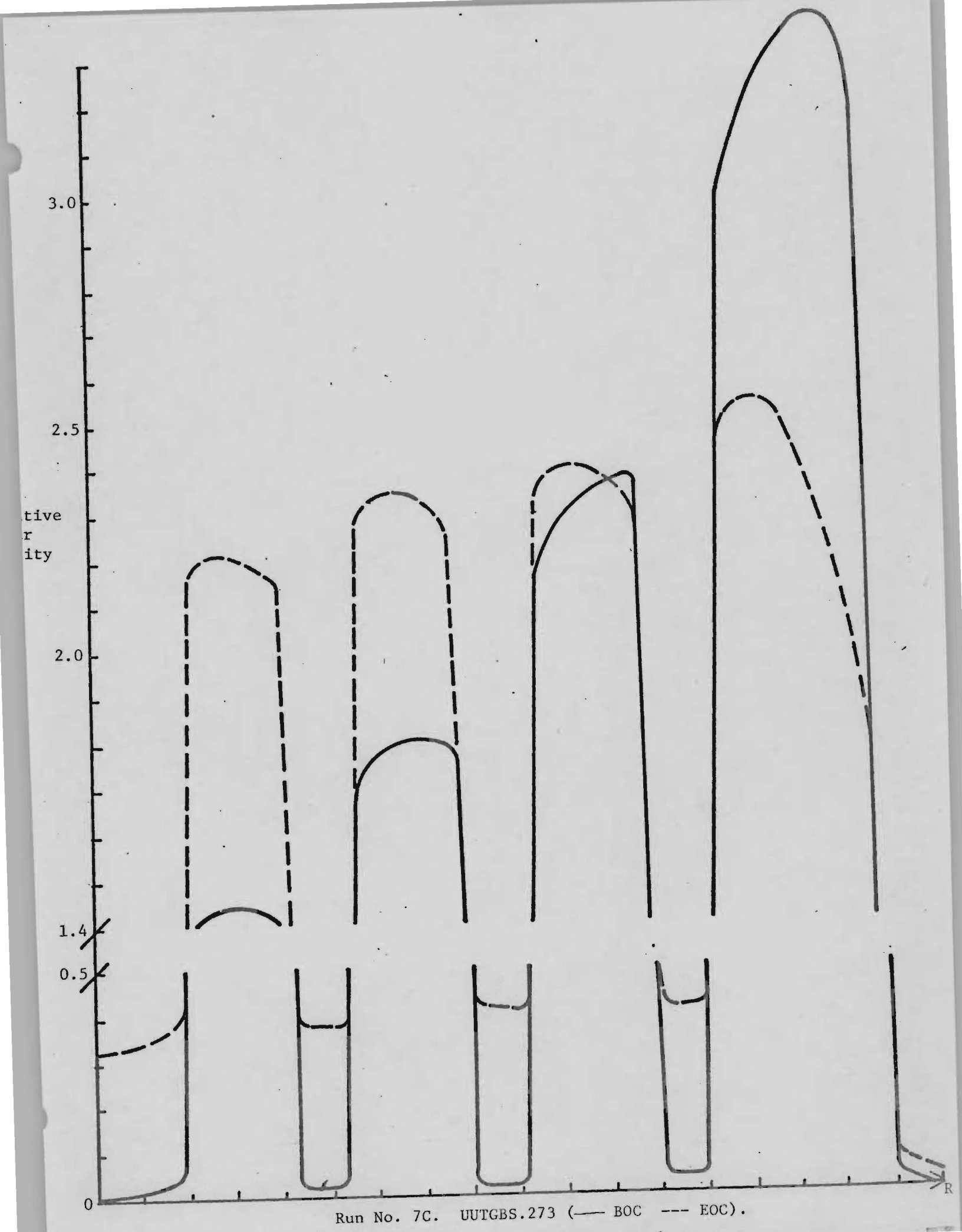

Run No. 7C. UUTGBS.273 (—— BOC --- EOC).

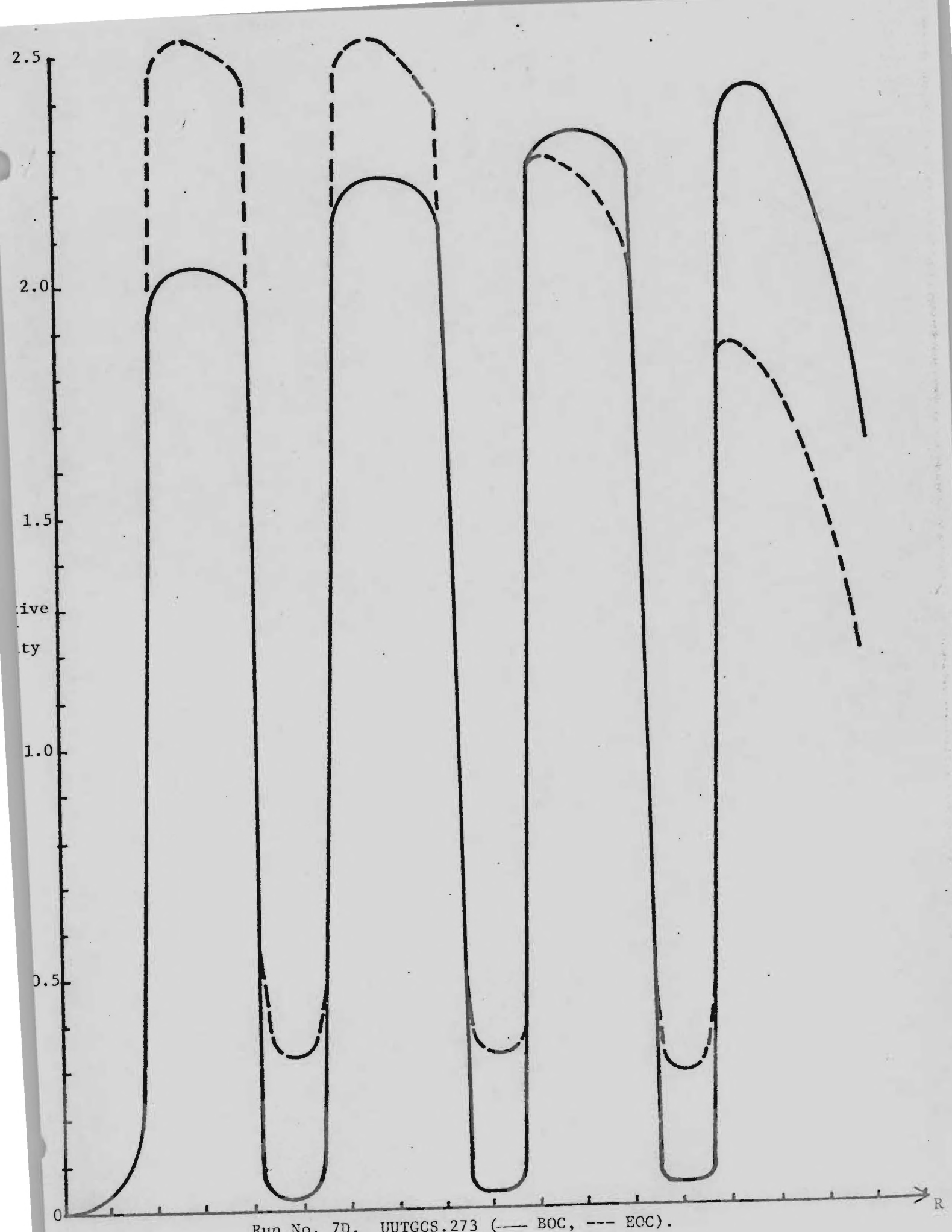

Run No. 7D. UUTGCS.273 (—— BOC, --- EOC).

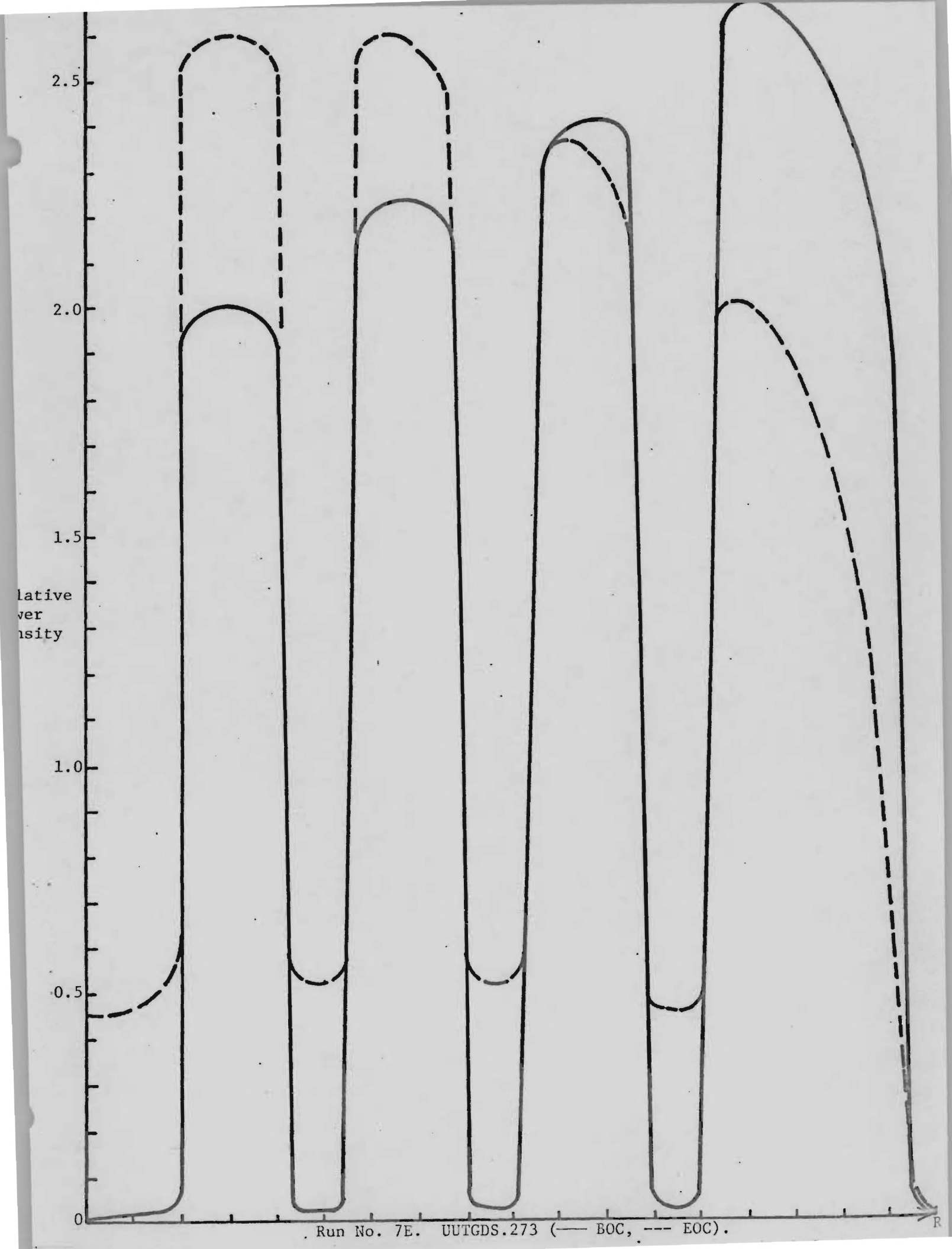

Run No. 7E. UUTGDS.273 (—— BOC, --- EOC).

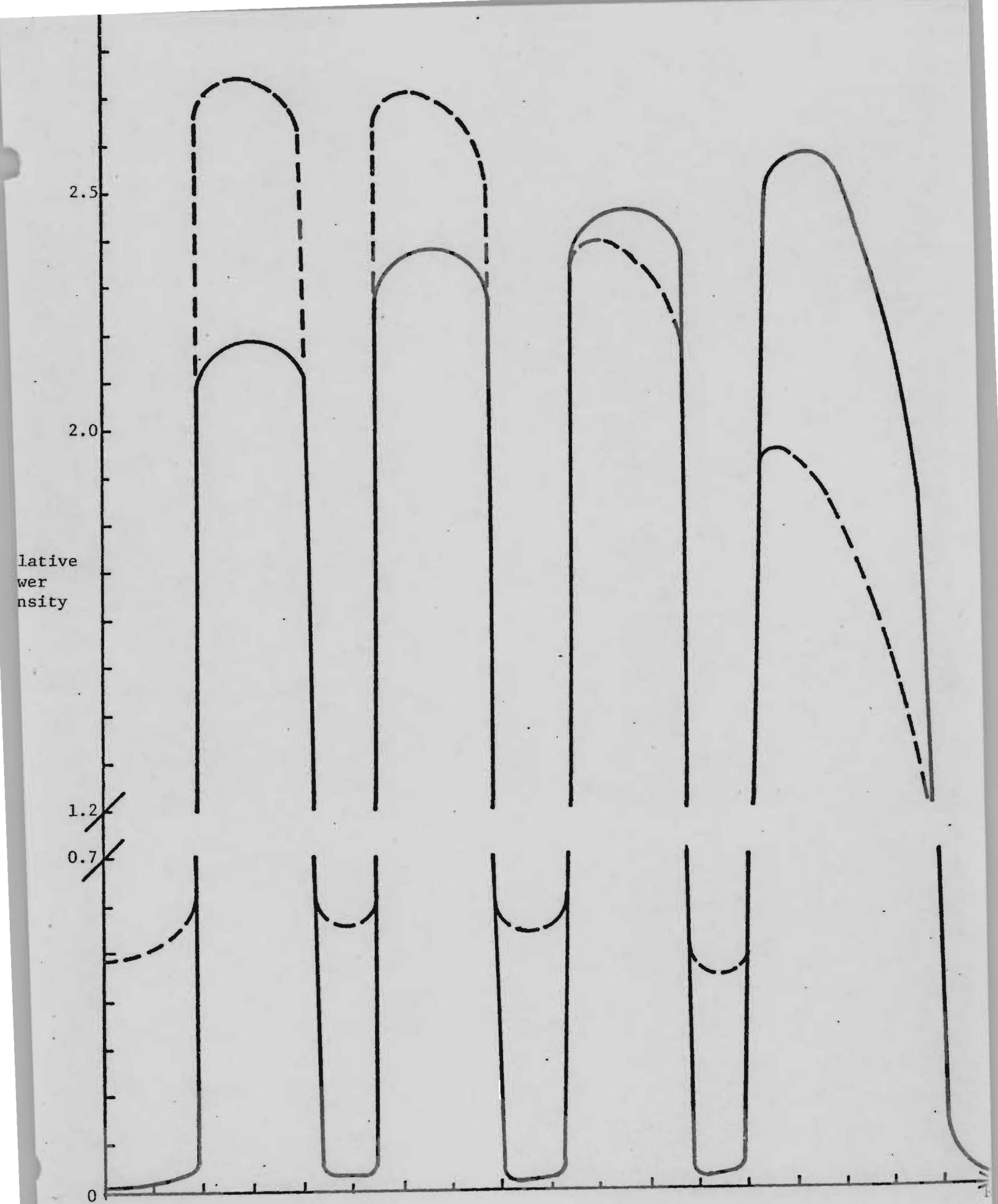

Run No. 7F. UUTGES.273 (—— BOC, --- EOC).

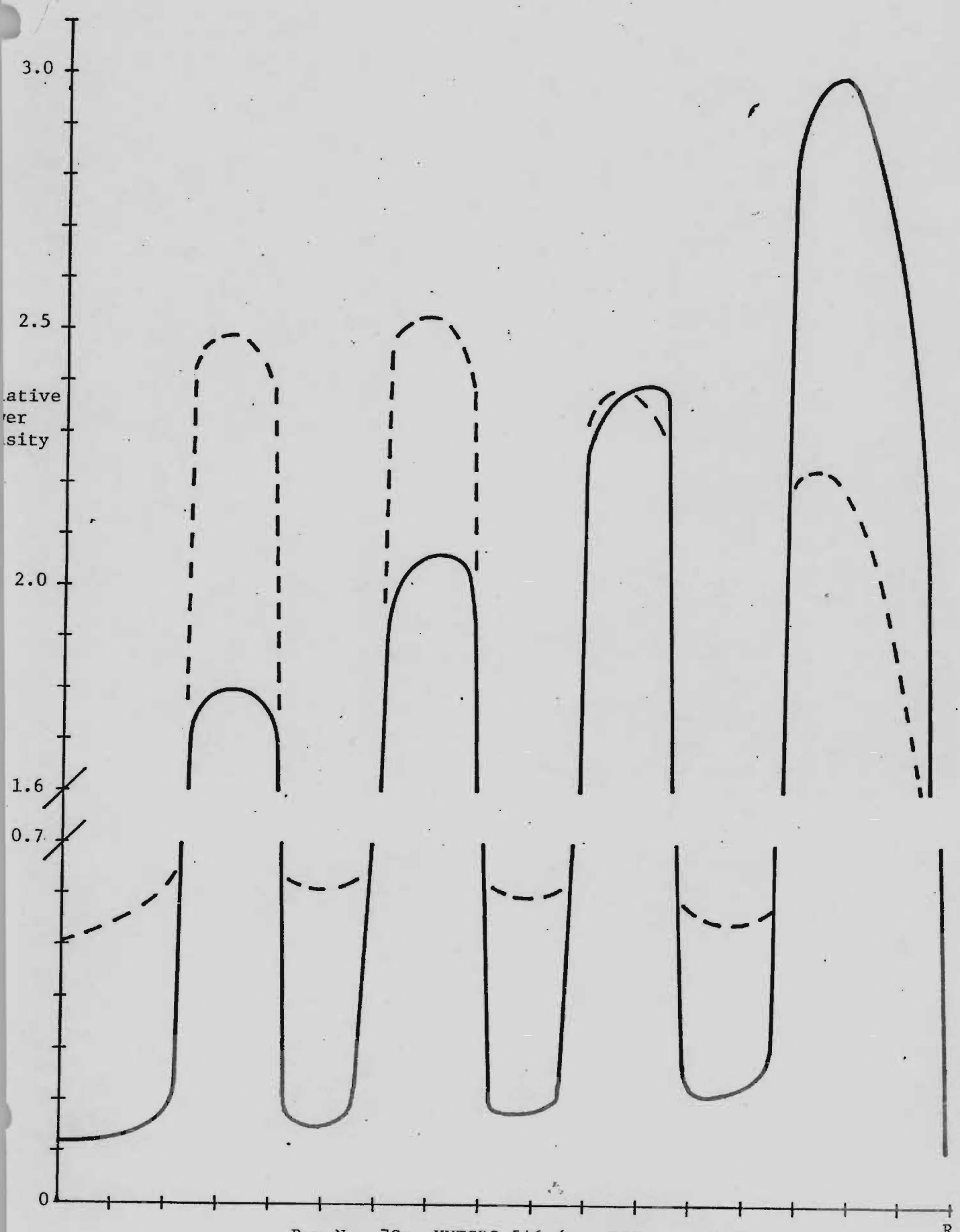

Run No. 7G. UUTGBS.546 (—— BOC, --- EOC).

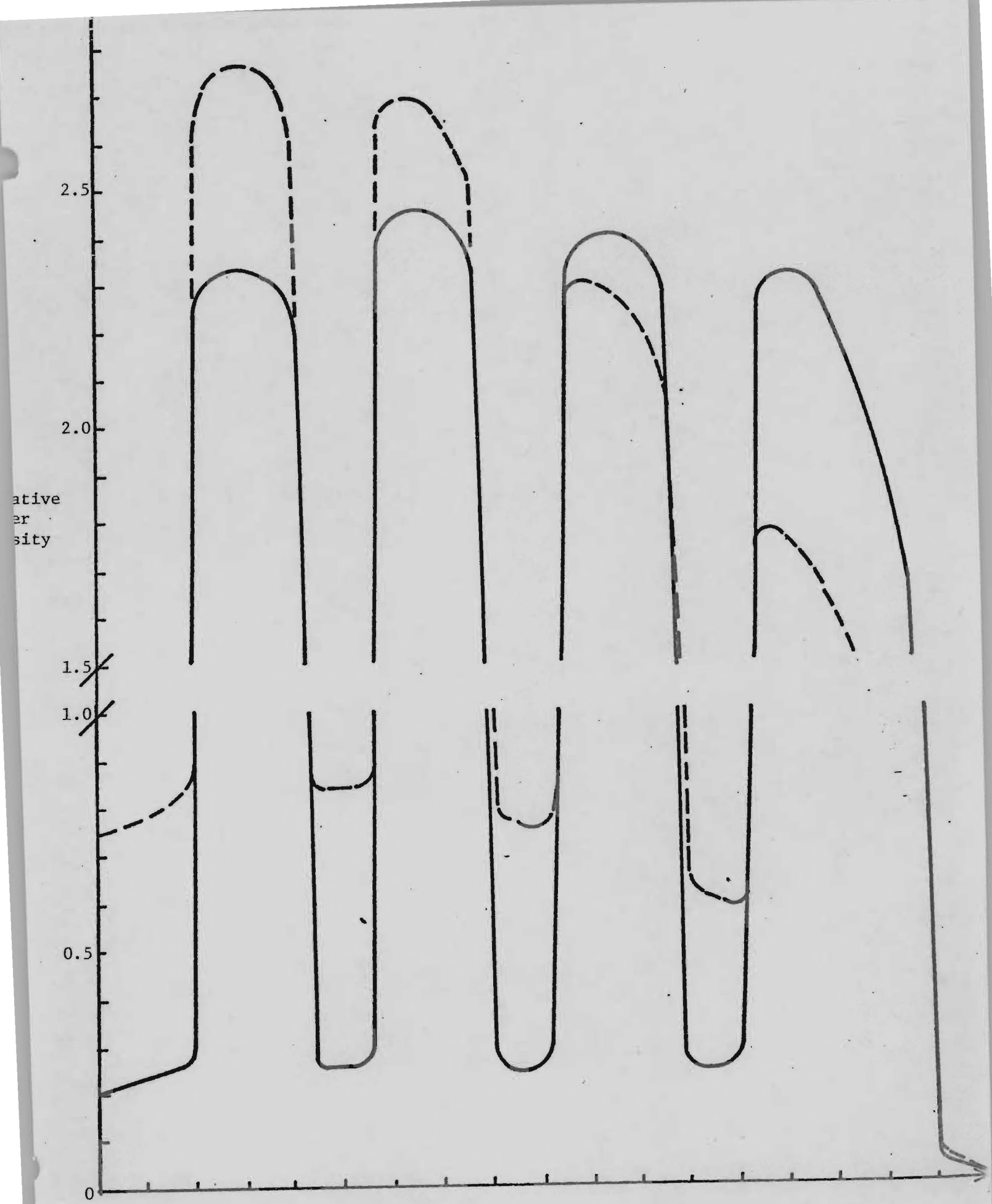

Run No. 7H. UUTGDS.546 (—— BOC, --- EOC).

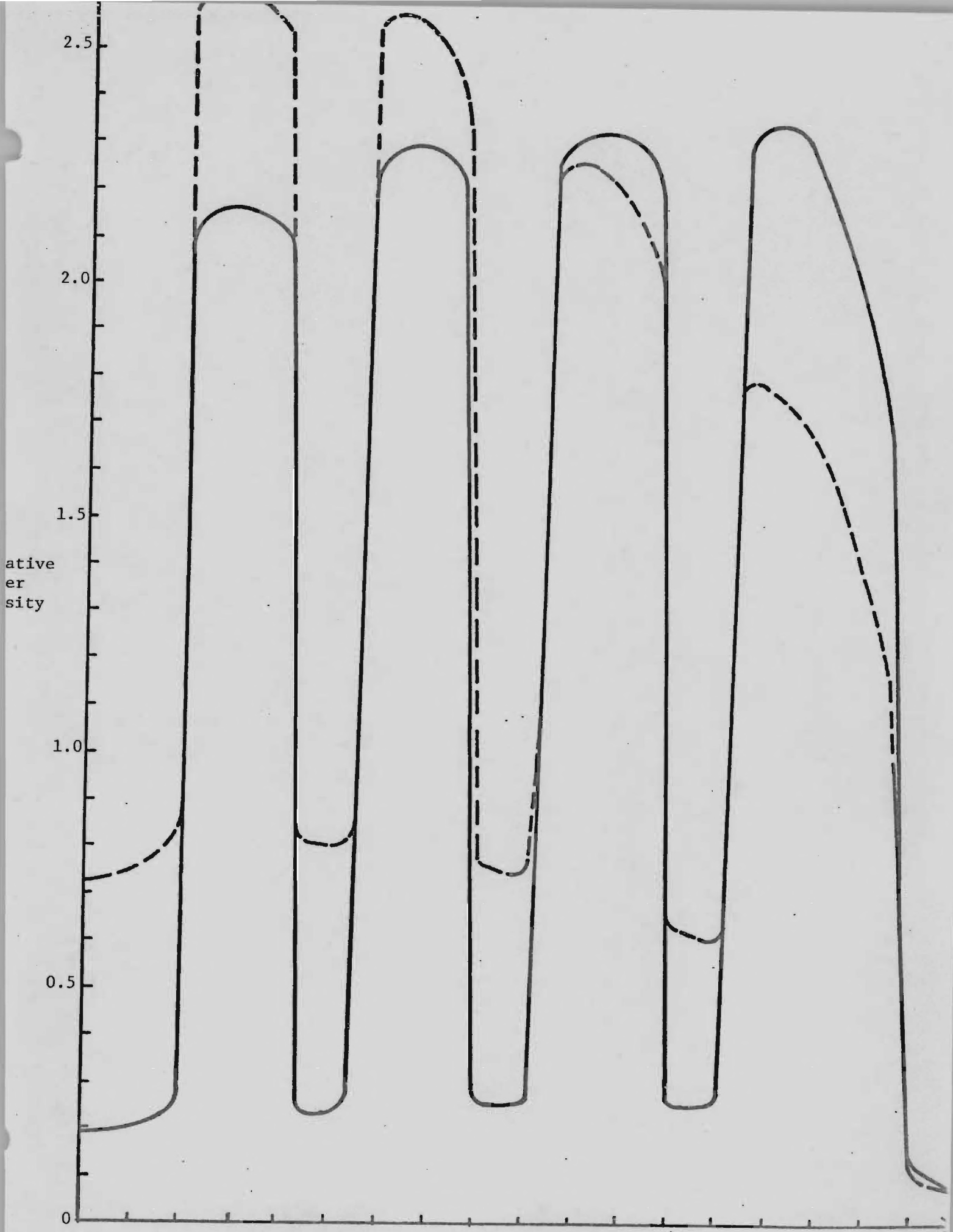

Run No. 7I. UUTGDS.EQI (——BOC, --- EOC).

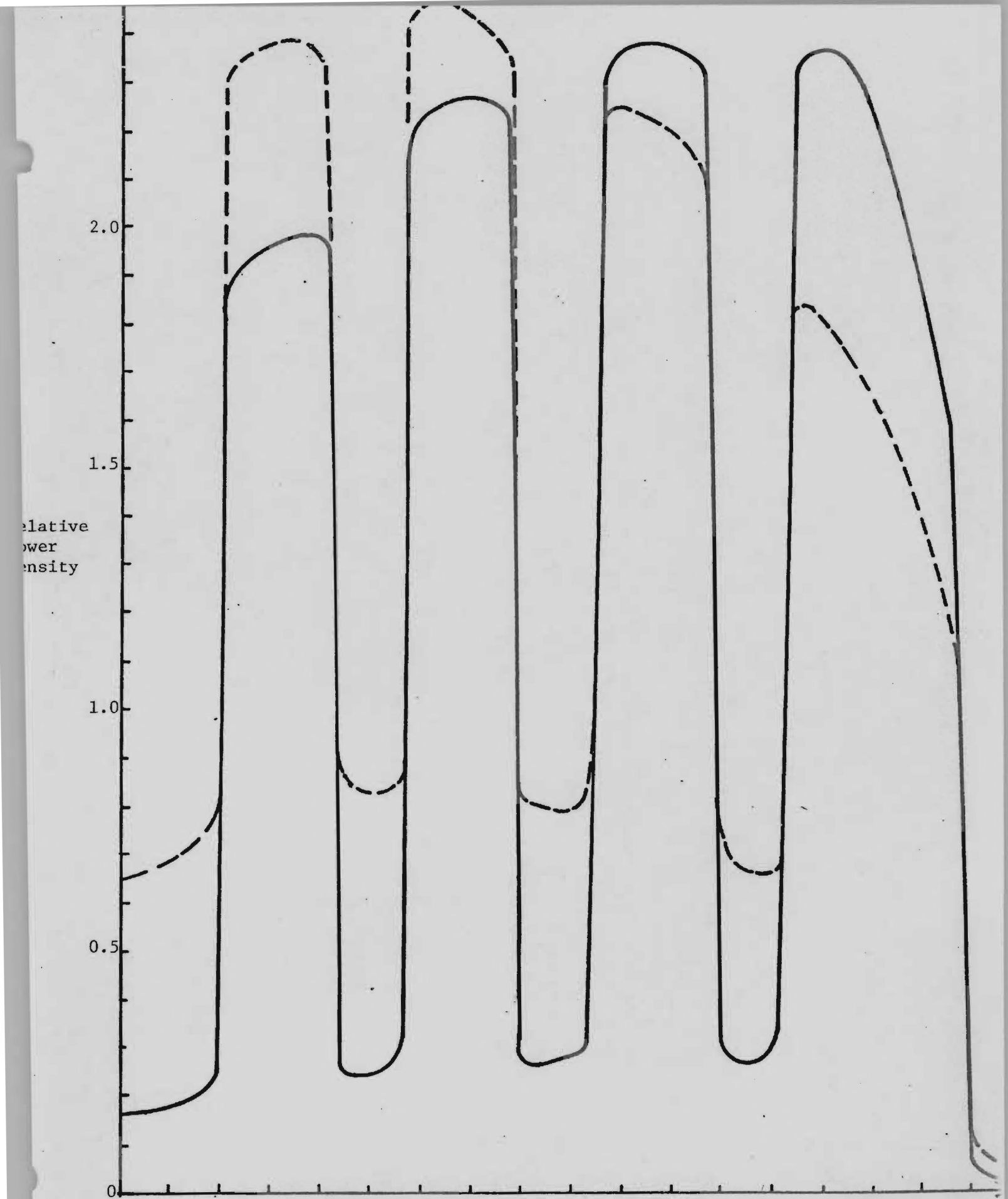

Run No. 7J. UUTGXD.546 (—— BOC, --- EOC).

ORNL Progress Report
March 1978

APPENDIX III

ALTERNATIVE FUEL CYCLES FOR BREEDER REACTORS*

D. E. Bartine, T. J. Burns, and J. R. White
Oak Ridge National Laboratory
Oak Ridge, Tennessee, U.S.A.

J. M. Kallfelz and D. M. Rowland
Georgia Institute of Technology
Atlanta, Georgia, U.S.A.

ABSTRACT

The impact of various "alternative" nuclear fuel cycles, particularly those involving thorium and ^{233}U, is addressed. Due to recently accentuated concerns regarding possible use of nuclear power reactor fuel as a source of weapons fissile material, such fuel cycles are of interest since they possess certain inherent proliferation-resistant chracteristics. In particular, the impact on breeder reactors is considered. Both "homogeneous" (fissile core region surrounded by fertile blankets) and "heterogeneous" (fertile blankets intermixed with core assemblies) designs are addressed. Additionally, the breeding and growth characteristics of symbiotic systems involving ^{233}U production reactors in safeguarded energy centers and dispersed reactors operating on proliferation-resistant $^{233}U/^{238}U$-based fuel are examined. The neutronic calculations indicate that such symbiotic systems have the potential of supporting reasonable energy growth rates.

(Presented at the Miami International Conference on Alternative Energy Sources, Miami Beach, FL, December 5-7, 1977.)

*Research sponsored by the Department of Energy under Contract with Union Carbide Corporation.

INTRODUCTION

Recently accentuated concerns regarding the possible use of reactor fuel as a source of weapons material have led to an overall reassessment of various alternative fuel cycles. In particular, the recycle of plutonium and the development of plutonium-producing Liquid Metal Breeder Reactors (LMFBRs) have been questioned. Long-term viability and growth of fission-based nuclear generating capacity, however, must ultimately rely on both recycle fuel and breeder reactors. Prudence therefore dictates that any alternative cycle which has potential for reducing the attractiveness of breeder reactor fuel as a source of nuclear weapons material be examined. The denatured ($^{233}U/^{238}U/^{232}Th$) fuel cycle [1,2,3] is one such option being studied and one that extends to the recycle/breeder scenario the most prominent proliferation-resistant characteristic of the current once-through low-enriched ($^{235}U/^{238}U$) uranium cycle: an intrinsic "isotopic barrier." The fresh fuel consists of fissile ^{233}U denatured with ^{238}U to the extent that it cannot serve as a direct source of weapons-usable material (i.e., it would require the use of an isotope enrichment facility). This is in contrast to ^{239}Pu-based fuel cycles in which the fissile material in the fresh fuel is directly accessible via chemical separation and for which no denaturant analogous to ^{238}U exists.

In assessing the impact of the alternate fuel cycles, a $Pu/^{238}U$ reference LMFBR design [4] was selected and analyzed, and the performance parameters of alternate fissile/fertile fuel combinations were then calculated by replacing the reference core and blanket materials by the appropriate alternative material(s). For these initial studies no attempt was made to modify or optimize the designs to account for differences in the thermo-physical properties of the alternative fuel materials relative to the reference system. Such differences were considered only when obviously necessary, e.g., to ensure that the fuel and fertile pin maximum linear powers for the various materials were not exceeded.

The breeding performance of the alternate LMFBR fuel cycles is significantly lower than that of the reference system, one reason being the lower values of ν and the associated η (neutrons produced per fission and per fissile absorption, respectively) of ^{233}U relative to the fissile plutonium isotopes. Additionally, the replacement of ^{238}U by ^{232}Th as the core fertile material also has a deleterious effect resulting from the markedly lower fast fission effect of ^{232}Th relative to ^{238}U.

A further point which must be addressed regarding the denatured reactors is their self-sufficiency in terms of the fuel material, ^{233}U. Since the denatured systems contain ^{238}U in addition to ^{232}Th, ^{239}Pu is produced via neutron capture. Thus, in evaluating the self-sufficiency of a fast breeder reactor, the ^{233}U component of the overall breeding ratio is of primary importance since the bred plutonium cannot be recycled back into the denatured system. Moreover, the ^{233}U component of the breeding ratio increases as the allowable denatured "enrichment" (percent of uranium atoms which are ^{233}U) is increased, since such an increase allows more Th to replace ^{238}U in the fuel material. One potential means for improving

the self-sufficiency of a denatured reactor, namely the utilization of a "heterogeneous" or radial "parfait" core design [5-13], has been investigated. Although initially conceived as a means to increase the breeding performance (as well as to assuage certain safety-related problems), the heterogeneous design (which has fertile fuel assemblies interspersed with fissile driver assemblies) is of particular interest for these alternate cycles because of its greater breeding flexibility. However, since all denatured reactors require an initial inventory of ^{233}U, as well as varying amounts of ^{233}U as makeup material, a second class of reactors must be considered when evaluating the denatured fuel cycle. The function of these systems would be to produce the ^{233}U required by the denatured reactors. Possible LMFBR candidates for this role, using various combinations of fissile and fertile material for both a "classical" or homogeneous model (i.e., two core enrichment zones surrounded by fertile blanket regions) and a "heterogeneous" core, have been considered. Some examples of such reactors are a ^{233}U/Th breeder and various "transmuter" reactors which burn plutonium and produce ^{233}U, such as a Pu/Th LMFBR, or a breeder with Pu/^{238}U fuel elements and ThO_2 in various fertile regions. All of these systems, since they are not denatured, must be subject to rigorous safeguards, that is, operated only in nuclear weapon states or in internationally controlled energy centers. A symbiotic system, such as that depicted in Fig. 1, is envisioned in which the "inside" reactors consume plutonium and produce ^{233}U for the denatured reactors and vice versa.

MODELS AND CALCULATIONAL METHODS

Codes, Input Data

Nine-group cross-section sets were generated for various reactor regions, using the code system MINX/SPHINX/AMPX [14-16] and ENDF/B-IV input data. The results reported in this paper for reactor performance parameters were calculated with CITATION [17] using a two-dimensional cylindrical geometry. For a test case, comparison of results with those from a three-dimensional hexagonal geometry calculation validated the adequacy of the two-dimensional annular models utilized in this study.

Model

The model used for our studies was based on the design prescribed for the Large Core Code Evaluation Working Group (LCCEWG) in Ref. [4]. This LMFBR is not the commercial design of a specific organization, but is a compromise model determined after discussion among various members of the LCCEWG, and has general performance parameters felt to be typical of a possible future commercial LMFBR. Table I gives some of the principal features of this homogeneous core design.

The initial plutonium feed composition was typical of that produced by a LWR, as specified in the Clinch River Breeder Reactor Preliminary Safety Analysis Report and used in the Large Heterogeneous Reference Fuel Design Study (LHRFDS) [18], i.e., weight percents of about 67%, 19%, 10%, and

2.5% for ^{239}Pu, ^{240}Pu, ^{241}Pu, and ^{242}Pu respectively. The depleted uranium used for the fertile material was assumed to contain 0.25% ^{235}U.

General Methods

For the cases investigated, the fuel and fertile element volume fractions were maintained as in Ref. [4]. Atom densities for the various fuel and fertile element combinations were determined considering the different densities of the oxides involved, e.g., $(Pu/U)O_2$, UO_2 and ThO_2. For the heterogeneous models, the cylindrical models (described in more detail below) were established for fertile and fissile elements with the same volume fractions as those of Ref. [4]. Thus the calculations reported here do not include any optimization of the pin sizes to take advantage of the superior thermal properties of the materials used for the alternative cycles. For instance, mixed $(U,Th)O_2$ rods can sustain a larger maximum linear power than the base case $(U,Pu)O_2$ rods, and the same is true of ThO_2 compared to UO_2. Thus in principle the fuel and blanket rod radii could be somewhat larger, thereby increasing the fuel volume fraction [13,19].

Annual refueling, a plant capacity factor of 75%, and maximum burnup of 100,000 MWd/T were assumed. These constraints led to replacement of 1/3 of the fuel elements and 1/6 of the radial blanket elements for the homogeneous cores at each refueling, while for the heterogeneous cases these fractions were 1/2, 1/3, and 1/6 for the fuel, internal blanket, and radial blanket elements respectively.

Using the above assumptions, depletion calculations were performed until the equilibrium cycle was reached, i.e., the point at which the isotopic composition of the discharged elements does not change from cycle to cycle. The values reported here are for this cycle; for time-dependent parameters such as the breeding ratio, mid-cycle values are given. Using a code written to be compatible with CITATION, iterations were performed to adjust the initial first cycle fissile loading so that criticality was maintained with a minimum fissile inventory.

RESULTS FOR HOMOGENEOUS REACTORS

General Results

Overall breeding performance characteristics for homogeneous LMFBRs with certain alternative fuel cycles are presented in Table II. The breeding ratio was calculated utilizing the following definition:

$$BR = \frac{\text{fertile capture rate}}{\text{fissile absorption rate}} \quad . \qquad (1)$$

The common European practice of assigning "equivalence factors" [5,8,20] to the various fissile and fertile isotopes based on their relative worth

with respect to k_{eff} has not been followed. Since such equivalence factors depend on reactor type, the proper definition and use of such factors becomes difficult in studies of symbiotic systems involving various reactor types. The studies of the symbiotic characteristics of such systems reported here are based on the actual mass flows calculated for the various fissile isotopes.

It must be noted however that Eq. (1) represents an approximation in that it assumes that the fissile production rate is equal to the fertile capture rate. For Pu/^{238}U fueled systems, the difference between the two rates is insignificant due to the short half-life (large decay constant) of the intermediate nuclide, ^{239}Np. For alternative fuel cycles involving ^{232}Th, however, the use of Eq. (1) does represent a slight approximation due to the much longer half-life of ^{233}Pa.

The designation of a compound fissile doubling time (CFDT) in Table II also represents a modification in parameter definition necessitated by the alternative cycles. Since some of the bred fissile material produced in a given reactor may not be available for recycle in the reactor, the commonly used terminology of a "reactor doubling time" is somewhat misleading. The designation of a compound fissile doubling time is employed to emphasize this difference. The parameter, however, is defined in a manner similar to that used for the compound system doubling time for a single fuel cycle system (e.g., Pu/U):

$$\text{CFDT} = \frac{0.693 \times (\text{fissile mass, initial core + 1 reload})}{(0.98 \text{ eq. cycle fissile discharge} - \text{eq. cycle fissile charge})} \qquad (2)$$

The compound fissile doubling time is thus a measure of the rate of excess fissile production. The value of 0.98 used in Eq. (2) represents a recovery factor (i.e., assumes 2% losses).

As discussed above, the overall breeding performance of the various alternative cycles is reduced relative to the reference case (the Pu/U case listed first in Table II). The replacement of $^{238}UO_2$ by ThO_2 as the fertile material as well as the substitution of $^{233}UO_2$ for PuO_2 as the fissile material reduces the overall breeding ratio and increases the CFDT. Moreover, increasing the denatured uranium "enrichment" (the atom percent ^{233}U), and thereby allowing more Th in the fuel, results in lower values for the breeding ratio (and increased fissile doubling times). However, Fig. 2 illustrates a desirable effect of higher enrichment for denatured reactors, namely the increase in the ^{233}U component of the breeding ratio. Note that in this figure and elsewhere in this article, the term "X% denatured U" means denatured uranium with X% ^{233}U enrichment.

Certain characteristics of three possible candidate reactors for the safeguarded area ^{233}U producers are given in Table III. Clearly, each system has its own unique properties. From the standpoint of ^{233}U production

capability, the hybrid Pu/Th LMFBR is clearly superior. However, it does require a large quantity of fissile Pu as makeup since it essentially "transmutes" plutonium into ^{233}U. The $Pu/^{238}U + ThO_2$ radial blanket LMFBR generates significantly less ^{233}U but also markedly reduces the required plutonium feed. In fact, for the case illustrated, this system actually produces a slight excess of plutonium. The third possible LMFBR system considered is the $^{233}U/Th$ breeder which is characterized by a very small excess ^{233}U production. Moreover, it does not provide a means for utilizing the plutonium which is bred in the denatured systems.

Energy Center and Dispersed Reactor Symbiosis

Potentially, the reactor types used in the energy center represent a higher proliferation risk than the dispersed denatured reactors, although with adequate control of the center this risk could be made quite small. Furthermore, there are many obvious reasons to avoid generation of too large a percentage of the world's total nuclear power capacity in such centers. Hence, there is a strong incentive to minimize the number of inside reactors. The amount of power generated by the dispersed reactors relative to that generated inside the energy centers is a crucial symbiotic parameter. The power ratio (i.e., outside power/inside power) typically results in a symbiotic "window" constrained on one side by ^{233}U production and by plutonium production on the other. Moreover, once initiated, a system of dispersed denatured LMFBRs and energy center LMFBRs is characterized by an asymptotic power ratio, at which point the relative growth rate of each fissile inventory is identical. This asymptotic value can be viewed as the "natural" symbiotic power ratio. Additionally, a true compound system doubling time can be calculated at this value of the power ratio since each component of the system is increasing at the same rate.

This asymptotic value is determined by assuming that the inventory of each fissile isotope is compounded continuously (in a manner similar to that used to calculate a reactor's compound doubling time). Figure 3 illustrates the time-dependent behavior of a symbiotic system's power ratio using a logical initial value, namely, no denatured reactors because of an initial lack of ^{233}U. It should be noted that the asymptotic value is approached regardless of the starting configuration. Also indicated on Fig. 3 is the power window bounded by P_{min} and P_{max}, outside of which the system cannot operate without some external supply of fissile material, e.g., already-bred LWR plutonium. Table IV gives some symbiotic system parameters for certain reactor combinations. As indicated, a trade-off clearly exists concerning system doubling time and asymptotic power ratio achieved.

HETEROGENEOUS CORE DESIGNS

Development of Heterogeneous Core Concepts

The term "heterogeneous core" is used, in general, to describe LMFBR designs which are comprised of distinct fertile regions interspersed with fissile regions in the core. This concept is in contrast to that of the "classical"

or homogeneous LMFBR core, which has fertile material mixed homogeneously with the fissile material.

While studies of this concept were conducted in the 1960's at Risley [6,7], interest in heterogeneous core designs was recently revived by a paper presented by Mougniot et al. [5] at the 1975 European Nuclear Conference at Paris, describing French investigations of this topic. The emphasis of this latter paper was on the potential improvement in the doubling time of a LMFBR which this concept offers. Also discussed was the fact that, for certain situations, a heterogeneous core may also have a lower positive sodium void coefficient than for a homogeneous design. Some early LMFBR designs and studies, such as the Westinghouse modular reactor [21] and the annular core investigated by Spenke [22], used a heterogeneous design primarily to improve the sodium voiding characteristics. The investigation by Sehgal et al. [21] of an LMFBR fueled with modular assemblies, each containing a fuel and blanket region, was also an attempt to incorporate this advantage into a reactor design.

Due to the apparent success of the French LMFBR program, including considerable operating experience with a demonstration LMFBR plant, it was natural that their studies of the heterogeneous core would stimulate international interest in this concept. Further, with the growing concern about excessively large doubling times for commercial oxide-fueled LMFBRs, the potential high breeding gains (0.35-0.40) of a heterogeneous core with such fuel clearly made it a concept of high interest for designers. The last several years have seen considerable international activity in this area [8-13,24,25], including a national U.S. study [18] to assess heterogeneous and homogeneous designs under various imposed constraints.

Some Characteristics of Heterogeneous Cores

Presently, some disagreement exists on whether the potential for improved breeding ratio and doubling time characteristics in heterogeneous cores is real. Some investigators state that the heterogeneous core has a markedly improved breeding potential [5,9,10-12], while others conclude that this is not the case [23,25]. This disagreement can be attributed to several factors:

(a) The heterogeneous core can be optimized for improved breeding potential or reduced sodium void reactivity: in some designs the latter advantage is emphasized to the detriment of the former.

(b) The performance characteristics of various "heterogeneous core" designs cover a much wider range than those of "classical" or "homogeneous" cores being considered. Partially this is because the "classical" core designs are now much more similar to each other than are the various proposed heterogeneous core designs. Also, for the same general concept, the heterogeneous core performance is sensitive to such factors as the fuel element size, ring placement, etc. Some examples of this sensitivity are discussed in Refs. [10,24]. For instance, a "tightly-coupled" core (small internal fertile regions) has markedly different characteristics than a "loosely-coupled" core.

(c) There is considerable difficulty in defining which classical core to compare with the heterogeneous design. Some aspects of this problem are evident from a survey of the heterogeneous core references cited above, as well as from the results of the LHRFDS study [18]. Comparison of a reactor of each type, for example, with the same average enrichment and critical mass is precluded by the intrinsic differences in the two designs.

(d) For different MW(e) capacity reactors or reactors with different constraints on core size, the conclusions can be different. For instance, some studies of "pipe" type LMFBR systems have had a stringent physical constraint on the total core and blanket size, while the French and Italian studies are for a Superphenix [26,27] "pot" type LMFBR, for which this limitation is somewhat more flexible. One clear disadvantage of a stringent size constraint is that the increased core size when heterogeneity is introduced may require a reduced radial blanket size.

(e) The comparison is further complicated by other factors related to fuel management, fuel fabrication costs, etc. For instance, some studies assume the same pin size for the internal fertile elements as for the radial blanket, as in Level I of LHRFDS [18]. Due to the high fissile production rate in the internal elements, however, they must be replaced more frequently than those of the radial blanket to avoid excessive pin temperatures. In other studies a smaller pin has been assumed but this decreases the volume percent of fertile material in these regions, with an associated decrease in the breeding ratio. For their studies of an 1800 MW(e) heterogeneous core, the French assume an internal fertile pin size intermediate between the driver and radial blanket pin sizes [12]. The requirement for three pin sizes, however, also affects the fabrication costs.

The fact still remains, however, that many studies have reported considerably improved breeding ratio (BR) and/or doubling time results for the heterogeneous core, compared to some "equivalent" homogeneous systems [5,9-12,24].

Despite the various sophisticated arguments about what constitutes an "equivalent" classical system (which as indicated above is a complex issue), it appears that a simple procedure for comparisons can be established as a valid basis - at least to compare the breeding potential of the two systems. Some particular "classical" LMFBR design that has been through an optimization process for the homogeneous design is adopted. The fertile and fissile assemblies are then arranged in heterogeneous designs (a process necessitating an increase in the enrichment of the fissile assemblies) to determine whether, for some configuration, the breeding potential is improved. While the heterogeneous design should not have any significant operating parameters which are obviously worse than for the classical design (e.g., maximum pin temperature), the evaluation of all such parameters is clearly the subject of a large study such

as the LHRFDS [18]. (Of course, some nominal characteristics of the elements for the two designs, e.g., duct venting, may differ.) If the heterogeneous concept shows higher breeding potential, further arguments about whether the heterogeneous system design parameters (pin size, element size, etc.) are optimized seems irrelevant to answer the original question: does the heterogeneous concept have improved breeding potential? Presumably "optimization" of the heterogeneous design will further improve its performance. The above procedure has been employed in this study.

Clearly, the term "breeding potential" is ambiguous since an improved breeding ratio does not necessarily result in a reduced doubling time. Among other differences, heterogeneous cores typically require higher critical loadings, a factor which has a detrimental effect on the doubling time. However, in most cases this latter effect is outweighed by the increase in breeding gain, resulting in a lower doubling time.

Some contributing factors to the higher breeding gain (and reduced doubling time) in a heterogeneous core are:

(a) The space dependence of the neutron flux, $\phi(E,\vec{r})$, in the core is an advantage. That is, it is not only a question of putting more fertile material where the total flux is higher - which could also be accomplished in a homogeneous core with a revised fuel pin and assembly containing a higher heavy metal volume - but also of the energy spectrum of the neutron flux at these locations.

(b) The core "internal conversion ratio" (BI) is quite high, approaching 1.0. The resulting reduced requirement for excess reactivity at the start of the cycle permits a design with fewer control rods, which is a clear advantage for the breeding in the upper blanket.

(c) A relatively flat flux in the heterogeneous core leads to an increased value of the fractional breeding gain in the surrounding blanket regions.

Point (a) is illustrated by calculations performed in Italy [10] and reported in detail in [24]. Using the CNEN code CIAP-1D [28] for several heterogeneous core models, the generalized adjoint function $\psi_g^*(r)$ was determined for the total breeding ratio (BR) and for the internal conversion ratio (BI) for the "core" (which includes both the fissile driver assemblies and the internal blanket assemblies). These functions reflect the importance of a neutron at a given location (r) and in a particular energy group (g) to either the BR or BI.

For a $(Pu/U)O_2$ heterogeneous model with a general configuration similar to that of Fig. 4, the difference between ψ^* for low and high energy neutrons ($\psi_{20}^* - \psi_5^*$) is illustrated in Fig. 5. As indicated, the quantity plotted is generally positive for the fertile regions and negative for the fissile regions, reflecting the importance of a soft fertile region spectrum and hard fissile region spectrum to the internal conversion rate.

Figure 5 also illustrates the spatial variation of the spectrum within the core -- in precisely the manner which is advantageous to BI (and BR). The proportion of the low energy neutrons (represented by the quantity, ϕ_{20}/ϕ_5, is appreciably greater for the fertile regions, as expected. It should be noted that a "classical" core with a "homogeneous" mixture of fissile and fertile material in the core does not have this feature; in the homogeneous core, both $\phi_g(\vec{r})$ and $\psi_g^*(\vec{r})$ typically vary monotonically over the core.

The energy "shape" of $\phi_g(\underline{r})$ in the fertile regions is not the sole criterion for an improved BI however. The absolute values of the important group fluxes in the fertile regions (relative to those in the fissile regions) must also be considered. As can be seen in Table V, the absolute values for this model are favorable to an increased BI. Using the approximate centers of neighboring core regions, the ratio $\phi_g(\text{fissile})/\phi_g(\text{fertile})$ is roughly 0.7 for the low energy group and 1.4 for the high energy group.

Of course a higher BR does not necessarily mean an improved doubling time. However, many of the cited reports which compare the two design concepts under varying assumptions report a clear reduction in the doubling time for a heterogeneous core relative to the homogeneous design. A quote from Ref. [11] summarizes the view of the SNR-2 designers:

> "The present results indicate that the heterogeneous design has improved core performance data and long-term breeding potential. An improvement of safety is expected, but is still to be proved by detailed safety calculations. If this is achieved, the development of an heterogeneous core design will be recommended for SNR-2."

The design of heterogeneous cores is, of course, quite complicated and requires considerable experience and iteration steps. For example, Spenke, who has years of experience in this field, reported [30] that after studying a great number of configurations at Interatom they arrived at a heterogeneous design that had essentially the same fissile loading as for their SNR-2 homogeneous core. This contrasts with the commonly accepted rule in the U.S. that heterogeneous cores have appreciably higher fissile loadings.

Furthermore, it should be made clear that even if the neutronics properties of such cores were completely known, there are other areas, particularly mechanical and thermodynamic problems, which would need further theoretical and experimental investigation, as indicated by the above quotation.

Models Used

For the heterogeneous core models, the fuel element parameters were the same as those given in Table I for the homogeneous reactor models.

The fertile and fissile element region arrangement is shown in Fig. 4. This layout is similar to models developed at NIRA, the Italian participant in the Superphenix project, which was reported in Refs. [8,10,24]. The

core fertile elements have the same composition as those of the radial blanket. These models have been designed to obtain a fairly flat power distribution during operation and utilize a single fissile element enrichment (an economic advantage because of standardization of the fuel cycle operations) [12].

The fertile regions of the denatured reactors consisted of ThO_2 assemblies while the driver pins contained both UO_2 and ThO_2, the quantity of the latter material depending on the enrichment of the denatured uranium. It should also be noted that a heterogeneous case analogous to the 12% denatured homogeneous case was not analyzed. The 12% value represents the minimum enrichment (i.e., the core assemblies containing ^{233}U and ^{238}U but no ^{232}Th) for the homogeneous reactor model employed. For the fuel assembly design and reactor configuration assumed, the use of internal fertile blanket regions increases the required fissile loading. Thus, the fissile enrichment of the driver assemblies must be increased to compensate for this effect. In light of this effect, the lowest fissile enrichment considered for the heterogeneous cases was 20%.

For the safeguarded energy center transmuter reactors, cases with fresh fuel pins of either $(Pu/U)O_2$ or $(Pu/Th)O_2$ were considered. The former case has the advantage of employing a fuel material for which much developmental experience exists. A reactor utilizing the latter fuel, on the other hand, would have greater production rate of ^{233}U. All blanket and internal fertile zones of the transmuter reactors contained ThO_2 as the fertile material.

Results for Heterogeneous Cores

The approximate power distributions calculated at the beginning and end of the initial cycle for a denatured heterogeneous reactor are shown in Fig. 6. This result assumes that all energy from fission is deposited at the point where the fission occurs, and does include the capture-gamma energy deposition. A detailed coupled neutron-gamma transport calculation would be necessary for a more accurate curve. The depicted curve, however, does illustrate some characteristics of heterogeneous cores which make further study of their thermal and mechanical characteristics imperative, e.g., large changes in the internal fertile element power and changes in the overall distribution shape during the cycle. For the equilibrium cycle the former change is less drastic on the average for the fertile annular regions, as is the difference between the power production of the outer and inner fissile regions.

The spectral change between fertile and fissile regions for the denatured reactors also contributes to an increase in the $^{233}U/^{239}Pu$ production ratio for the heterogeneous cores, relative to that for the homogeneous cases. For 20% denatured cases, the average per atom ratio of ^{232}Th capture to ^{238}U capture was about 15% higher for the core fissile and fertile regions of the heterogeneous reactor than for the homogeneous core.

Figure 7 demonstrates that the use of a heterogeneous design for the denatured LMFBRs increases the overall breeding ratio, and moreover that the use of ThO_2 internal blanket assemblies markedly improves the ^{233}U to plutonium

production ratio. In fact, it appears feasible to design a "self-sufficient" denatured heterogeneous LMFBR using 30% denatured uranium as a fuel.

The use of the heterogeneous designs for the safeguarded center results in a significant increase in the ^{233}U production rate, even if $(Pu/U)O_2$ drivers are maintained, as indicated by Fig. 8.

One of the significant results is that the use of heterogeneous designs for one or both components tends to increase the asymptotic power ratio as well as decrease the overall system doubling time, as illustrated in Table VI. It is also interesting to note that the compound system doubling time reaches a minimum as the enrichment of the denatured fuel is increased up to a certain point (around 30%) and then starts to increase.

INFLUENCE OF NUCLEAR DATA

Because there was only minor interest in the ^{233}U-Th cycle for fast breeder reactors until the last several years, there has been much less experimental and analytical investigation of the significant nuclear data for this cycle relative to that for the Pu-^{238}U cycle. Hence, the estimated error limits for the significant nuclear data of the former cycle are considerably higher than for the latter cycle.

A nuclear data change (and also a design change, such as adaptation of the heterogeneous core concept) which influences the breeding ratio can have a much stronger influence for a case with a low breeding ratio, characteristic of the alternative cycles, than for a case with a high breeding ratio. The doubling time is roughly inversely proportional to the breeding gain, i.e., the breeding ratio minus 1; thus a 0.10 change in the breeding ratio is clearly much more likely to influence the doubling time significantly if the original breeding ratio is 1.1 rather than 1.3.

As an example of this influence, we have considered the effect of a new evaluation of the ^{232}Th capture cross section by Macklin and Halperin [31]. As shown in Fig. 9, their evaluation is roughly 10 - 20% lower than the ENDF/B-IV values over a wide energy range. We performed calculations for two of the homogeneous cases (20% denatured and Pu/Th transmuter), using group cross section values approximating the curve in Fig. 9. The reductions in the breeding ratios were about 0.05 and 0.07 respectively, which corresponds to about a 50% decrease in breeding gain for both these cases. While the symbiotic power ratio for a system employing both these reactors changed only slightly, the increase in the system doubling time was much more significant, increasing by approximately a factor of three.

Before viewing these results too pessimistically it should be emphasized that other important data for the ^{233}U/Th cycle may have compensating errors. More importantly, there is conflicting information which indicates that the ENDF/B-IV thorium capture data may not be as much in error as suggested by [31]. At Argonne National Laboratory, recent calculations [32]

with ENDF/B-IV of the per atom ^{232}Th capture to ^{235}U fission ratios for two gas cooled fast reactor critical experiments gave calculation/experiment values of 1.0±2%. Corrections for foil environment have not yet been applied, but are estimated to be less than 2 - 3% [32].

While the impact of current inaccuracies of the basic nuclear data on the viability of the various alternative fuel cycles is significant, it is important to note that many unfavorable changes can be accommodated by design modifications. Moreover, efforts to determine more accurate data and reduce the uncertainties for significant nuclear parameters involved in alternative cycles have increased considerably in the last year.

CONCLUDING REMARKS

The denatured fuel cycle, as outlined above, clearly represents a trade-off between nuclear performance and proliferation concerns. The denatured fuel cycle reduces the possibility of using fresh recycle fuel for weapons purposes due to the chemical inseparability of the fissile component. However, it also reduces the energy growth rate sustainable in a breeder-based economy.

In particular, the question of allowable denatured enrichment is crucial. As the results given above indicate, the nuclear performance benefits from a relatively high fissile enrichment (up to perhaps 30% ^{233}U in ^{238}U for the heterogeneous reactors). However, from a safeguards standpoint, a much lower enrichment is desirable.

The introduction of any new cycle, of course, involves many factors, most of which can be characterized as "developmental uncertainties." Such uncertainties may delay the introduction of certain reactors and eventually, when resolved, eliminate some systems as impractical. The influence of present nuclear data uncertainties on the performance has been discussed. The need for more studies of the mechanical and thermal properties of the heterogeneous core concept has also been mentioned; the French are planning experimental studies of these characteristics in their Rhapsodie and Phenix fast reactors [33].

Development of the thorium fuel cycle is necessary for the alternative fuel cycles, and this would involve significant new research and development programs. At present the information available on the behavior in a fast breeder reactor of the mixed oxides proposed for the alternative fuel cycles is much less than that for $(Pu/U)O_2$ fuel. Furthermore, reprocessing procedures for the alternative cycles will require considerable development.

While the above factors and uncertainties may have considerable impact on the eventual performance values and paths followed, the calculations reported here indicate adequate compound system doubling times may eventually be attained with the proposed symbiotic systems of dispersed and energy center LMFBRs.

The impact of the denatured fuel cycle on breeder-based nuclear power will clearly be significant, resulting in reduced power growth capability compared to a system based only on the Pu/U. Additionally, owing to the requirement for safeguarded energy centers, implementation of the denatured fuel cycle will require changes in international institutional arrangements as well as international agreement on what constitutes "adequate" denaturing. Thus considerations other than the purely technical aspects addressed here will clearly impact the viability of the denatured fuel cycle.

REFERENCES

1. U. S. Dept. of State. Committee on Atomic Energy. (D. E. Lilienthal, Chairman) "..A Report on the International Control of Atomic Energy," U. S. Dept. of State Publication 2498, U. S. Government Printing Office, Washington D. C., pp. 127-198 (March 1946).

2. H. A. Feiveson and T. B. Taylor, "Security Implications of Alternative Fission Futures," Bull. At. Scientist, 32, 14 (December 1976).

3. T. J. Burns and D. E. Bartine, "Feasibility of Denatured LMFBRs," Trans. Am. Nucl. Soc., 26, 285 (June 1977).

4. Letter from Edouard Kujawski, Fast Breeder Reactor Department, General Electric, to Members of the Large Core Code Evaluation Working Group, SUBJECT: Transmittal of Design for Use in Large Core Code Evaluation, (January 29, 1976).

5. J. C. Mougniot, J. Y. Barre, P. Clauzon, D. Giancometti, G. Neviere, J. Ravier and B. Sicard, "Gains de Regeneration des Reacteurs Rapides a Combustible Oxyde et a Refrigerant Sodium," Nuclear Energy Maturity, Proceedings of the Paris Conference. Progress in Nuclear Energy Series 1976. Pergamon Press, Oxford and New York.

6. R. T. Ackroyd, J. E. Mann, M. A. Perks, "Notes on the Effect of the Heterogeneous Core Construction on Breeding Gain and Doubling Time," Internal Risley document, 1968 (Private communication, R. T. Ackroyd).

7. R. T. Ackroyd, M. A. Perks, "Low Inventory, Short Doubling Time, High X and Good Voiding Characteristics from Reactors with Heterogeneous Cores," Internal Risley document, 1968 (Private communication, R. T. Ackroyd).

8. G. Bruna, J. M. Kallfelz and G. Palmiotti, "Advances in the Heterogeneous Core Concept," NIRA External Report T-NA-E-10004-F, Nucleare Italiana Reattori Avanzati, Genoa (1976).

9. U. Wehman, "Safety Aspects in Nuclear Core Design of LMFBR's," Proc. Int. Meeting on Fast Reactor Safety and Related Physics, Chicago (October 5-8, 1976).

10. G. B. Bruna, G. P. Cecchini, G. Gastaldo, J. M. Kallfelz, G. Palmiotti, M. Salvatores, D. Rowland, D. Bartine, T. Burns, "Studies of the Heterogeneous LMFBR Core Concept for Several Fuel Cycles and Its Sensitivity to Design and Cross-Section Changes," Trans. Am. Nucl. Soc., 26, 558 (June 1977). See also many other summaries in these transactions concerning the heterogeneous core concept, particularly on pages 552-562, e.g. the following two references.

11. H. Spenke, U. Wehmann, S. Pilate, R. de Wouters, E. Kiefhaber, "Physics Studies of a Heterogeneous Core Concept for SNR-2," Trans. Am. Nucl. Soc., 26, 561 (June 1977).

12. B. Sicard, J. C. Mougniot, H. Sztark, J. C. Cabrillat, C. Giacometti, M. Carnoy, P. Clauzon, "Preliminary Physics Studies of a Large Fast Core Based on the Heterogeneous Concept," Trans. Am. Nucl. Soc., 26, 553 (June 1977).

13. R. A. Doncals, et al, "Transposition of Fuel and Blanket Assemblies in LMFBRs," Presentation at Am. Nucl. Soc. Meeting, New York, June 12-16, 1977.

14. C. R. Weisbin, P. D. Soran, R. E. MacFarlane, D. R. Harris, R. J. LaBauve, J. S. Hendricks, J. E. White and R. B. Kidman, "MINX: a Multigroup Interpretation of Nuclear X-Sections from ENDF/B," LA-6488-MS (ENDF-237) Los Alamos Scientific Laboratory (September 1976).

15. N. C. Paik, et al, "Physics Evaluations and Applications Quarterly Progress Report for Period Ending July 31, 1974," WARD-XS-3042-7, Westinghouse Advanced Reactors Div. (July 1974).

16. N. M. Greene, J. L. Lucius, L. M. Petrie, W. E. Ford, III, J. E. White and R. Q. Wright, "AMPX: A Modular Code System for Generating Coupled Multigroup Neutron-Gamma Libraries from ENDF/B," ORNL-TM-3706, Oak Ridge National Laboratory (March 1976).

17. T. B. Fowler, D. R. Vondy and G. W. Cunningham, "Nuclear Reactor Core Analysis Code: CITATION," ORNL-TM-2496, Rev. 2, Oak Ridge National Laboratory (July 1971).

18. "Ground Rules Large Heterogeneous Reference Fuel Design Study," Combustion Engineering, Inc., Windsor, Conn. (October 22, 1976).

19. T. G. Ayers, M. T. Benedict, F. L. Culler, Jr., J. L. Everett, III, R. V. Laney, C. D. Perkins, C. Starr, C. Walske, "LMFBR Program Review by the Following Members of the LMFBR Review Steering Committee." See Addendum to Vol. II, "Addendum to the Report of the Task Force - Role of the CRBRP. Alternative Plan," Energy Research and Development Administration (April 6, 1977).

20. C. R. Adkins, "The Breeding Ratio with Correlation to Doubling Time and Fuel Cycle Reactivity Variation," Nuclear Technology 13, p. 114 (1972).

21. R. J. Steck (Comp.), "Liquid-Metal Fast Breeder Reactor Design Study," USAEC Report WCAP-3251-1, Westinghouse Electric Corp., January 1964.

22. H. Spenke, "Reducing the Void Effect in a Large Fast Power Reactor," in Fast Reactor Physics, Proc. Symposium Karlsruhe 30 Oct. - 3 Nov. 1967, p. 365, Vol. II, I.A.E.A., Vienna, 1968.

23. B. R. Sehgal, Ching-In Lin, and W. B. Loewenstein, "A High-Breeding Gain/Low-Sodium Void Coefficient LMFBR Core," in Report EPRI NP-3, Electric Power Research Institute, P.18, August 1975.

24. G. B. Bruna, G. P. Cecchini, J. M. Kalfelz, G. Palmiotti, and M. Salvatores, "Studies of the Heterogeneous LMFBR Core Concept and Its Sensitivity to Design and Cross Sections Variations," NIRA Report, Nucleare Italiana Reattori Avanzati, Genoa, Italy (1977).

25. W. P. Barthold, J. Beitel, E. Khan, C. Tzanos, "Potential and Limitation of the Heterogeneous Reactor Concept," Trans. Am. Nucl. Soc., 26, 552 (1977).

26. J. Chaumont, et al., "Conception du Coeur et des Assemblages d'une Grande Centrale a Neutrons Rapides," Nuclear Energy Maturity, Proc. of the Paris Conference, 21-25 April 1975 Progress in Nuclear Energy Series 1976, Pergamon Press. Oxford and New York (1976).

27. "Technical Data, Fast Reactors," Nuclear Engineering International, April 1975 Supplement, p. 408.

28. I. Dal Bono, V. Leproni and M. Salvatores, "The CIAP-1D Code" RT/FI (68)9, Comitato Nazionale Energia Nucleare, Rome (1968).

29. A. Gandini, "A Generalized Perturbation Method for Bilinear Functionals of the Real and Adjoint Neutron Fluxes," J. Nuclear Energy, 21, 755 (1967).

30. H. Spenke, presentation of Ref. [11] at Am. Nucl. Soc. Meeting, New York, June 12-16, 1977.

31. R. L. Macklin, J. Halperin, "^{232}Th(n,γ) Cross Section from 2.6 to 800 keV," Nucl. Sci. Engr., 64, 849 (1977).

32. C. L. Beck, M. J. Lineberry, et al., "A Review and Analysis of Fast Integral Experiments Related to ^{233}U and Thorium," ZPR-TM-291, Argonne National Laboratory, September 1977. (Referenced with permission of author.)

33. B. Sicard, CEA-Cadarache, private communication (Sept. 1977).

TABLE I. PARAMETERS OF BASIC HOMOGENEOUS CORE LMFBR DESIGN USED IN THIS STUDY

Power (MWe)	1200
Power (MWth)	3085
Fuel Density (1% TD)	92
Core Height (in.)	42
Axial Blanket Height (in.)	13
Rods/Assembly	271
Spacers	Wire
Channel Pitch (in.)	5.47
Rod Pitch/Diameter (P/D)	1.20
Rod OD (in.)	0.260
Cladding Thickness (in.)	0.012
Fuel Gap (in.)	0.0055
Channel Wall Thickness (in.)	0.080
Channel Gap (in.)	0.080
Fuel Volume Fraction (%)	43.3
Structure Volume Fraction (%)	17.4
Sodium Volume Fraction (%)	39.3
Cylindrical Model	
Inner Core Max. Radius (in.)	40.3
Outer Core Max. Radius (in.)	56.4
Radial Blanket Thickness (in.)	15.3

TABLE II. ALTERNATE OXIDE-FUELED HOMOGENEOUS LMFBR PERFORMANCE PARAMETERS (2% losses, 1 year ex-reactor inventory)

Core		Uranium	Axial	Radial	Breeding	CFDT
Fissile	Fertile	enrichment	blanket	blanket	ratio	(yr)
Pu	^{238}U	-	^{238}U	^{238}U	1.272	12.7
Pu	^{238}U	-	^{238}U	^{232}Th	1.272	13.0
^{233}U	^{238}U	~12%	^{238}U	^{232}Th	1.127	24.3
^{233}U	^{238}U	~12%	^{232}Th	^{232}Th	1.121	26.6
^{233}U	$^{238}U/^{232}Th$	20%	^{232}Th	^{232}Th	1.086	43.2
^{233}U	$^{238}U/^{232}Th$	40%	^{232}Th	^{232}Th	1.048	116.4
^{233}U	^{232}Th	100%	^{232}Th	^{232}Th	1.020	-696.4

TABLE III. PERFORMANCE CHARACTERISTICS OF SOME OXIDE-FUELED ^{233}U PRODUCTION HOMOGENEOUS LMFBRs

Fuel material	Blanket material	Net eq. cycle production (kg/GWe-year)		Breeding ratio
		^{233}U	Pu	
$^{233}U/Th$	Th	+ 15.2	-	1.020
$Pu/^{238}U$	Th	+154.2	+ 30.4	1.272
Pu/Th	Th	+582.6	-492.8	1.144

TABLE IV. EQUILIBRIUM CYCLE SYMBIOTIC PARAMETERS OF OXIDE-FUELED HOMOGENEOUS LMFBRs
(2% losses, 1 year out-of-reactor time)

Energy center reactor LMFBR	Dispersed LMFBR	Power ratio Min.	Power ratio Asym.	Power ratio Max.	CSDT[a] (yr)	Energy growth rate (%)
$(Pu/U)O_2 + ThO_2$ RB	~12% denatured	0.00	0.30	0.42	14.5	4.8
$(Pu/U)O_2 + ThO_2$ RB	20% denatured	0.00	0.55	1.00	17.3	4.0
$(Pu/U)O_2 + ThO_2$ RB	40% denatured	0.00	1.00	2.63	23.7	2.9
Pu/Th	~12% denatured	1.13	1.32	1.57	29.0	2.4
Pu/Th	20% denatured	2.52	2.83	3.79	40.9	1.7
Pu/Th	40% denatured	6.55	6.92	9.93	88.7	0.8
-	(Pu/U)		∞		12.7	5.4

[a]CSDT = Compound System Doubling Time

TABLE V. RADIAL SPATIAL VARIATION OF CERTAIN GROUP FLUXES FOR A HETEROGENEOUS CORE MODEL [24][a]

Region	ϕ_{20}	ϕ_5	ϕ_{20}/ϕ_5
1. FERT	1.161	2.597	0.447
2. FISS	0.780	9.497	0.082
3. FERT	1.096	6.791	0.161
4. FISS	0.837	11.02	0.076
5. FERT	1.144	6.892	0.166
6. FISS	0.852	10.66	0.080
7. FERT	1.104	6.942	0.159
8. FISS	0.604	10.43	0.057

[a]Values are at points near the center of the designated core regions, numbered from core center. ϕ_g is in arbitrary units, with energy limits for groups given in Fig. 5.

TABLE VI. PERFORMANCE IMPROVEMENT WITH HETEROGENEOUS OXIDE DESIGNS IN SYMBIOTIC SYSTEMS

Energy center reactor		Dispersed reactor		Power ratio			CSDT
Driver	Blanket	Driver	Blanket	Min.	Asym.	Max.	(yr)
Pu/U	Th	D20*	Th	0.96	1.76	5.76	15.7
Pu/U	Th	D20	Th	1.23	2.25	17.2	16.1
Pu/U	Th	D30	Th	2.16	3.97	∞	15.7
Pu/U	Th	D40	Th	3.31	5.82	∞	17.4
Pu/Th	Th	D20*	Th	2.10	2.85	8.41	18.5
Pu/Th	Th	D20	Th	2.71	3.69	25.1	18.5
Pu/Th	Th	D30	Th	4.73	6.59	∞	17.0
Pu/Th	Th	D40	Th	7.26	9.87	∞	18.6

*Axial extensions of driver contain depleted U; D20 means 20% denatured.

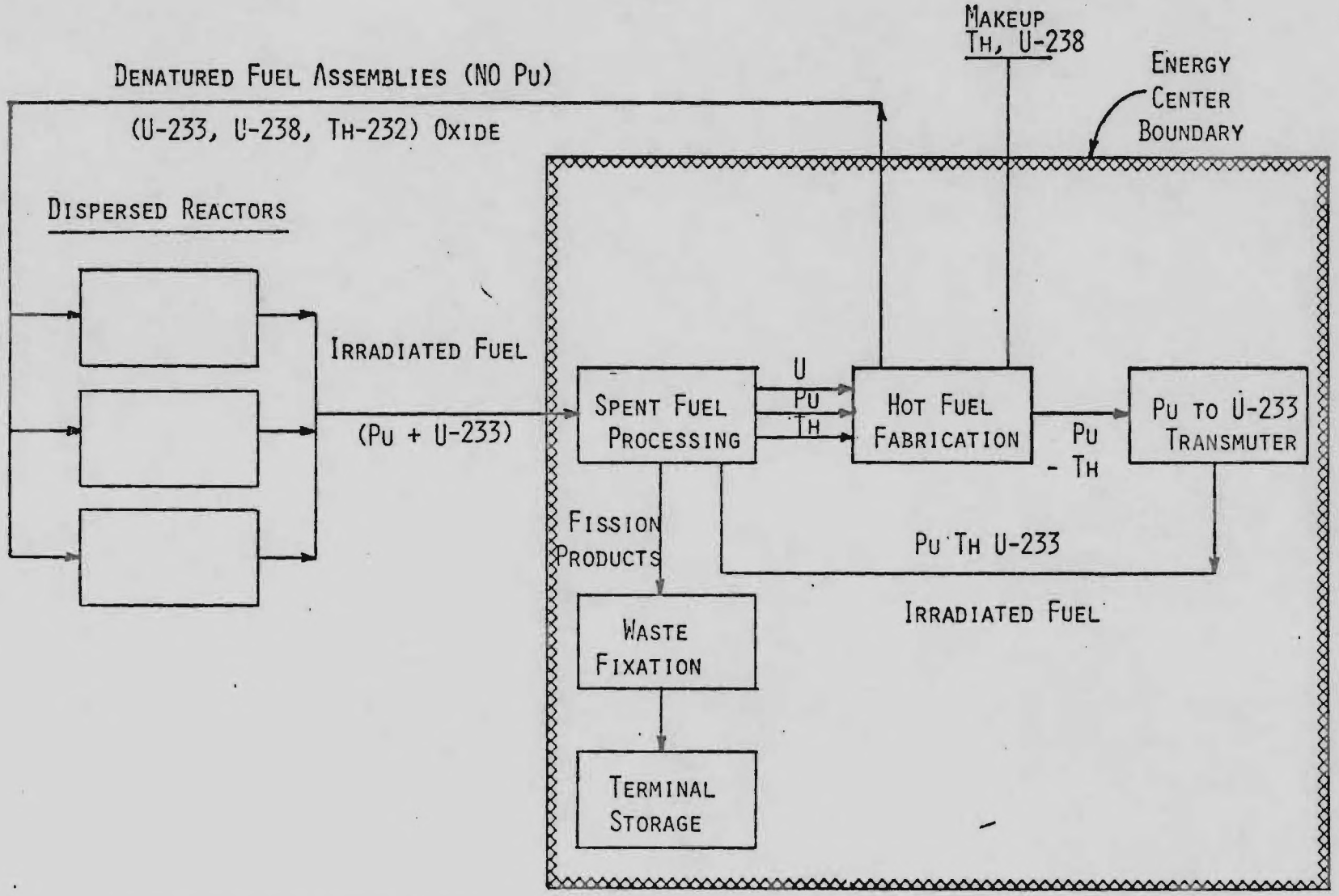

Fig. 1. Schematic Fuel Flow for Denatured Dispersed/Energy Center Symbiosis.

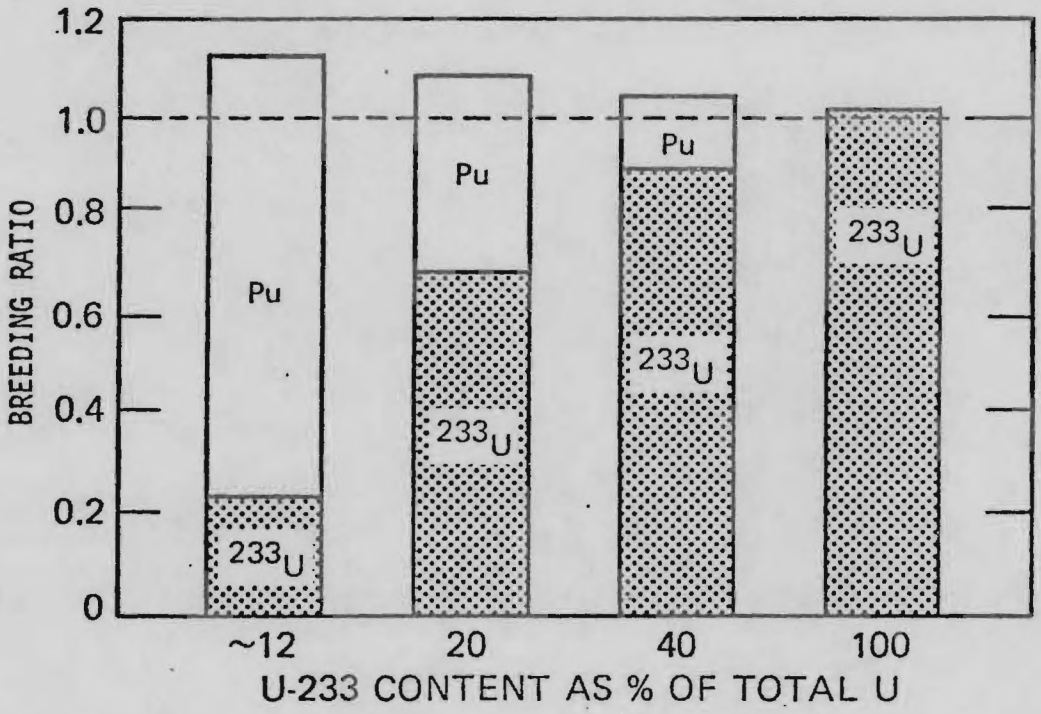

Fig. 2. Alternate LMFBR Fuel Cycle Breeding Ratio Components.

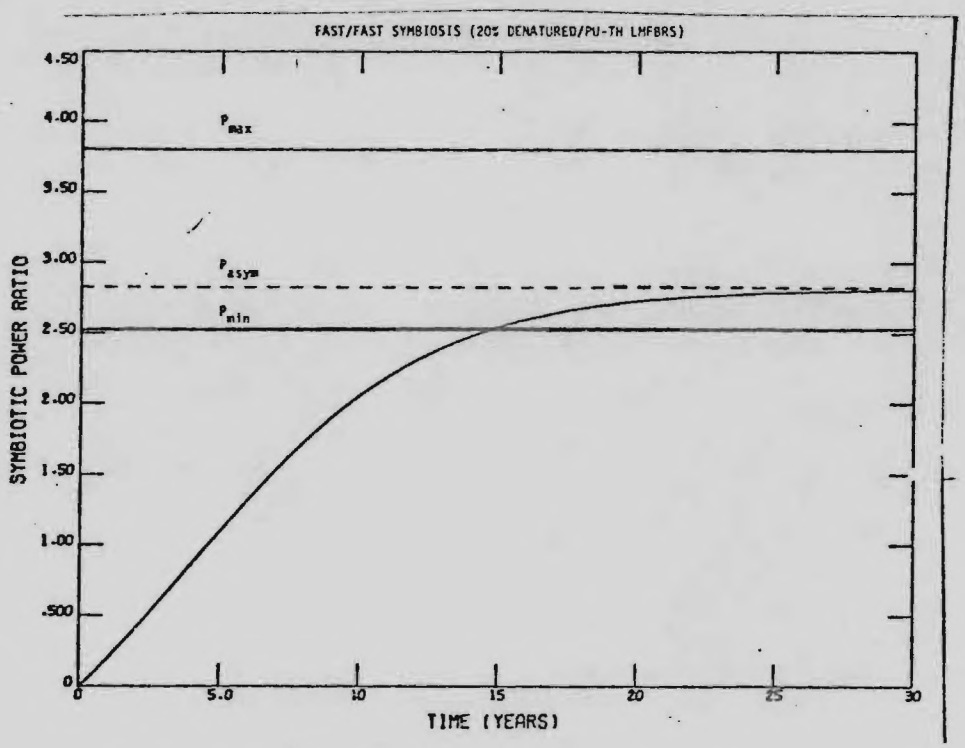

Fig. 3. Time-Dependent Behavior of Power Ratio of Symbiotic System.

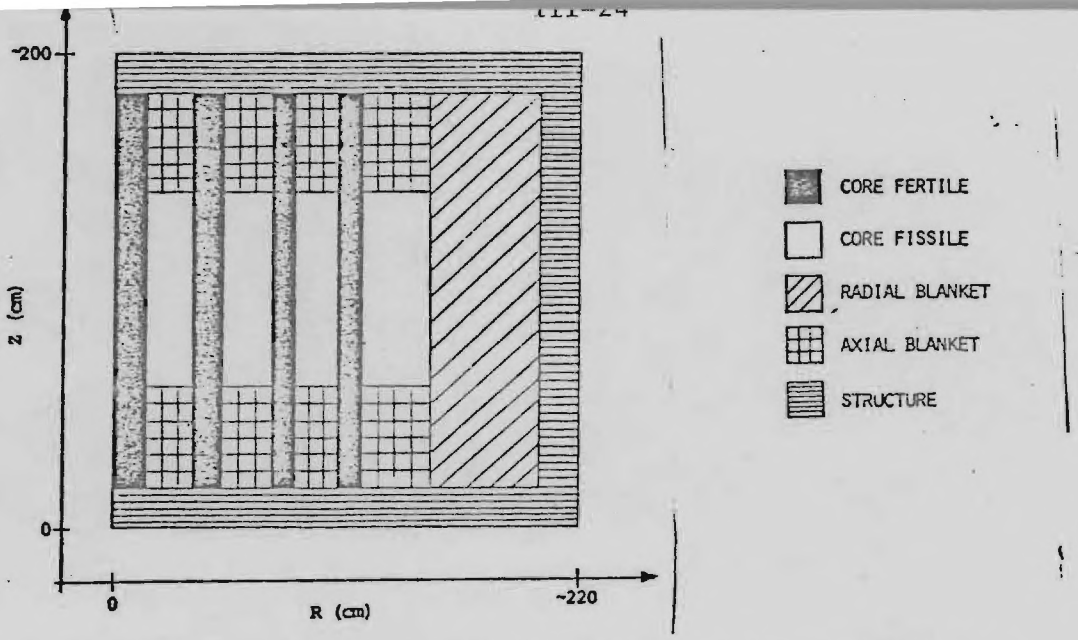

Fig. 4. General Layout of Heterogeneous Core Models.

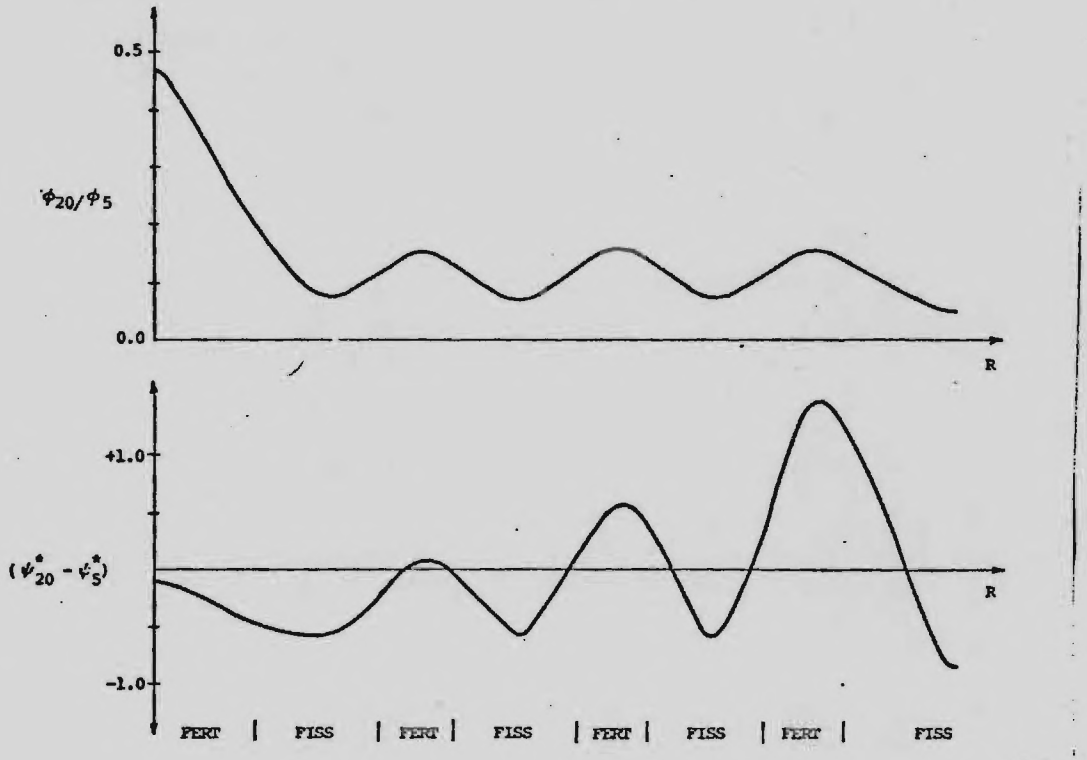

Fig. 5. Neutron Flux (ϕ_g) and Generalized Adjoint (ψ^*_g) Radial Dependence for a Heterogeneous Core. (Energy groups 5 and 20 have boundaries of 0.821 - 1.35 MeV and 454 - 748 eV, respectively.)

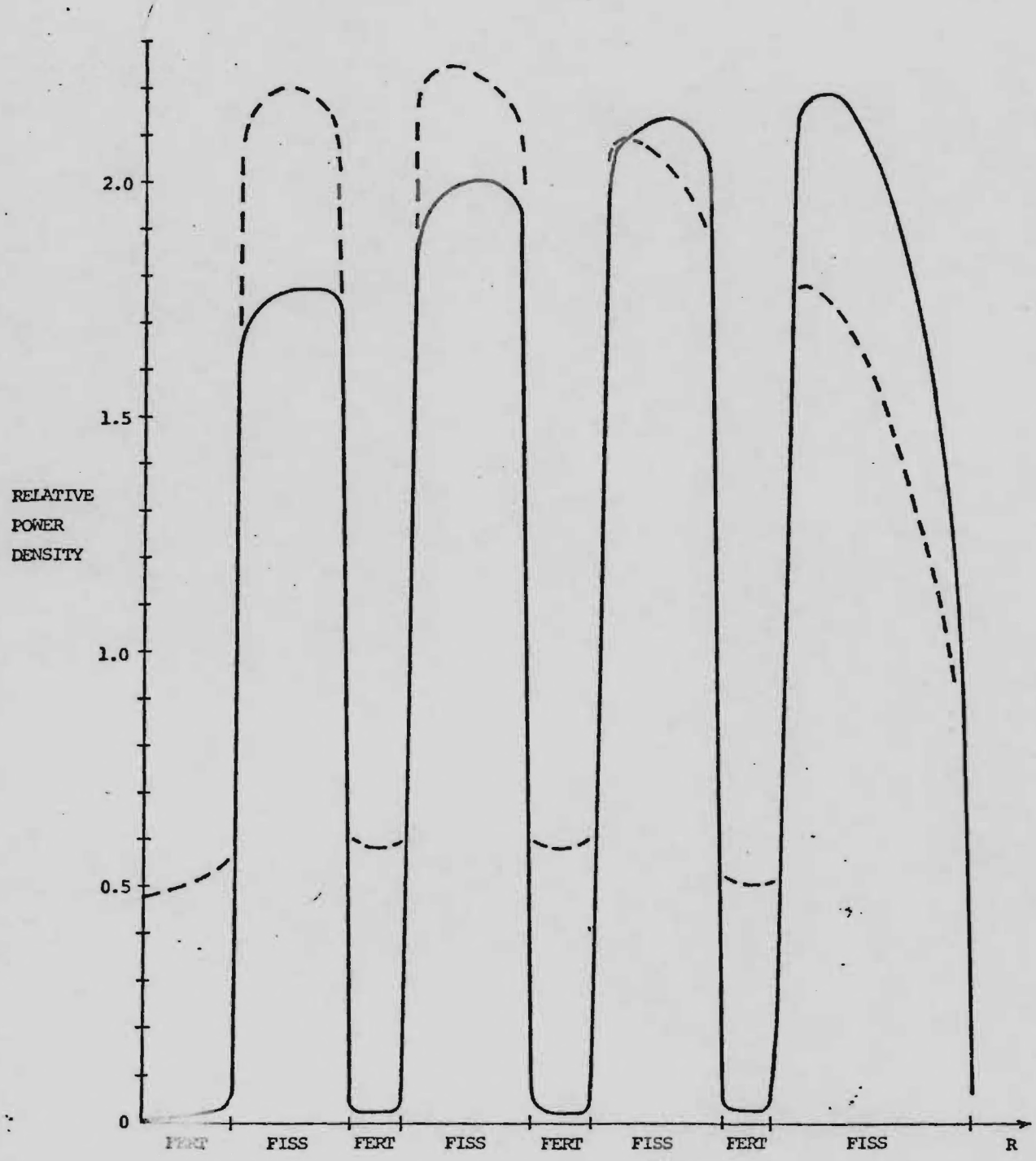

Fig. 6. Radial Power Distributions for a Typical Denatured Heterogeneous Core Configuration. (Solid line, beginning of cycle; dashed line, end of cycle.)

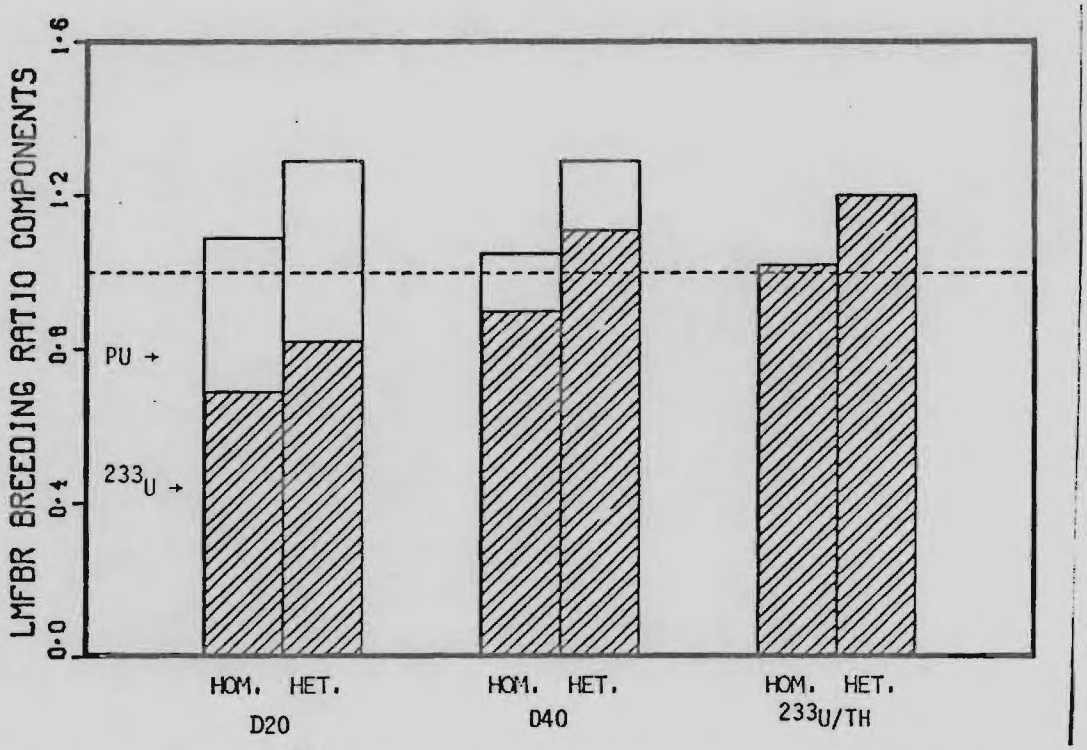

Fig. 7. Increases in ^{233}U Fraction of Bred Fuel with Heterogeneous Denatured Designs. Note: D20 means 20% denatured.

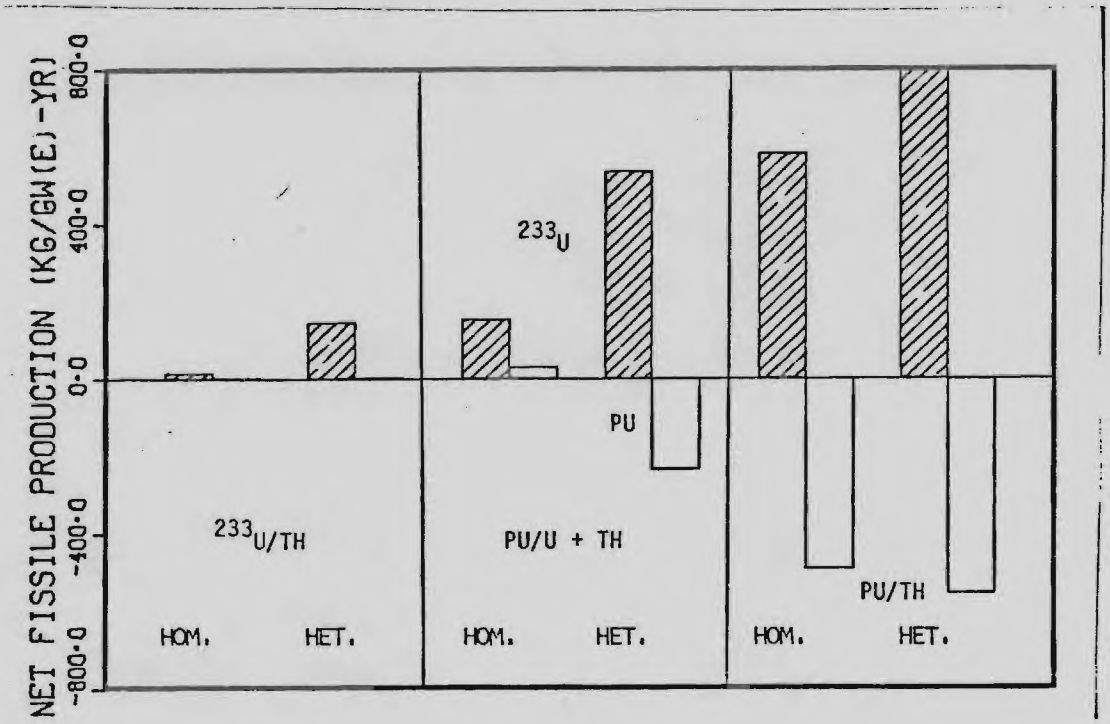

Fig. 8. Increases in ^{233}U Production with Heterogeneous "Transmuters."

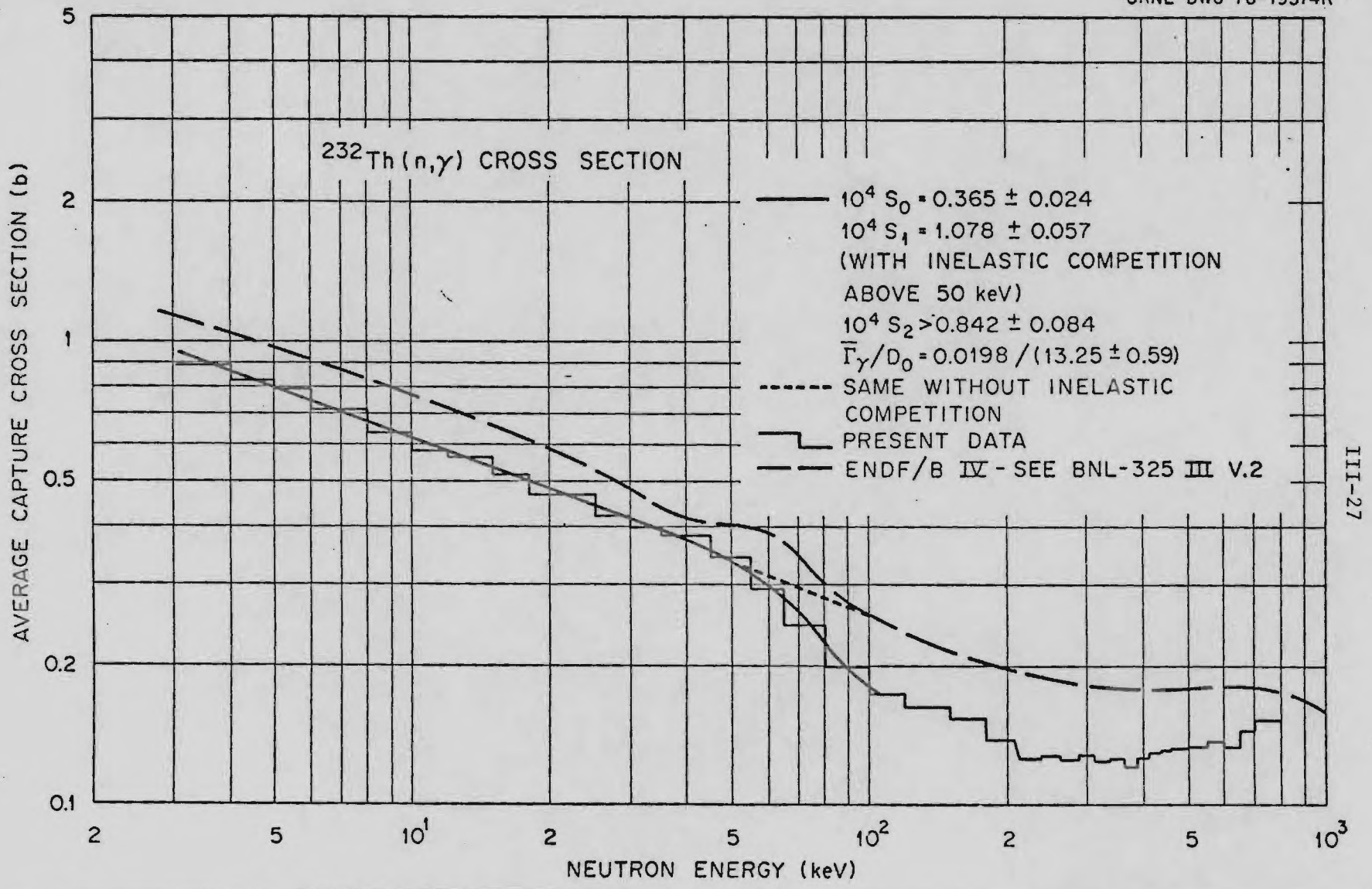

III-27

Fig. 9. Comparison of $^{232}Th(n,\gamma)$ Cross Section Values from ENDF/B-IV with Those from Evaluation by Macklin and Halperin [31].

ORNL Progress Report
March, 1978

APPENDIX IV.

Determination of "Base" Models for Heterogeneous LMFBR Cores, Based on GE LCCEWG Model [13].

1. Geometry - Using the NIRA Model 1 [9] as a guide for determining the number of rows in each region, the GE LCCEWG core [13] was divided into alternating fertile and fissile regions (see Fig. IV-1, 1200 MWe Core Layout). The area of each region was then determined using the hexagonal fuel assumbly pitch of 5.47 inches (13.89 cm) and the number of fuel assemblies per region (see Table IV-1). Core and axial blanket heights are as for the GE model, given on page III-18 (107.7 cm and 33.3 cm, respectively). Additionally, the shield dimension from the GE model was added to the core radius (i.e., 195 - 182.06 = 12.94 cm).

2. Outside the Fence Denatured Reactor Nuclide Concentrations

   A. Fertile Inside Core - Same as Tom Burns' calculation (DU20TT.HM1) except that no concentration was added for channel (51).*

   B. Fertile Outside Core - Same as Tom Burns' calculation (DU20TT.HM1) except that no concentration was added for channel (51) and control (61).

   C. Core Fissile - No channel (51) concentration added. Cladding (31) and Na concentration the same as the GE LCCEWG model [13]. Assuming that PuO_2 and $U^{238}O_2$ have the same weight density and that $U^{233}O_2$ and $U^{238}O_2$ have identical molecular densities, the

*The two-digit numbers after various materials refers to the identification numbers of these materials on the ORNL cross section tape.

same concentrations from the GE model region CZ2 were used for O_2 and U^{238}. Moreover, the initial concentration for U^{233} before the k search is the same as that of Pu for the GE model.

D. Axial Blanket - Channel (51) and control (61) concentrations are zero. Na and clad (31) concentration the same as the GE model. ThO_2 determined by correcting the concentration of UO_2 as follows:

$$N^{ThO_2} = N^{UO_2} \times \frac{10}{10.5} \times \frac{238 + 32}{232 + 32}$$

$$= (.009019)(.974)$$

$$= .008784$$

(units of all densities are 10^{24} atoms/cc)

E. Radial Blanket - Same as Tom Burns' calculation (DU2TT.HM1). Note that he used 10 g/cc as the density for ThO_2.

F. Shielding - Same as the GE Model.

Table IV-2 gives the resulting CITATION input parameters for this model.

3. Inside the Fence Pu/Th Reactor Nuclide Concentrations

A. Fertile Inside Core - Same as 2 above.

B. Fertile Outside Core - Same as 2 above.

C. Core Fissile - Using the densities listed in GE Model CZ2 and assuming the same density for $U^{238}O_2$ and PuO_2 and that the number of ThO_2 molecules can be determined as in 1D above, the following calculations were made for an enrichment of 30%:

$$\frac{Pu + x}{(Pu + x) + (Th - .974x)} = .3$$

where $Pu = 1.722 \times 10^{-3}$

$Th = (.974)(7.248 \times 10^{-3})$

$= 7.060 \times 10^{-3}$

(see 2.D. for derivation of the factor .974)

$x = .9053 \times 10^{-3}$

After the above atom exchange was calculated, Pu isotope concentrations were determined to be consistent with the following Pu isotope weight percentages listed in Table VII, Large Heterogeneous Core Study Guidelines (14):

Pu 239	67.3%
Pu 240	19.2%
Pu 241	10.1%
Pu 242	2.4%

The approximately 1% of Pu 238 was ignored.

D. Axial Blanket - Same as 2 above.

E. Radial Blanket - Same as 2 above.

F. Shielding - Same as 2 above.

Table IV-3 gives the resulting CITATION input parameters for this model.

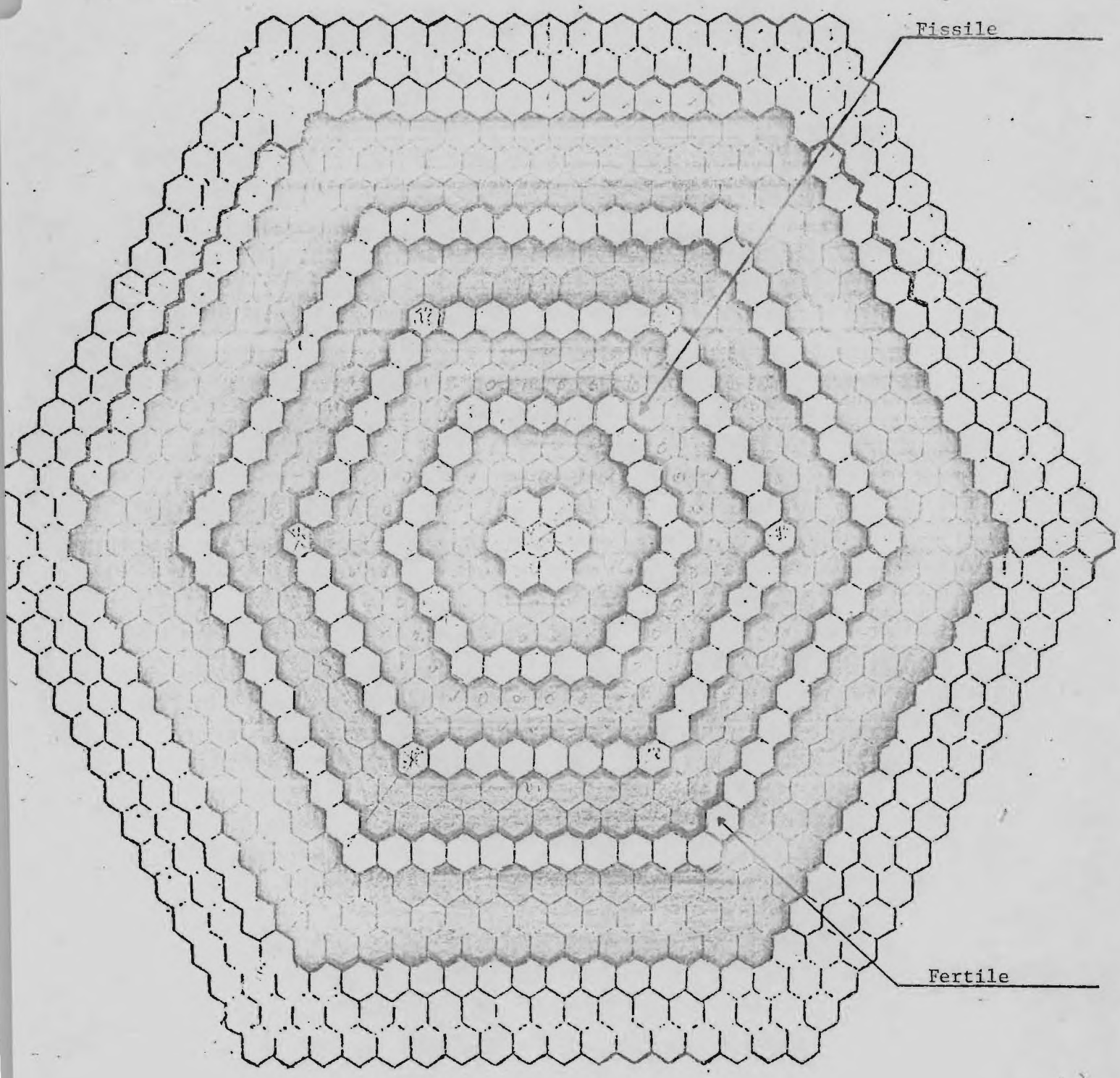

Fig. IV-1. Layout for Heterogeneous Core "Base Models, based on GE LCCEWG Reactor [13].

TABLE IV-1

Calculation of Effective Radii for Various Regions

Pitch = 5.47" = 13.8938 cm

1.

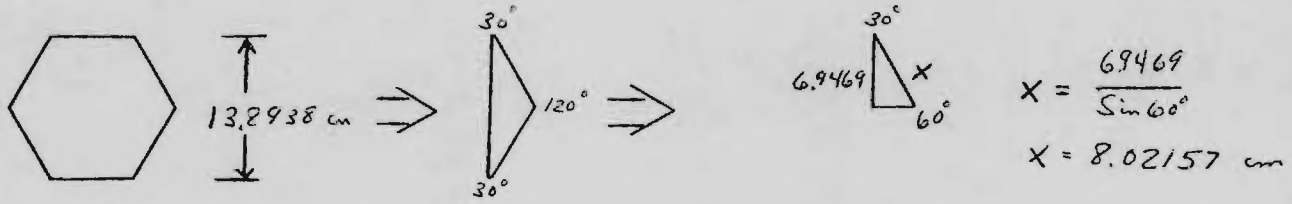

$X = \frac{6.9469}{\sin 60^\circ}$

$X = 8.02157$ cm

2. Area of Hexagon = $2.59808\,\ell^2$ (from CRC)
$= (2.59808)(8.02157)^2$
$= 167.17831\ cm^2$

3. Region I
No. of Hex = 7
Area = $7\,(167.17831\ cm^2) = 1170.2315\ cm^2$
Equivalent Circle = $R = \sqrt{A/\pi}$
$= 19.300298$ cm
Vol (½ core height) = $9004\ cm^3$ (½ height = 53.86 cm)

4. Region II
No. of Hex = 6 + 6 + 10 + 8 = 30
$Area_{II} = 30(167.17831\ cm^2) = 5015.3493$
$Area_{TOT} = Area_I + Area_{II} = 6185.5974$
Equivalent Circle = $R = \sqrt{A_T/\pi}$
$= 44.372703$

$\Delta R_{II} = R_{TOT} - R_I$
$= 25.072405$

5. Region III
No. of Hex = 24
$Area_{III} = 24(167.17831) = 4012.2794$
$Area_{TOT} = Area_{TOT\ II} + Area\ III = 10197.876$
Equivalent Circle = $R_{TOT} = \sqrt{\frac{A_{TOT}}{\pi}}$
$= 56.97442$
$\Delta R_{III} = R_{TOT} - R_{TOT\ II}$
$= 12.601717$

6. Region IV
No. of Hex = 30 + 36 = 66
Area IV = $66(167.17831) = 11033.768$
Area TOT = $Area_{TOT\ III} + Area\ IV = 21231.644$
Equivalent Circle = $R = \sqrt{A/\pi}$
$R_{TOT} = 82.208525$
$\Delta R_{IV} = R_{TOT} - R_{TOT\ III}$
$= 25.234105$

continued/

TABLE IV-1
(continued)

7. Region V

No. of Hex = 42
Area V = 42(167.17831) = 7021.489
Area TOT = Area $_{TOT\ III}$ + Area IV = 2$\mathfrak{L}$231.644
Equivalent Circle = R = $\sqrt{A/\pi}$
R_{TOT} = 94.832755
$\Delta R_V = R_{TOT} - R_{TOT\ IV}$
= 12.62423

8. Region VI

No. of Hex = 48 + 54 = 102
Area VI = 102(167.17831) = 17052.187
Area TOT = $Area_{TOT\ V}$ + Area VI = 45305.32
Equivalent Circle = R = $\sqrt{A/\pi}$
R_{TOT} = 120.08801
$\Delta R_{VI} = R_{TOT} - R_{TOT\ V}$ = 25.25526

9. Region VII

No. of Hex = 60
Area VII = 60(167.17831) = 10030.698
Area TOT = Area $_{TOT\ IV}$ + Area $_{VII}$ = 55336.018
Equivalent Circle = R = $\sqrt{A/\pi}$
R_{TOT} = 132.71774
$\Delta R_{VII} = R_{TOT} - R_{TOT\ IV}$
= 12.62973

10. Region VIII

No. of Hex = 66 + 72 + 78 = 216
Area VIII = 216(167.17831) = 36110.514
Area TOT = $Area_{TOT\ VII}$ + Area VIII = 91446.532
Equivalent Circle = R = $\sqrt{A/\pi}$
R_{TOT} = 170.61164
$\Delta R_{VIII} = R_{TOT} - R_{TOT\ VII}$ = 37.8939

11. Region IX

No. of Hex = 84 + 90 + 96 - 270
Area IX = 270(167.17831) = 45138.143
Area TOT = $Area_{TOT\ VIII}$ + Area IX = 136584.67
Equivalent Circle = R_{TOT} = 208.50959
$\Delta R_{IX} = R_{TOT} - R_{TOT\ VIII}$ = 37.89795

continued/

TABLE IV-1
(continued)

12. Summary

		ΔR_i	R_{outer}
(Fertile)	Region I	19.300	19.300
(Fuel)	Region II	25.072	44.372
(Fertile)	Region III	12.602	56.974
(Fuel)	Region IV	25.234	82.208
(Fertile)	Region V	12.624	94.832
(Fuel)	Region VI	25.235	120.087
(Fertile)	Region VII	12.630	132.717
(Fuel)	Region VIII	37.894	170.611
(Rad. Blkt.)	Region IX	37.898	208.509
(Shield)	Shield X	12.94	221.449

See Figure, page III-24, for a schematic diagram of this model.

TABLE IV-2

Input Dimensions and Atom Densities for Base Case (UUTGXX) for Denatured LMFBR

```
TYPE UUTGXX.000
//*UUTGXX.000
//GO.FT05F001 DD *
GGGGGG
UUTGXX TAK FRIOF LMFBR, GE MODEL, FERT IN,
FISS 20% U233, 3085 MWTH, GAMMA E CORRECTION 1.065
001
  0  0  0  0  0  0  0  0  0  0  0  0  0  0  0  0  0  0  0  0  3
  0  0  0  0  0  0  0  1  0  0  0  1  0  1
200100 10  2  3                                              5  2  2  1  2  5
  2.          .1          1.          0.          1.          1.
003
  0  0  0  0  7  0  0  0  0  0  1  1
  .0001       .00001        0.000       .0001
                           3085.       1.065       .5
004
  4 19.300    5 25.072    3 12.602    5 25.234    3 12.624    5 25.255
  3 12.630    7 37.894    7 37.898    3 12.940
 11 53.860    7 33.350    3 12.790
005
  1  2  1  2  1  2  1  2  5  6
  3  4  3  4  3  4  3  4  5  6
  6  6  6  6  6  6  6  6  6  6
012
  1  1  0  2  0  1  0  0 FERT IN     (Fertile Regions in Core)
  2  2  0  1  0  1  0  0 CORE FISS   (Core Fissile Regions)
  3  3  0  2  0  1  0  0 FERT, OUT   (Fert. Regions in Ax. Blkt. Above/Below
  4  4  0  2  0  1  0  0 AX BLKT                    Core Fert. Regions)
  5  5  0  2  0  1  0  0 RAD BLKT
  6  6  0  2  0  1  0  0  STRUCT     (Shield)

018
 15 17 23 25    11 19 24       26    31 41 43 51    61
020
  1  1  0  0
 11 1.366-02 31 9.800-03 41 6.070-03 43 2.732-02 51 0.000
  2  2  0  0
 15 1.722-03 17 1.800-05 19 7.230-03 41 8.080-03 43 1.804-02 31 1.476-02
 51 0.000-03
  3  3  0  0
 11 1.366-02 31 9.800-03 41 6.070-03 43 2.732-02 51 0.000-05 61 0.000

  4  4  0  0
 11 8.784-03 31 1.476-02 41 8.080-03 43 1.757-02 51 0.000-05 61 0.000

  5  5  0  0
 11 1.366-02 31 9.800-03 41 6.070-03 43 2.732-02
  6  6  0  0
 31 8.508-02
999
```

NUCLIDES

```
/*  11: Th 232      15: U 233       17: U 235       19: U 238       23: Pu 239
    24: Pu 240      25: Pu 241      26: Pu 242      31: SS          41: BLKT
    43: 0           51: Control Channel             61: Control Chan w/rod in
    71: Fiss Prod. (31,51 & 61 comp. defined by Tom Burns)
```

TABLE IV-3
Input Dimensions and Atom Densities for Base
Case (PTTGXX) for a Pu/Th Heterogeneous LMFBR
(See Table IV-2 for region and material definitions)

```
 TYPE PTTGXX.000
//*PTTGXX.000
//GO.FT05F001 DD *
035000
INSIDE THE FENCE LMFBR, GE MODEL, FERT TH,
FISS PU(LHEDS COMP), 3085 MWTH, GAMMA CORRCTION 1.065
001
  0  0  0  0  0  0  0  0  0  0  0  0  0  0  0  0  0  0  0  0  3
  0  0  0  0  0  0  0  1  0  0  0  1  0  1
200100 10  2  3                                              5  2  2  1  2  5
  2.            .1            1.            0.            1.            1.
003
  0  0  0  0  7  0  0  0  0  0  1  1
  .0001         .00001          0.000         .0001
                               3085.         1.065          .5
004
  4 19.300     5 25.072     3 12.602     5 25.234     3 12.624     5 25.255
  3 12.630     7 37.894     7 37.898     3 12.940
 11 53.860     7 33.350     3 12.790
005
  1  2  1. 2  1  2  1  2  5  6
  3  4  3  4  3  4  3  4  5  6
  6  6  6  6  6  6  6  6  6  6
012
  1  1  0  2  0  1  0  0 FERT IN
  2  2  0  1  0  1  0  0 CORE FISS
  3  3  0  2  0  1  0  0 FERT OUT
  4  4  0  2  0  1  0  0 AX BLKT
  5  5  0  2  0  1  0  0 RAD BLKT
  6  6  0  2  0  1  0  0  STRUCT

018
 15 17 23 25    11 19 24       26    31 41 43 51    61
020
  1  1  0  0
 11 1.366-02 31 9.800-03 41 6.070-03 43 2.732-02 51 0.000
  2  2  0  0
 23 1.767-03 24 5.047-04 25 2.661-04 26 6.292-05 41 8.080-03 31 1.476-02
 43 1.804-02 11 6.131-03 51 0.000-03
  3  3  0  0
 11 1.366-02 31 9.800-03 41 6.070-03 43 2.732-02 51 0.000-05 61 0.000

  4  4  0  0
 11 8.784-03 31 1.476-02 41 8.080-03 43 1.757-02 51 0.000-05 61 0.000

  5  5  0  0
 11 1.366-02 31 9.800-03 41 6.070-03 43 2.732-02
  6  6  0  0
 31 8.966-02

999

/*
```

Table V . Summary of Heterogenous Reactor Calculations for Models Based on Reactor Proposal by GE for LCCEWG Study [13].

NAME	GEOMETRY	k @ BOL	BR	
UUTGXS.273	Base	1.030	1.284	
UUTGAS.273	-10% Fiss width	1.030	1.294	
UUTGBS.273	-25% Fiss width	1.030	1.316	
UUTGCS.273	-10% Fiss width, -5% out Fiss	1.030	1.280	
UUTGDS.273	-16% Fiss width, -5% out Fiss	1.030	1.286	
UUTGES.273	-16% Fiss width, -7% out Fiss	1.030	1.280	
UUTGXD.546	-23%/+23% fiss/fert width	1.030	1.280	Dimen. Search
UUTGDS.546	-16% Fiss width , -5% out Fiss	1.030	1.282	
UUTGDS.EQI	-16% Fiss width , -5% out Fiss	1.030	1.302	
UUTGBS.546	-25% Fiss width	1.050	1.273	
UUTGAS.27A	-10% Fiss width	1.030	1.319	

NAME	GEOMETRY	k @ BOL	BR	
PUUGXS.273	Base	1.030	1.387	
PUUGAS.273	-10% Fiss width	1.030	1.417	
PUUGBS.273	-25% Fiss width	1.030	1.475	
PUUGCS.273	-16% Fiss width	1.030	1.438	
PUUGDS.273	-16% Fiss width, -5% out Fiss	1.030	1.425	
PUUGES.273	-16% Fiss width, -7% out Fiss	1.030	1.419	
PUUGYS.273	-16% Fiss width, -33% out Fiss	1.030	1.379	
PUUGDS.546	-16% Fiss width, -5% out Fiss	1.007	1.430	
PUUG1S.273	-1/3 outer Fiss Ring	1.030	1.356	

Table V (continued)

NAME	GEOMETRY	k @ BOL	BR	
PTTGXS.273	Base	1.030	1.235	
PTTG1S.273	-1/3 outer Fiss Ring	1.030	1.200	
PTTGAS.273	-10% Fiss width	1.030	1.269	
PTTGBS.273	-25% Fiss width	1.030	1.337*	
PTTGCS.273	-10% Fiss width, -5% out Fiss	1.030	1.257	
PTTGDS.273	-10% Fiss width, -7% out Fiss	1.030	1.252	
PTTGCS.546	-10% Fiss width, -5% out Fiss	0.986	1.277	
				*Not EOC

NAME	GEOMETRY	k @ BOL	BR	
PUTGXS.273	Base	1.030	1.363	
PUTG1S.273	-33% outer Fiss Ring	1.030	1.307*	
PUTGAS.273	-10% Fiss width	1.030	1.401*	
PUTGBS.273	-25% Fiss width	1.030	1.448	
PUTGCS.273	-10% Fiss width, -5% out Fiss	1.030	1.373	
PUTGCS.546	-10% Fiss width, -5% out Fiss	0.995	1.387	
				*Not EOC

*Example of Geometry Description: "-10% Fiss width, -7% out Fiss" means an initial 10% decrease in the widths of all fissile annuli, and an additional 7% decrease in the width of the center fissile annulus. (See sec. 2.4)

GITNE - 78/2

INVESTIGATIONS OF HETEROGENEOUS LMFBR CORES WITH ALTERNATIVE FUEL CYCLES

by J. M. Kallfelz and A. Livrieri

Progress Report for ORNL Subcontract 3986
June 1978

ABSTRACT

Investigations of heterogeneous LMFBR cores for alternative fuel cycles are being performed at the Georgia Institue of Technology under ORNL Subcontract 3986, and this report covers the April-June (1978) quarter. Results are given for a $(Pu/U)O_2$ reference reactor and transmuter and denatured reactors, all based on the GE design designated as the "starting-point" reference reactor in the initial guidelines of the Proliferation-Resistant LMFBR Core Design Studies (PRLCDS). The pin size of these designs was that of CRBR, and the resulting breeding performance for all classes of reactors was inferior to that of models with larger pins which we previously studied. The PRLCDS guidelines do not prescribe the pin size, and we discuss the pin size, fuel volume fraction, and their influence on breeding performance. Finally, the planned work for the next quarter of this project is discussed.

1. GE Model From LHRFDS Study

For the Proliferation-Resistant LMFBR Core Design Studies (PRLCDS) [2], the GE heterogeneous level II design [3] of the Large Heterogeneous Reference Fuel Design Study (LHRFDS) [4] was chosen as the reference $(Pu/U)O_2$ design in the original guidelines [9] which stated that this reference design shall be updated only if necessary. Given the present interest in this model, we have performed calculations for various fuel cycles using the PRLCDS model as our base design. The results for the reference $(Pu/U)O_2$ design were reported in our March 1978 progress report, and are repeated here for completeness.

1.1 Reference $(Pu/U)O_2$ Design

The GE report [3] gives a description of their $(Pu/U)O_2$ design, and we have used the r-z model described therein for our calculations. From the data given in this reference [3], we were unable to derive consistent values for the atom densities in the various regions. Since the fuel pins used in this model are those of the CRBR, we used the CRBR region densities of Ref. [5] given in Appendix A for our preliminary calculations, changing only the fuel enrichment to obtain criticality. Our calculations should not reproduce the GE results precisely, since GE used slightly larger fuel elements than for CRBR (271 vs. 217 pins/element) and fertile pins smaller than those of CRBR. However, our preliminary quasi-equilibrium cycle [1] calculations are adequate to investigate the general characteristics of the GE model.

Results for our calculations of the $(Pu/U)O_2$ design are given in Table 1 and Figs. 1 and 2. The GE report [3] does not define the time in

Table 1. Results for Our Calculations of the GE PUU Heterogeneous Model from LHRFDS [3].

CYCLE DAYS	0	136.5	273	409.5
K_{eff}	1.007	1.010	1.013	1.015
Breeding Ratio	1.408	1.389	1.348	1.294
P_{max} (W/cc)	672	692	693	684
Fissile Mass (FM) [kg]				
Pu-239	4472	4756	5007	5230
Pu-241	677	614	562	518
U-235	327	305	286	269
(a) FM(409.5)-FM(136.5) [kg]			(b)	(a)
(b) FM(273) -FM(0) [kg]				
Pu-239			+535	+474
Pu-241			-115	- 96
U-235			- 41	- 36
Total			+379	+342
Capture Rates [sec^{-1}]				
Th-232				
U-238	0.487			
Pu-240	0.019			

Fig. 1. Power Distribution for Our Quasi-Equilibrium Cycle Calculation of the GE Heterogeneous PUU Model from LHRFDS [3].

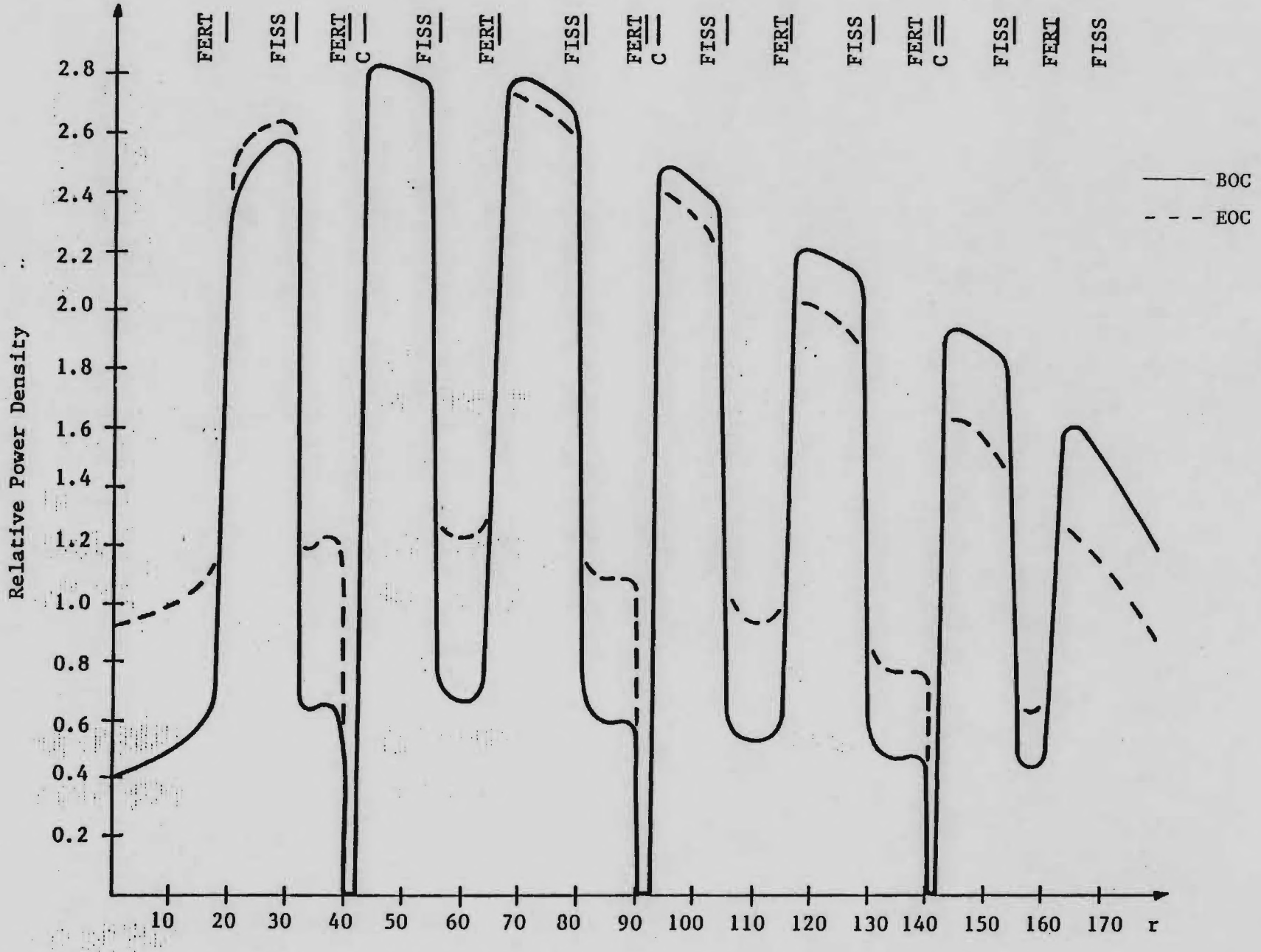

Fig. 2. Radial Linear Power Profile (Core Midplane) for GE Heterogeneous PUU Model from LHRDFS [3]. Our Calculations are for the Quasi-Equilibrium Cycle [1].

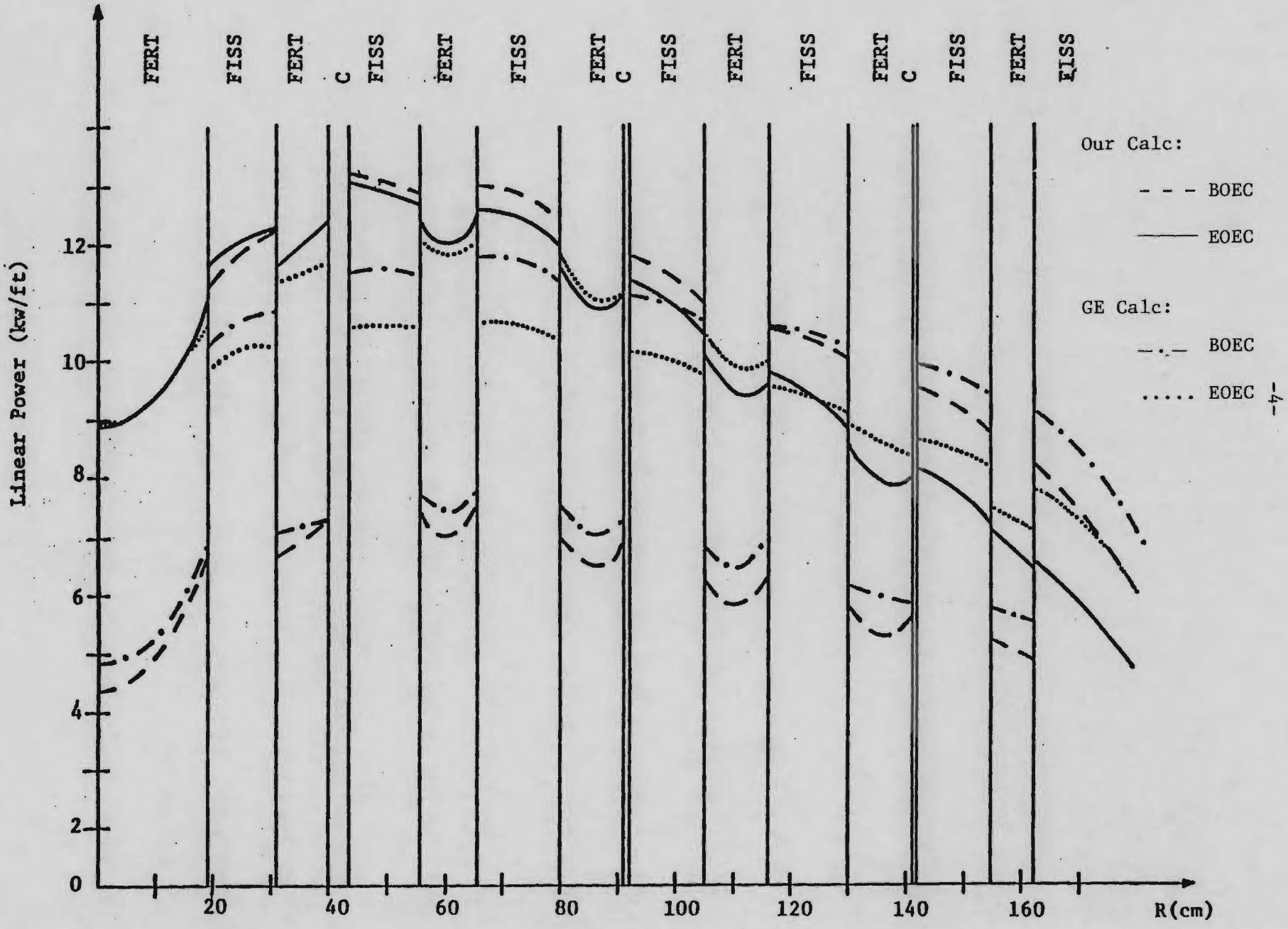

the cycle for which the performance indices are quoted, but assuming their breeding ratio value of 1.336 is for the middle of the equilibrium cycle, our value of 1.348 for the middle of the quasi-equilibrium cycle is in good agreement. Figure 2 presents the radial layout of the various core regions for this model, and allows a comparison of the radial linear power profile for our results and those of GE. Due to the approximations in our model discussed above, we would not expect precise agreement, but the general behavior of the curves is approximately the same for the two cases, with the GE power distribution being somewhat flatter than for our case.

The breeding ratio for the GE model is generally appreciably smaller (about 10%) than the results for PUUG cases in section 4 of Appendix I of our previous report [1]. The fissile loading for the GE LHRFDS model is also somewhat higher than the latter cases. Thus, the 16.7 year doubling time of the GE model [3] is somewhat higher than the 12-13 year values given in Table 4.4 of [1] for our models. The principal reason for this difference is probably the fact that for the LHRFDS use of .23 in OD CRBR fuel pins was required. The base model we used [6] had somewhat larger fuel pins (.26 in OD) with a smaller pin P/D ratio and a larger fuel volume fraction than for the CRBR. Various studies [7] have indicated that the minimum doubling time for a heterogeneous core is obtained with a fuel pin somewhat larger than that of the CRBR. There appears to be a small inconsistency between the stated fuel pin size and fuel volume fraction for the GE LCCEWG model [6] used as the basis for our original models; this inconsistency will be discussed in section 2, below.

1.2. Transmuter and Denatured Reactors Based on the GE LMRFDS Reference Design

Using the same basic model, we have performed calculations for the same alternative fuel cycles considered in our previous calculations [1]. The atom densities for the various cases were obtained as described in Appendix IV of [1]. Volume fractions of the various constituents were the same for all models.

(1) PUT - $(Pu/U)O_2$ drivers, and ThO_2 fertile regions. The driver densities were the same as for those of the base case, while the concentration of the ThO_2 in the various fertile regions was obtained from the following expression:

$$N^{ThO_2} = N^{UO_2} \times \frac{10.0}{10.5} \times \frac{238 + 32}{232 + 32} = 0.974 \times N^{UO_2} \quad .$$

(2) PTT - $(Pu/Th)O_2$ drivers, and ThO_2 fertile regions. The fertile region densities were as for the PUT case. We assumed that in $(Pu/U)O_2$, Pu and U atoms can be exchanged on a one-for-one basis, and that for a given amount of Pu/cc in $(Pu/Th)O_2$ fuel, the ThO_2 molecular density would be 0.974 (calculated in the previous paragraph) of the UO_2 molecular density in $(Pu/U)O_2$ fuel. Thus we used the following expression to estimate the fuel constituent densities for the input value of 36% enrichment, which we estimated to be approximately the value needed at BOL.

$$\frac{N^{Pu} + X}{(N^{Pu} + X) + (N^{Th} - .974X)} = 0.36$$

where

N^{Pu} = 1.3066 E-3, the sum of the densities of plutonium isotopes 239-242 in CRBR core zone 1 (see Appendix A),

and

N^{Th} = 5.613 E-3, 0.974 times the density of uranium in the same zone.

The resulting X value is 1.196 E-3.

The above approximation is consistent with density values for $(Pu/U)O_2$ and $(Pu/Th)O_2$ fuel of 10.35 g/cc and 10.23 g/cc, respectively, given in the ORNL revision of the data sheets from the HEDL September 1977 Design Characteristics books [8].

Results for the "new" PUT and PTT cases based on the PRLCDS reference model are given in Tables 2 and 3, respectively. Comparing these results with those of our "old" models reported in [1], we can see that:

(1) The fissile loading and breeding ratio for the new model are generally about 20-30% higher, and 5-10% lower, respectively, than the values for the old model.

(2) For the new models the change in the maximum power density during the cycle is appreciably smaller than for the old cases.

(3) While the total fissile production during a cycle is generally appreciably higher for the old models, the production of U-233 is much larger for the new models.

For the denatured UUT case, we have first assumed the U-233 atom density to be the same as that of the plutonium in the PUT case, with the other densities unchanged. Then we reduced the density of U^{235} and

Table 2. Results for the PUT Heterogeneous Reactor Based on the GE Model from LHRFDS [3].

CYCLE DAYS	0	136.5	273	409.5
K_{eff}	0.999	1.012	1.022	1.029
Breeding Ratio	1.362	1.335	1.281	1.215
P_{max} (W/cc)	694	726	727	713
Fissile Mass (FM) [kg]				
Pu-239	4967	4676	4419	4188
Pu-241	752	683	621	577
U-233		537	999	1399
U-235	101	92	83	75
(a) FM(409.5)-FM(136.5) [kg]			(b)	(a)
(b) FM(273) -FM(0) [kg]				
Pu-239			-548	-488
Pu-241			-131	-106
U-233			+999	+862
U-235			- 18	- 17
Total			+302	+251
Capture Rates [sec^{-1}]				
Th-232	0.383			
U-238	0.110			
Pu-240	0.020			

Table 3. Results for the PTT Heterogeneous Reactor Based on the GE Model from LHRFDS [3].

CYCLE DAYS	0	136.5	273	409.5
K_{eff}	1.000	1.015	1.026	1.035
Breeding Ratio	1.310	1.283	1.230	1.166
P_{max} (W/cc)	711	742	741	726
Fissile Mass (FM) [kg]				
Pu-239	5363	4886	4469	4099
Pu-241	812	738	677	625
U-233		689	1277	1783
(a) FM(409.5)-FM(136.5) [kg]			(b)	(a)
(b) FM(273) -FM(0) [kg]				
Pu-239			-894	-787
Pu-241			-135	-113
U-233			+1277	+1094
Total			+ 248	+ 194
Capture Rates [sec^{-1}]				
Th-232	0.491			
U-238				
Pu-240	0.021			

U^{238} in the core fissile to arrive at an enrichment of 19.1%, replacing the removed uranium with thorium. This enrichment would have allowed comparison with cases in [1] with the same denaturing, but for our new model it was impossible to go critical with this enrichment.

We thus reduced this constraint, and achieved criticality with 22.7% denaturing. The results, shown in Table 4, indicate a k_{eff} value which had a much smaller change during the cycle than was the case for the old UUT cases [1]. Otherwise, the comparison between the new and old UUT cases shows the same trends indicated by points (1)-(3) above for the PUT and PTT cases.

1.3. Compound Fissile Doubling Time

For the cases discussed above we have performed calculations of the compound fissile doubling time (CFDT) defined as in [1]:

$$\text{CFDT} = \frac{0.693 \times (\text{fissile mass, initial core + 1 reload})}{(0.98 \text{ quasi-eq. cycle fissile discharge}) - (\text{quasi-eq. cycle fissile charge})}$$

The value of 0.98 corresponds to 2% losses, and we have assumed that one reload is 1/2 an initial core.

The CFDT results for all cases are given in Table 5. These values are considerably larger than those for the "old" models reported in [1]: roughly 13, 17, 24 and 33 years for the PUU, PUT, UUT and PTT reactors, respectively.

As mentioned earlier for the PUU case, the principal reason for the poorer breeding performance of the "new" model is probably the fact that for the LHRFDS the use of small (0.23 in OD) CRBR fuel pins, with a corresponding small fuel volume fraction, was required. Remembering that

Table 4. Results for the UUT Heterogeneous Reactor Based on the GE Model from LHRFDS [3].

CYCLE DAYS	0	136.5	273	409.5
K_{eff}	1.012	1.011	1.010	1.008
Breeding Ratio	1.245	1.237	1.216	1.186
P_{max} (W/cc)	776	788	778	757
Fissile Mass (FM) [kg]				
U-233	4837	4816	4797	4779
U-235	118	108	98	90
Pu-239		161	309	443
(a) FM(409.5)-FM(136.5) [kg]			(b)	(a)
(b) FM(273) -FM(0) [kg]				
Pu-239			+309	+282
U-233			- 40	- 37
U-235			- 20	- 18
Total			+249	+227
Capture Rates [sec^{-1}]				
Th-232	0.377			
U-238	0.125			
Pu-240				
Percent Denatured	22.7			

Table 5. Compound Fissile Doubling Time (CFDT) for Various Cases Based on the GE Model from LNRFDS [3].

Case	CFDT (Yr)
PUU	20.3
PUT	41.1
PTT	100.5
UUT	41.0

the original PRCLDS guidelines stated that the GE LHRFDS "reference" model should be updated only if necessary, it is interesting to note that for both the heterogeneous and homogeneous reactors, the participants in PRCLDS have increased the fuel pin size in their preliminary models [10,11]. Westinghouse [11] considers 0.31 in OD pins for all their heterogeneous models, while GE [10] uses OD values of 0.29, 0.31, and 0.34 in for the fuel pins of their homogeneous PUU, PTT, and UUT reactors, respectively. For the denatured UUT case, one of the Westinghouse heterogeneous designs in this study has an enrichment of only 13% [11]. We will discuss the fuel volume fraction in more detail in the following section.

2. Pin Size and Fuel Volume Fraction (FVF)

As indicated previously, there have been various studies of the relation between pin size, fuel volume fraction, and breeding characteristics. For the Pu/U cycle, an ANL paper at the Gatlinburg meeting [7] gives results for heterogeneous and homogeneous cores. For homogeneous cores, the CSDT drops appreciably with pin size up to the maximum outside diameter they considered, 8.38 mm. For the loosely coupled heterogeneous core they considered, there was only a very small drop in the CSDT when going from 7.62 to 8.38 mm OD pins.

Similar trends resulted from a Westinghouse study of $(U\text{-}Th)O_2$ systems [11], which indicated a strong decrease in the CSDT with increasing fuel volume fraction (FVF) up to about 0.52 FVF for the homogeneous reactor, while the heterogeneous reactor CSDT decreased only slightly as the FVF increased from .40 to .45.

As mentioned in section 1, the preliminary PRLCDS designs of GE [10] and WARD [11] all have larger pins than the 0.26 in OD pins of our old models [1]. Furthermore, for the homogeneous designs GE used pin size OD values varying from 0.29 in for the PUU model to 0.34 in for the UUT case, with the corresponding fuel volume fraction varying from 0.427 to 0.466. WARD studied a 0.31 in pin for the reference, transmuter, and denatured heterogeneous designs. For the $(Pu/U)O_2$ driver reactors they also considered the 0.23 in CRBR pin, which for the PUU case had a CSDT three years larger than the 16 year value for the 0.31 in pin. (CSDT not corrected for pre-equilibrium buildup.)

For the ORNL/Ga Tech studies of alternative fuel cycles the same pin size was used for all cases, for both homogeneous and heterogeneous

designs. Obviously for our future studies we should incorporate information on optimum pin sizes presently becoming available through the PRLCDS. Particular attention should be paid to the pin size for the homogeneous designs, since their breeding performance is apparently more sensitive to pin size than is the case for heterogeneous designs.

In this context some comments on calculating fuel volume fraction are in order. It appears that generally the FVF is calculated assuming the pellet swelling has closed the pellet-clad gap, i.e., the volume of the fuel is determined from a pellet diameter equal to the ID of the clad. For instance, the GE PRLCDS report [10] gives an assembly pitch of 6.38 cm, a pin OD of 0.29 in, and a clad thickness of 0.012 in Assuming the fuel fills the clad, for 271 pins/assembly we calculate a pin cross-sectional area of 15.06 in^2. With an equivalent element cross section area (based on the element pitch) of 35.25 in^2, the resulting FVF is 42.7%, the value given by GE [10].

On the other hand, for the numbers given for the GE LCCEWG model [6] used as a basis for our studies, we are unable to arrive at the quoted FVF using the above method. The element pitch is 5.47 in (13.893 cm), the pin OD is 0.26 in (.6604 cm), and the fuel gap is 0.0055 in (0.01397 cm). With 271 pins/assembly, the area inside the clad is 76.48 cm^2. With an equivalent element cores section area of 167.18 cm^2, the resulting FVF would be 0.457, appreciably higher than the 0.433 value given by GE for the LCCEWG model [6]. The FVF value calculated before the fuel swells is 0.416; if we assume that the fuel swells to fill <u>half</u> of the gap area, we arrive at a FVF of 0.436, which is close to the stated value of 0.433.

Obviously the required coolant volume fraction depends on various factors, e.g., pin size, maximum linear power, flow rate, core ΔT, axial peaking factor, core height, etc. However, it may be useful for studies of the influence of pin size on breeding ratio to assume that the core height, core ΔT, Na flow rate and axial peaking factors are the same. Then roughly the volume of sodium per pin should be proportional to the maximum pin linear power. If the later value is approximately the same, and the pins per assembly is the same, then the sodium cross-sectional area inside the various assemblies should be roughly the same.

We have checked this assumption against the results given by GE for their PRLCDS [10], for which the core height and core ΔT are the same; the parameters of interest are given in Table VI.

Table VI. Parameters for GE Homogeneous Core PRLCDS Designs [10]

Parameter	Reference	Transmuter	Denatured
Core height (in)	48	48	48
Pins/Asby	271	271	271
Asby Pitch (in)	6.38	6.63	7.12
Pin OD (in)	0.29	0.31	0.34
Pin P/D	1.20	1.17	1.15
Coolant Vol. Fract (%)	40.1	37.9	35.8

With the above values, we calculate the following results for the coolant cross-sectional area:

Table VII. Parameters Related to Energy Removal, for GE-PRLCDS Designs

Parameter	Reference	Transmuter	Denatured
(a) Coolant area inside element [in^2] (horizontal cross-section)	11.53	11.45	12.43
(a)/(a) for reference reactor	1.00	.993	1.078
Fuel type	$(Pu/U)O_2$	$(Pu/Th)O_2$	$(U233/U_t)O_2$*
(b) Power-to-melt for fuel used in various designs [12] (kw/ft)	20.5	21.0	23.6
(b)/(b) for reference reactor	1.00	1.02	1.15

*U_t = uranium tailings, with 0.2 wt% U235.

From Table VII we see that the coolant per pin varies less than 8% for the three models, and that the only appreciably higher value is for UO_2, which also has an appreciably higher linear power-to-melt, as determined by WARD. The pin sizes and enrichments for the linear power guidelines deviate somewhat from the values used by GE, and of course the GE design actual average linear powers are probably not in the same ratio as the power-to-melt values. It appears that the suggested approximation for determining the necessary coolant volume would be adequate for survey calculations of the influence of pin size on breeding parameters.

3. Neutron Leakage by Zone

Because of errors discovered in the transport cross sections of the ORNL data set which we have been using for our calculations, we attempted to make a comparison with some results available from NIRA to estimate the influence of this error on the neutron leakage by zone. To this end we executed CITATION [13] runs requesting the edit options which print neutron balance information, including zone-wise leakage (IEDG5 and IEDG6 of card 3, section 001). This option functions on the CITATION versions we have used in Italy and at Georgia Tech.

This option is apparently inoperative on the ORNL X-10 CITATION version, since this information was not printed on an output of the run for which these edit options were requested. This option is valuable for a number of purposes, such as determining the information we desired on the influence of diffusion coefficient changes, estimating effective bucklings, and investigating basic physics differences for reactors operating on various alternative fuel cycle. Therefore, we feel that this option should be checked, and initiated on the X-10 CITATION version if in fact it is presently inoperative.

4. Work Planned for Next Quarter

For the July-September 1978 quarter, our planned activities will concentrate on investigations of the models being developed for the Proliferation Resistant Large Core Design Study PRLCDS [2], and on the influence of new cross section data on performance indices of LMFBRs operating on various fuel cycles:

(1) The first priority work will be: to analyze the characteristics of the oxide-fuelled LMFBRs being developed for the PRLCDS, to determine the significant differences between these designs and the designs we have used for our previous studies [1], and to make recommendations as to how the PRLCDS results should be incorporated into our future studies. This analysis will be performed both by use of reported results from the contractors involved in the PRLCDS, and by our own calculations of their models, extending our investigations of preliminary models which we reported in sections 1. and 2. Partial results available for the oxide GE homogeneous models [10] and WARD heterogeneous models [11] have been previously mentioned. With the final "data sheets" (format prescribed in section J of [2]) for these models which have just been received at ORNL, we will be able to perform accurate calculations of the parameters of interest for these models. We plan to use some of the comparison techniques used by HEDL in their "cross-cutting physics analysis" [14] for these studies.

(2) Influence of Cross Section Changes.

Our calculations have been performed with ENDF/B-IV nuclear data, which was also prescribed for the PRLCDS [2]. Many recent investigations indicate that for this data base the Th232 capture cross section is too

high, [15-17], the U-233 σ_f is too low over a wide energy range [18], and that other changes are in order. These changes have been incorporated into ENDF/B-V data, which is presently becoming available. Investigations of the influence of these changes have been reported for some classes of reactors. HEDL has reported such studies for homogeneous LMFBRs [19], and the previously cited WARD report [11] gives results for a 20% reduction in Th232 σ_c for a $(U/Th)O_2$ heterogeneous design. We will use the same scoping method we described briefly in [20] for a limited study performed previously, i.e., we will use the differential cross section curves such as those in [15-19] to estimate approximate changes to the group cross sections input into CITATION for our reactor calculations. We will consider homogeneous and heterogeneous designs for the reference, transmuter, and denatured classes of reactors.

1. J. M. Kallfelz, A. Livrieri and D. M. Rowland, "Investigations of Heterogeneous LMFBR Cores with Alternative Fuel Cycle," GITNE-78/1, Progress Report for ORNL Subcontract 3986, Georgia Institute of Technology, March 1978.

2. J. C. Chandler et al., "The Proliferation Resistant Preconceptual Core Design Study, TC-1082, Hanford Engineering Development Laboratory, March 1978.

3. D. P. Johnson, "Large Heterogeneous Reference Fuel Design Study," GEFR 00110 (L), General Electric Fast Breeder Reactor Department, Sunnyvale, Calif. (May 1977).

4. "Ground Rules, Large Heterogeneous Reference Fuel Design Study," Combustion Engineering, Inc., Windsor, Conn. (October 22, 1976).

5. J. Lake, "LMFBR Nuclear Analytical Model," WARD Internal Memo LRA-73-251, August 17, 1973.

6. Letter from Edouard Kujawski, Fast Breeder Reactor Department, General Electric, to Members of the Large Core Code Evaluation Working Group, SUBJECT: Transmittal of Design for Use in Large Core Code Evaluation, (January 29, 1976).

7. W. P. Barthold and J. C. Beitel, "Physics Aspects in the Design of Heterogeneous Cores," Proceedings of the ANS Reactor Physics Division Topical Meeting," Gatlinburg, Tenn. April 1978.

8. G. F. Flanagan, Memo to T. E. Cole and H. F. Bauman, ORNL, Dec. 14, 1977, "Revised Reactor Design Characteristics for Use by Burns and Roe for Fuel Center Calculations," with attached copies of ORNL revision of the data sheets from the HEDL September 1977 Design Characteristics books.

9. C. E. Weber (RDD/TA), telex to F. Mynatt, SUBJECT: Proliferation-Resistant LMFBR Core Design Studies," Sept. 1977.

10. H. S. Bailey and B. Talwar, "Advanced LMFBR Core Design, Proliferation Resistant LMFBR Core Design Study, Status Review for PRLCDS Working Group, April 25-26, 1978, Argonne, Illinois," GE Fast Breeder Reactor Dept, Sunnyvale, Calif.

11. P. W. Dickson, "PRLCDS Review Meeting, Westinghouse Advanced Reactors Division, Nuclear Design Effort, Argonne Nat. Lab. Meeting, April 25-26, 1978," Westinghouse Advanced Reactors Div.

12. A. Biancheria et al., "Contribution to Meeting on PRLCDS, April 25-26, Overview of Fuel and Blanket Rod Groundrules," Westinghouse Advanced Reactors Division.

13. T. B. Fowler, D. R. Vondy and G. W. Cunningham, "Nuclear Reactor Core Analysis Code: CITATION," ORNL-TM-2496, Rev. 2, Oak Ridge National Laboratory, July 1971.

14. J. C. Chandler et al., "Cross-Cutting Physics Analysis," HEDL, April 20, 1978, Presentation at PRLCDS Working Group Meeting at ANL, April 25-26, 1978.

15. R. L. Macklin and J. Halperin, "^{232}Th(n,γ) Cross Sections from 2.6 to 800 keV," Nucl. Sci. Engr. 64, 849 (1977)

16. G. de Saussure and R. L. Macklin, "Evaluation of the ^{232}Th Neutron Capture Cross Section Above 3 keV," ORNL/TM-6161, Dec. 1977.

17. W. P. Poenitz, "Revised Th-232 (n,γ)-Evaluation," Argonne National Laboratory Memo, Jan. 16, 1978.

18. W. P. Poenitz, "U-233 (n,f) Cross Section," Argonne National Laboratory Memo, Oct. 31, 1977.

19. J. C. Chandler et al., "Effects of Revised Cross Section Data," HEDL, Feb. 15, 1978, Presentation at Feb. 16, 1978 PRLCDS meeting.

20. D. E. Bartine, et al., "Alternative Fuel Cycles for Breeder Reactors," Proceedings Int. Conf. Alternative Energy Sources, Miami Beach, Florida, Dec. 5-7, 1977.

HOT-FULL-POWER NUCLEAR NUMBER DENSITIES

LMFBR - 975 MWt Demo Plant (720°F inlet, 980°F outlet) - BOC, first core
all values $\times 10^{24}$/cc

Region	Pu-238	Pu-239	Pu-240	Pu-241	Pu-242	U-235	U-238	O	Fe	Cr	Ni	Mo	Mn	Na	B-10	B-11	C	REMARKS
ENDF/B		9	8	7	6	12	10	2	19	21	18	16	20	1	4	25	3	
1	1.320-5	8.882-4	2.534-4	1.333-4	3.168-5	4.091-5	5.722-3	1.388-2	1.285-2	3.730-3	2.548 3	2.888-4	3.530-4	9.188-3				Core Zone 1 Fuel.
2	1.923-5	1.294-3	3.693-4	1.942-4	4.616-5	3.689-5	5.159-3	1.395-2	1.285-2	3.730-3	2.548-3	2.888-4	3.530-4	9.200-3				Core Zone 2 Fuel.
3						2.906-5	1.318-2	2.642-2	8.693-3	2.524-3	1.724-3	1.958-4	2.388-4	5.667-3				Radial Blanket, "core" region.
3						2.908-5	1.319-2	2.643-2	8.704-3	2.527-3	1.726-3	1.956-4	2.391-4	5.762-3				Radial Blanket, lower axial extension.
4						1.661-5	7.533-3	1.510-2	1.393-2	4.044-3	2.763-3	3.131-4	3.827-4	8.506-3				Upper Axial Blanket, core zone 1.
4						1.661-5	7.536-3	1.510-2	1.393-2	4.045-3	2.763-3	3.132-4	3.828-4	8.535-3				Upper Axial Blanket, core Zone 2.
5									5.201-3	1.510-3	1.032-3	1.189-4	1.429-4	2.041-2				Control - lower "expandable" Na transition region.
6									1.049-2	3.045-3	1.977-3	2.066-4	2.901-4	5.574-3				Radial Blanket Fission Gas Plenum.
7									1.565-2	4.542-3	3.012-3	3.261-4	4.315-4	8.939-3				Core Zone 1 Fission Gas Plenum.
7									1.565-2	4.543-3	3.013-3	3.262-4	4.316-4	8.970-3				Core Zone 2 Fission Gas Plenum
8									1.801-2	5.229-3	3.572-3	4.048-4	4.949-4	7.297-3	6.224-3	2.524-2	8.225-3	Central Control, 61 pin, natural B_4C. [a]
9									1.803-2	5.233-3	3.575-3	4.052-4	4.953-4	7.419-3	6.226-3	2.525-2	8.226-3	Row 4 Control, 61 pin, natural B_4C. [b]
9									1.803-2	5.233-3	3.575-3	4.052-4	4.953-4	7.419-3	1.574-2	1.574-2	8.226-3	Row 4 Control, 61 pin, 50% enriched B_4C. [b]
9									1.803-2	5.233-3	3.575-3	4.052-4	4.953-4	7.419-3	1.257-2	1.891-2	8.226-3	Row 4 Control, 61 pin, 4-50% enriched + 2-natural B_4C [b]
10									1.801-2	5.229-3	3.572-3	4.048-4	4.949-4	7.298-3	6.224-3	2.524-2	8.224-3	Row 7 (flats) Control, 61 pin, natural B_4C. [a]
11									1.803-2	5.233-3	3.575-3	4.052-4	4.953-4	7.430-3	6.227-3	2.526-2	8.228-3	Row 7 (corners) Control, 61 pin, natural B_4C. [b]
12									1.672-2	7.757-3	5.300-3	6.006-4	7.342-4	1.161-2				Control Rod Lower Attachment Region.
13									1.938-2	5.627-3	3.844-3	4.356-4	5.325-4	1.461-2				Fuel Rod Lower Attachment Region.
14						2.905-5	1.318-2	2.641-2	9.280-3	2.699-3	1.841-3	2.086-4	2.550-4	5.335-3				Radial Blanket, upper axial extension.
16									2.249-2	6.527-3	4.459-3	5.054-4	6.179-4	1.334-2				Radial Blanket Lower Rod Attachment Region
17									4.298-2	1.248-2	8.523-3	9.659-4	1.181-3	9.959-3				Control Assemblies, lower shield.
18									4.582-2	1.330-2	9.087-3	1.030-3	1.259-3	3.796-3				Fuel Assemblies, lower shield.
19									4.235-2	1.404-2	1.703-2	9.331-4	1.141-3	2.489-3				Radial Reflector.
20									5.484-3	1.304-2	5.775-2			2.401-3				Radial Restraint.
21									1.985-2	5.761-3	3.936-3	4.461-4	5.453-4	7.521-3				Control, lower He gas plenum (central + row 7 flats).
21									1.984-2	5.760-3	3.935-3	4.459-4	5.451-4	7.471-3				Control, lower He gas plenum (Row 4 + row 7 corners).
22									1.927-2	5.593-3	3.811-3	4.301-4	5.295-4	7.189-3				Control, upper He gas plenum (central + row 7 flats).
22									1.930-2	5.603-3	3.818-3	4.309-4	5.305-4	7.391-3				Control, upper He gas plenum (Row 4 + row 7 corners).
23									3.031-2	8.800-3	6.012-3	6.813-4	8.329-4	9.667-3				Control Rod Top End Caps (central + row 7 flats).
23									3.036-2	8.814-3	6.022-3	6.824-4	8.342-4	9.918-3				Control Rod Top End Caps (Row 4 + row 7 corners).
24									1.468-2	4.260-3	2.911-3	3.299-4	4.032-4	1.588-2				Control, upper "compressible" Na transition (central + row 7 flats)
24									1.470-2	4.267-3	2.916-3	3.304-4	4.039-4	1.624-2				Control, upper "compressible" Na transition (Row 4+ row 7 corners).
25									2.978-2	8.644-3	5.905-3	6.692-4	8.181-4	9.781-3				Core Zone 1 Upper Fuel Rod Expansion Region.
25									2.976-2	8.640-3	5.903-3	6.689-4	8.177-4	9.823-3				Core Zone 2 Upper Fuel Rod Expansion Region.
26									8.628-3	2.505-3	1.711-3	1.939-4	2.370-4	1.853-2				Radial Blanket Rod Upper Expansion Region.
27						1.664-5	7.546-3	1.513-2	1.287-2	3.736-3	2.553-3	2.893-4	3.536-4	9.440-3				Lower Axial Blanket, core zone 1.
27						1.663-5	7.544-3	1.512-2	1.287-2	3.736-3	2.553-3	2.893-4	3.536-4	9.441-3				Lower Axial Blanket, core zone 2.
28									4.163-2	1.208-2	8.256-3	9.355-4	1.144-3	5.511-3				Radial Blanket Assemblies, lower shield.

J.A. Lake 8/9/73

[a] temperature distribution @ 11.65 inches withdrawn.

[b] temperature distribution @ 36 inches withdrawn.

TABLE 5 - REGIONWISE HOT-FULL-POWER ELEMENTAL NUMBER DENSITIES. FORMAT X.XXX - N is X.XXX $.10^{-N}$. ALL VALUES ARE $\times 10^{24}$/CC. "ENDF/B" INDICATES THE LIBRARY NUMBER OF THE MATERIAL ON THE WMLLIBR LIBRARY TAPE CONTAINING PROCESSED 30-GROUP ENDF/B-III CROSS SECTION DATA.

JAL
8/17/73